GENERATING POINT CLOUD BY USING SFS WITH SOLAR LIGHT SOURCE TO BUILT 3D SURFACE BY CATIA

WITTAYA AUEPRASERT

**A THESIS SUBMITTED IN PARTIAL FULFILLMENT
OF THE REQUIREMENTS FOR
THE DEGREE OF MASTER OF ENGINEERING
(INDUSTRIAL ENGINEERING)
FACULTY OF GRADUATE STUDIES
MAHIDOL UNIVERSITY
2010**

Thesis
entitled

GENERATING POINT CLOUD BY USING SFS WITH SOLAR LIGHT SOURCE TO BUILT 3D SURFACE BY CATIA

………………………………………

LCDR. Wittaya Aueprasert
Candidate

………………………………………

Lect. Kiattisak Sritrakulchai, Ph.D.
Major advisor

………………………………………

Lect. Kanokwon Kingphadung, D.Eng
Co-advisor

………………………………………

Lect. Thitikorn Limchimchol, Ph.D.
Co-advisor

………………………………………

Prof. Banchong Mahaisavariya,
M.D., Dip Thai Board of Orthopedics
Dean
Faculty of Graduate Studies,
Mahidol University

………………………………………

Asst. Prof. Thanakorn Naenna, Ph.D.
Program Director
Master of Engineering Program in
Industrial Engineering
Faculty of Engineering , Mahidol University

Thesis
entitled

GENERATING POINT CLOUD BY USING SFS WITH SOLAR LIGHT SOURCE TO BUILT 3D SURFACE BY CATIA

was submitted to the Faculty of Graduate Studies, Mahidol University
for the degree of Master of Engineering (Industrial Engineering)
on
June 1, 2010

……………….……….….………
LCDR. Wittaya Aueprasert
Candidate

……………………..…..………………
Lect. Manusak Janthong, Dr.-Ing
Chair

……………………..…..……….….……
Lect. Kiattisak Sritrakulchai, Ph.D.
Member

……………………..…..……………...…
Lect. Kanokwon Kingphadung, D.Eng
Member

……………………..…..………………..
Lect. Thitikorn Limchimchol, Ph.D.
Member

……………………..…..……………...…
Prof. Banchong Mahaisavariya,
M.D., Dip Thai Board of Orthopedics
Dean
Faculty of Graduate Studies,
Mahidol University

……………………..…..……………...…
Asst. Prof. Rawin Raviwongse, Ph.D.
Dean
Faculty of Engineering, Mahidol University

ACKNOWLEDGEMENTS

This thesis would not have been possible without the help, support and patience of my advisors' team. First and foremost I offer my sincerest gratitude to my professor, Dr. Kiattisak Sritrakulchai, who gave a good guidance for thesis. Special thanks go to Dr. Kanokwon Kingphadung and Dr. Thitikorn Limchimchol who gave comments and appreciate suggestion.

I would like to thank also teaching staff but more importantly the Industrial Engineering staff in the Faculty of Engineering, Mahidol University - for their kindness and helpful all times when I studied at there.

Finally, special thanks to my parents, Mr. Pajon and Mrs. Urawan Aueprasert, I know they take care of me all way and all time that main cause of my successful. My wife, Mrs. Thapanun Aueprasert, who consistently believes, supports and encourages to me. Finally I would like to thank my friends, who helped me along this course, especially friends who consent to using their photographs in my thesis.

Wittaya Aueprasert

GENERATING POINT CLOUD BY USING SFS WITH SOLAR LIGHT SOURCE TO BUILT 3D SURFACE BY CATIA

LCDR. WITTAYA AUEPRASERT 5037353 EGIE/M

M.Eng. (INDUSTRIAL ENGINEERING)

THESIS ADVISORY COMMITTEE : KIATTISAK SRITRAKULCHAI, Ph.D., KANOKWON KINGPHADUNG, D.Eng. , THITIKORN LIMCHIMCHOL, Ph.D.

ABSTRACT

This research presents an application of the solar position to shape from shading (SPF) technique, a technique for producing 3D objects by utilizing information on image elements along with a reflectance of light. The technique aims to develop a process of 3D surface creation for photos, particularly taken from off-building areas such as building views, etc., which can be utilized in engineering design. The trial software created imports image data and pre-calculated data for finding solar light direction, whereas it exports point clouds for building 3D surfaces with the use of Computer Aided Three-dimensional Interactive Application (CATIA) software.

The developed process and created software enhances surface quality. Surface quality consists of correcting shape, surface resolution, and defect meshes, depend on image clearing, image resolution, and light direction are shadow effects and divergence failure. Temperature, air pressure, and elevation are less influential in solar position calculation, so the only equipment needed is a camera, compass, and watch. Surface creation is performed in two ways: bas-relief 3D surface and expanding height 3D surface. High quality bas-relief 3D surfaces which, while expanding the height of 3D surface, when it has been improved by CATIA, qualifies. Moreover combination of each partial well point cloud was used for solving shadow effects and making more robust surfaces.

KEY WORDS: SHAPE FROM SHADING / SOLAR POSITION / 3D SURFACE / POINT CLOUD

179 pages

การสร้างกลุ่มข้อมูลจุดด้วยวิธี SFS กับทิศทางแสงอาทิตย์ เพื่อสร้างพื้นผิว 3 มิติด้วยโปรแกรม CATIA

GENERATING POINT CLOUD BY USING SFS WITH SOLAR LIGHT SOURCE TO BUILT 3D SURFACE BY CATIA

น.ต. วิทยา เอื้อประเสริฐ 5037353 EGIE/M

วศ.ม.(วิศวกรรมอุตสาหการ)

คณะกรรมการที่ปรึกษาวิทยานิพนธ์: เกียรติศักดิ์ ศรีตระกูลชัย, Ph.D., กนกวรรณ กิ่งผดุง, D.Eng., ฐิติกร ลิ้มชิมชล, Ph.D.

บทคัดย่อ

งานวิจัยนี้นำเสนอการประยุกต์หลักการหาตำแหน่งของดวงอาทิตย์กับเทคนิควิธี Shape from Shading (SFS) ซึ่งเป็นเทคนิควิธีที่ใช้ข้อมูลรูปภาพและข้อมูลทิศทางแสงตกกระทบวัตถุในรูปภาพในการสร้างข้อมูลวัตถุ 3 มิติ ขึ้นมาใหม่ จุดประสงค์เพื่อพัฒนาวิธีสำหรับสร้างพื้นผิว 3 มิติ จากการถ่ายภาพภายนอกอาคาร เช่น สิ่งปลูกสร้าง ทิวทัศน์ และ อื่นๆ สำหรับไว้ใช้งานออกแบบทางวิศวกรรมได้ งานวิจัยนี้ได้สร้างซอฟแวร์เครื่องมือทดลอง โดยมีข้อมูลนำเข้าซอฟแวร์เป็นข้อมูลภาพและข้อมูลสำหรับคำนวณผลลัพธ์ทิศทางแสงอาทิตย์ ข้อมูลนำออกเป็นข้อมูลในลักษณะกลุ่มข้อมูลจุด ซึ่งเป็นลักษณะที่นำไปใช้สร้างพื้นผิว 3 มิติโดยซอฟแวร์ CATIA ได้

ผลการทดสอบกระบวนการและซอฟแวร์ที่สร้างขึ้นมาพบว่า คุณภาพของพื้นผิว, คุณภาพพื้นผิวคือความถูกต้องของรูปร่าง, รายละเอียดของพื้นผิว และ โครงข่าย 3 เหลี่ยมที่เสีย, ซึ่งขึ้นอยู่กับ ความคมชัดของภาพ ความละเอียดของภาพ และ ทิศทางของแสง ผลกระทบทิศทางแสงคือ ผลกระทบจากเงา และผลกระทบจากการลู่ออกจากผลลัพธ์ และพบว่าอุณหภูมิ ความกดอากาศ และความสูงจากระดับน้ำทะเล ส่งผลกระทบต่อการคำนวณตำแหน่งดวงอาทิตย์น้อย เป็นผลให้ อุปกรณ์ที่ใช้ในการถ่ายภาพมีเพียง กล้องถ่ายภาพ เข็มทิศ และนาฬิกา การสร้างพื้นผิวมี 2 ลักษณะคือ พื้นผิว นูนต่ำ กับพื้นผิว 3 มิติ ผลของพื้นผิวนูนต่ำมีคุณภาพดีมาก ส่วนพื้นผิว 3 มิติขยายความสูง เมื่อปรับปรุงพื้นผิวด้วย CATIA แล้วก็ได้คุณภาพดี นอกจากนี้ภาพที่มีผลกระทบจากเงาสามารถแก้ไขด้วยการรวมแต่ละกลุ่มข้อมูลจุดที่ดี จะได้พื้นผิวที่สมบูรณ์มากยิ่งขึ้น

179 หน้า

CONTENTS

CONTENTS (cont.)

CONTENTS (cont.)

CONTENTS (cont.)

CONTENTS (cont.)

CONTENTS (cont.)

LIST OF TABLES

LIST OF FIGURES

LIST OF FIGURES (cont.)

LIST OF FIGURES (cont.)

Figure **Page**

LIST OF FIGURES (cont.)

LIST OF FIGURES (cont.)

CHAPTER I
INTRODUCTION

1.1. Background and Problems statement

At the beginnings of this work, researcher intends to take an advantage by which focuses on the use of information from photos to create the shape of the object for engrave work. Principles for creating 3-dimensional objects by utilizing some characteristics of taken photos have been found in several ways such as the Photometric Stereo principle, firstly presented by Woodham (1980)-reconstruction a object shape from images in same camera angle but different light source direction-, and the Geometric principle, firstly presented for by Hu (1962) - reconstruction object shape from figures which camera angles as number of figures-. However, despite such as useful principles, both of them are limited by extent of which a number of images must be taken and complicated pre-arrangement process before making photography is needed, leading to an inconvenience for the use of images taken outside preparation places. However, apart from these two principles, researcher also found other 2 more principles using only one image for reconstruction, namely the Shape from Texture principle, firstly presented by Gibson (1950a,1950b) and the Shape Form Shading principle (SFS), firstly presented by Horn (1989). The former, based on calculations from twisting pattern on material surface essentially relies on an image of the objects with pattern or creating pattern to the object; on the other hand, the latter, based on the use of data from only one image together with light source direction is obviously less complicated than the former – comparison requirements of all principle is shown in table 1.1- . In this research, finally Shape Form Shading principle (SFS), because is the easiest to gather information and is flexible for selecting place to take photos, not limited to only photographic studio, has been chosen.

Table 1.1 Requirements of each image principle.

Principle	Requirements
Geometric	Data of images from different view.
Photometric Stereo	Data of images more thane one and their light sources.
Shape from Texture	Data of an image with texture.
Shape Form Shading	Data of an image and light source.

SFS principle aims to find object shape from an image; nonetheless, an error caused by incorrect light direction is a significant concern in performing this principle- which to find correct light direction against the object rarely happens without preparation of light source before taking photos. Such an important error will occur in only taken real images, not in synthetic images which particularly are created for testing image processing study. Hence, as far as the Shape Form Shading principle (SFS) is used for studying in this research, it is necessary to correct the light source direction, causing light preparation for photographing to be limited only in photographic studio.

From the foregoing preliminary, the use of SFS must consider the light source direction, and solar light source is inevitable to be used. The use of solar light benefits an ability to be used without prepared lightening devices and an ability to be used with large materials which are immobile into photographic studio. This may result in reducing in study costs. As a result, researcher is interested in applying direction of solar light source into SFS principle by aiming to conduct in the open area where the solar light can get into.

SFS principle can be applicable to product design which bas-relief work such as coins design, decorations design etc. That work need skillful sculptor and spent many times or use other tools such as 3D Scan and Laser Scan which despite high accuracy, require pretty much more expensive costs than those of SFS method which needs only digital camera and an individual computer. Besides, SFS is better fitting to materials outside photographic studio due to its movable camera and also more convenient when applied with solar light leading to an ability to generate 3D surface of large objects

Apart from engineering and product design applications, the result of this work may provide any other applications such as robot vision -which 3D object can be built into robot's perception device-, topographic survey –by which aerial photography can be used- and etc. According to the propose of this research, however, a study of possibility to use the solar light source direction with SFS to create 3D Surface will be emphasized on rather than others. Software for SFS calculations with Solar Light Source will be configured, and its result will finally be the cloud of points. Then, the use of existing tool, Computer Aided Three-dimensional Interactive Application (CATIA)-, for generating and improving 3D surface will be adopted. More significantly, if the quality of 3D surface from an image does not meet standard -check by eyes-, more images will be used for generating 3D surface by combining them together. This step also relies on CATIA.

1.2 Objective

1.2.1 To develop techniques for creating 3D surface from a digital camera photos with solar light.

1.2.2 To develop techniques for forming data sets as the Point cloud in Cartesian coordinate.

1.2.3 To use the Point cloud for creating 3D surface by using CATIA.

1.3 Scope of Work

1.3.1 Images Scope

- Images are used in only Bitmap type.
- Photos must be adjusted to the width and length equal.
- Photo size must not exceed 900x900 pixels.

- Photos must be compatible to background color by blending altogether with black ground prior to photographing or using imaging software to decorate background color image.

- In case of using CATIA for combining surface form more than 2 images; only top view image can be used.

1.3.2 Research Places and Times

- In Bangkok and suburban
- Photography location is not slanted.
- Photography is done in the period 09.00 to 16.00.

1.3.3 Object to Photograph

- Surface materials will be assumed with their reflectance as Lambert Cosine Law.
- Materials entirely have same color throughout the piece or are made up by the same color throughout the piece.
- Abedo was already assumed as constance to be equal 1

1.3.4 Method

- SFS principle used in this work will be selected only one, the most appropriate method,-Tsi-Shah're method-.
- Solar position principle used in this work will be selected only one, the most appropriate method,-Reda – Andreas're method-.

1.4 Expected results

1.4.1 Able to develop tool that has its result is the Point cloud by apply to SFS and Solar position.

1.4.2 Able to use CATIA for apply the point cloud to build 3D surface with sufficient quality to be finally used for product design utilization

CHAPTER II
LITERATURE REVIEW AND DESIGN CONCEPT

2.1 Literature Review

2.1.1 Shape Form Shading

A study of developing 2D figure into newly 3D object by using SFS approach has initially been recognized since 1970, according to a research conducted by Horn for his Ph.D. level. Then, SFS approach has been developed continuously, causing a great number of related documents to happen. At the same time, innovations on SFS approach have been occurring , and lots of techniques were applied into SFS principle such as Graph cut technique by Chang et Al (2008), wavelet-based technique by Hsieh et Al (1995), Newton-Raphson finite different technique by Tsai, Shah (1999), Fourier transform by Pentland (1990) as well as Heat equation by Robles-Kelly &Hancock(2007) etc.

SFS approach is rather complicated in mathematic calculation; however, it has been applied to utilize in various jobs for example: Horn (1981) presented use of SFS approach to find mountain geography, Bingham and Rees (1998) applied SFS approach to find shape of ice cap and ice sheet at Svalbard in the Eurepean Arctic sector, and Courteille et al (2007) used SFS approach for straightening curved images taken from digital cameras.

The aim of calculating SFS is to obtain height or depth - **unknown values**, whereas width and length must be known values. In SFS equation, to figure out these unknown values is called as direct SFS method, related to a variety of supporters such as Leclers&Bobick (1991), Cheung et Al(1997), and Vogel et Al (2007). However, most popularly used unknown values, was presented firstly by Horn, called gradient (p,q).

All of SFS methods need to use reflectance models to develop their equation. As known widely, in SFS methods, material surface should basically be designated as Lambertance surface- Lambert (1760) suggested this model. On the other hand, there are other reflectance models used for calculating such as Ahmed and Farag (2007) suggested reflectance model of Oren-Nayar(1995), and reflectance model of Pong(1975) was supported by Volgel et al (2008,2009) etc. However, compared with all other reflectance models, Lambert's reflectance model is used mostly for SFS methods because of its simply used pattern.

Until now there are a large number of techniques used for SFS methods including both unknown value model and reflectance model, causing grouping SFS approaches to be more complicated. However Zhang et al (1999) presented SFS approach can be divided into 4 groups -Minimization approach, Propagation approach, Local approach and Linear approach-. Grouping SFS approach based on Zhang's study is mostly used and referred. Apart from this, there still are other SFS approaches such as Global approach, Simple approach, Direct SFS etc.

Due to a lot of SFS methods, to properly choose SFS methods, there were two studies, conducted by Durou et al (2008) and Zhang et al (1999) which researcher are interested in. These two studies performed on the basis of comparison criteria. For the former, Durou et al compared methods of Zheng & Chellappa(1985), Lee & Kou(1991), Bichsel & Pentland (1992), Lee & Rosenfeld (1985), Pentland (1988), Tsi & Shah and found that the most error values and the least CPU times occurred in Tsi & Shah method; conversely, the least error values and the most CPU times happened in lee & Kuo method. For the latter, Zhang chose to compared methods of Falcone & Sagono(1997), Daniel & Durou (2000) , Tsi & Shah and showed that Falcone & Sagono method was good in smooth surface, whereas Daniel & Durou method was rather good in both Smooth and Non Smooth surface and also resulted in the least CPU time. By considering a few limitations in this work which is computer is individual and unable to process at high performance level, Tsi & Shah method is chosen because this method does not need occluding boundary –the edge of shadow on plane that perpendicular to the light source direction -, very difficult to find from real images. Besides this reason, Tsi & Shah method provided the least CPU times. However, Durou's study showed it causes the most error values, but still less different from any other methods. No matter which methods of SFS will be used, it is necessary to input two important data types -image data and light source data-. In this work, solar will be used as light source data for outdoor photographed image.

2.1.2 Solar Position

Natural phenomenon such as seasons caused by when the earth travels around the moon or tide caused by gravity between the earth and the moon unavoidably makes humans interested in studying astronomy. An advantage of such study is an ability to determine the position where stars or any other stuff in the universe are located. Previously, to navigate cruises, the main transportation at the time relied on calculating the position of the stars. More importantly, such a useful kind of astronomy has been performing continuously.

In calculating solar position, there have been a number of studies to support this until now. Many more methods for estimating solar position were presented: Michalsky (1988) suggested method that can estimate solar position between year 1950-2050 with maximum error equal 0.01 degrees, Blanco et al (2001) showeded method that can estimate solar position between year 1995 - 2015 with maximum error equal 0.008 degrees, Reda and Andreas (2004) presented method called Solar Position Algorithm (SPA) can estimate solar position between year 2000 BC.- 6000 with maximum error equal 0.0003 degrees, Grena (2008) presented method which was easier than Reda and Andreas method but performance was lower. Grena method can estimate solar position between years 2003 – 2022 with maximum error equal 0.0027 degrees.

Nowadays, SPA is the most accurate method for finding solar position and provides long using period; as a result, SPA is chosen as method for calculating solar position on this work with the reason of its long using period rather than the former because SFS methods need to be accurate up to 0.0003 degrees only.

2.2 Design concept

To develop images into 3D surface, various tools will be adopted on this study, are discussed as following:

2.2.1 Imaging

In real image, background, due to its different color shade may result in an inaccuracy for SFS calculation's performance; therefore, it is necessary to paint the same color shade as its background and for less CPU time image, it must be resized to 350 x 350 pixels. Besides, in this work, same materials within all images are required in order to adjust them toward the same directions before moving to next two steps called Cloud of point. Software used in this work names GIMP, is a high performance imaging freeware.

2.2.2 Gray scale

Before calculating SFS, this process needs to prepare all images' color in gray scale. To convert them into gray scale is not rather complicated; then, gray scale box will be explained in the upcoming topic 3.1.6. Otherwise, it is important for researcher to settle some supplementary processes into this step-such as to calculate maximum color shade value and to change image axis- by developing new tools with language software. The developed software program code is written by using Visual Basic(VB), will be explained in topic 3.2.2.

2.2.3 Solar position

This step aims to calculate SPA by utilizing Reda and Andreas (2004) approach and the result has shown as Zenith angle and Azimuth angle, the meaning of both will be explained in topic 3.1.3.

2.2.4 Transform

Both inconstant direction of taken photos and images rotated from imaging process as discussed on topic 2.2.1 have totally an effect on solar direction. It needs to be transformed to correct direction. This step will convert solar direction into (x,y,z) type, on the basis of Cartesian coordinate system.

2.2.5 SFS

This step is SFS calculation for finding height values in each pixel and reforms them into Cloud of point process. The method of calculation used in this step names Tsi-Shah which its detail will be explained in topic 3.1.2.

2.2.6 Generate Surface

This step concerns with an improvement in Cloud of point and develops it into 3D surface by using software called Computer Aided Three-dimensional Interactive Application (CATIA). CATIA will be explained in topic 3.2.3.

CHAPTER III
THEORETICAL BACKGROUND AND TOOLS

3.1 Theoretical Background

3.1.1 Background of Shape Form Shading

3.1.1.1 Reflectance Model: SFS calculation, in general, specify surface of material as Lambertance surface, knobbed surface in microstructure level, when the incident light hits material surface, reflected light is ideally scattered relevant to reflected light model, Lambert's cosine law, presented by Lambert (1760).

$$I_L = L\rho\cos\theta \tag{1}$$

I_L is radiant intensity (lambert brightness) , L is radiance , ρ is albedo almost assume as 1 , θ is an angle between direction of incident light on to surface normal and the direction of observation.

3.1.1.2 Unit surface normal And Light

Unit surface normal: N is 1 vector that has a 90-degree angle against material surface and unit surface normal N will be equal to

$$N = \frac{1}{\sqrt{1+p^2+q^2}}(-p,-q,1) \tag{2}$$

In calculating SFS, the position of light source or the direction of light is mostly defined or estimated. For example, taking a photograph with flash light, the direction of light seems to be the direction of a camera that causes $N \bullet L = 1$. Otherwise, in case of unknown direction of light, it, in particular, will be estimated.

3.1.1.3 Reflectance Map (This topic uses base information from Horn&Sjoberg(1978) and Nicodemus et Al (1977)): According to reflectance Map ,R (p, q) p and q are substitute for the slant as Gradient of pixel in the figure by which p represents a distance on Z axis against a distance on X axis; whereas, q represents a distance on Z axis against a distance on Y axis. In Cartesian coordinate system, X,Y and Z are defined as axis. When we give $z = f(x, y)$ by $p = \frac{\partial f(x, y)}{\partial x}$ and $q = \frac{\partial f(x, y)}{\partial y}$ if p = 0, that means z is independent of x; at the same time, q = 0, that means z is independent of y. Additionally, if p, q are equal to 0, it means there is no change on Z axis from that point.

R(p,q), Reflectance Map can be calculated by a number types of unknown, for example depth or height f(x,y) ,gradient(p,q) ,Slant(Sl) and Tilt (Tl) that will be explained in 3.1.2.2. From Lambert's cosine law in equation (2) will be

$$I_L = R(p,q) = \rho N \bullet L \qquad (3)$$

$$R(p,q) = L\rho \frac{\cos Sl_s - p\cos Tl_s \sin Sl_s - q\sin Tl_s \sin Sl_s}{\sqrt{1 + p^2 + q^2}} + \varepsilon \qquad (4)$$

Or

$$R(p,q) = L\rho \frac{p\cos Tl_s - q\cos\beta - \cos Sl_s}{\sqrt{1 + p^2 + q^2}} + \varepsilon \qquad (5)$$

Tl_s or Tilt of light is an angle distance between direction of light and X axis.

β is an angle distance between direction of light and Y axis.

Sl_s or Slant of light is an angle distance between direction of light and Z axis.

ε is brightness error.

From equation(5), in case of being calculated without consideration of Albedo, if Albedo remains its value as 1, and any error values are supposed to be nothing, the equation(12) will be changed into Simple SFS by A.Paul and R.Cooper(1994) as follows.

$$R(p,q) = L\frac{p\cos Tl_s - q\cos\beta - \cos Sl_s}{\sqrt{1+p^2+q^2}} \qquad (6)$$

3.1.1.4 Image irradiance equation: Images in Gray scale system have 256 color levels. Colors level will be used as an Irradiance, E(x,y). To convert colors scale level into Gray scale level, then Gray scale level in pixel (x, y) = E(x,y) which all pixels level of E(x,y) start from 0 to 1. This means E(x,y) needs to be normalized. E(x,y), when compared with Reflectance Map from 3.1.1.1, called image irradiance equation, will provide image irradiance equation, main equation in calculating SFS as follows.

$$E(x,y) = R(p,q) \qquad (7)$$

3.1.2 Shape form shading Tsai-Shah's linearization method with normalization. (This topic uses base information from Tsi & Shah (1994), Durou et Al (2007) and Shen&Yang (2005).)

Among a large number of SFS's algolithms, a selected Tsai-Shah algolithm is the most convenient to be applied to this work for reasons of non-required boundary condition, an easy format to write commanding code as well as a high performance by processing with computer.

3.1.2.1 First step is to alter the colour shade of figure into grey scale levels on each pixle which x,y point is valued as shade (x,y). The procedure will be mentioned in topic 3.1.6. The highest grey scale levels of all pixles is called as Maxshade.

3.1.2.2 Second step is to execute the direction of light before moving towards the process of calculation. The process is divided into 2 types as follows:

- The direction of light is in the form of (x, y, z)

If the direction of light on X axis , $x_s \neq 0$; therefore,

$$p_s = x_s / z_s \tag{8}$$

If the direction of light on X axis, $x_s = 0$; therefore,

$$p_s = \frac{0.001}{z_s} \tag{9}$$

If the direction of light on Y axis , $y_s \neq 0$; therefore,

$$q_s = y_s / z_s \tag{10}$$

If the direction of light on Y axis , $y_s = 0$; therefore,

$$q_s = \frac{0.001}{z_s} \tag{11}$$

- The direction of light is in the form of Tilt(Tl_s) and Slant(Sl_s)

$$q_s = \sin(Tl_s) \times \tan(Sl_s) \tag{12}$$

$$p_s = \cos(Tl_s) \times \tan(Sl_s) \tag{13}$$

3.1.2.3 Third step is to value all pixels of height function z(x,y)g at 0 and standard deviation function (Sn(x,y)) at 1. For initially calculating in a circle, Wn =0.01 is a standard deviation, and the remaining value can be determined as the small number less than 1.

3.1.2.4 in calculating (k), the higher number of times is set, the smoother value accordingly appears, but the longer calcalating time is taken. The most appropriate number of times suggested by J.D.Durou et al (2008) is more likely to be 6 times.

3.1.2.5 Fifth step is to calculate in circle for the first time an estimated q(x,y) and p(x,y) on the point at x = 0 : p = 0 and y = 0 : q = 0 in which p and q symbolize gradient. In case of $x \neq 0$: accordingly $p = \frac{z(x, y) - z(x-1, y)}{s}$ and in case of $y \neq 0$: accordingly $q = \frac{z(x, y) - z(x-1, y)}{s}$. Note that s represents distance between each point which Tsi-Shah quantified s to be equal to 1; then,

$$p = z(x+1, y) - z(x, y) : \text{กรณีที่ } x \neq 0 \tag{14}$$

$$q = z(x, y+1) - z(x, y) : \text{กรณีที่ } y \neq 0 \tag{15}$$

$$pq = 1.0 + p^2 + q^2 \tag{16}$$

$$pq_s = 1.0 + p_s^2 + q_s^2 \tag{17}$$

$$E_p(x, y) = \frac{shade(x, y)}{Maxshade} \tag{18}$$

Maxshade value obtained from the first step was taken to divide rather than 255 due to Abedo was already assumed to be equal 1.

$$R(x, y) = \frac{1 + p \times p_s + q \times q_s}{\sqrt{pq} \times \sqrt{pq_s}} \tag{19}$$

From equation (19), if $R(x, y)$ values less than 0, it will be changed to $R(x, y) = 0$.

$$dfz = -1 \times \frac{p_s + q_s}{\sqrt{pq} \times \sqrt{pq_s}} - \frac{p + q \times (1.0 + p \times p_s + q \times q_s)}{\sqrt{pq^3} \times \sqrt{pq_s}} \tag{20}$$

$$k_d = \frac{Sn(x,y) \times dfz}{Wn + Sn(x,y) \times dfz^2} \tag{21}$$

$$Sn^{next\_k}(x,y) = (1 - k_d \times dfz) \times Sn(x,y) \tag{22}$$

$$z^{next\_k}(x,y) = z(x,y) + k_d \times (R(x,y) - E_p(x,y)) \tag{23}$$

All calculating processes within the fifth step from the beginning to the end at equation(23) will repeatedly handle in the form of circle till completing all pixels of the figure, starting from x = 0 to x = the width of figure - 1 and from y = 0 to y = the length of figure - 1 As far as the series of calculations has been done, that means the first circle was rounded off.

3.1.2.6 This step, in fact, is to repeat the previous step by starting to perform the second circle by setting:

$Sn^{next}(x,y) = Sn(x,y)$ of the next series of calculation

$z^{next}(x,y) = z(x,y)$ of the next series of calculation

Calculation remains processing until reaching the expected number of k Since the fifth and sixth step have to be repeated several times, to provide much more understanding on the process, an explaination of both steps will specially be presented by determining k = 6, as shown in flowchart 3.1 which its detail will discuss in topic 3.2.1.

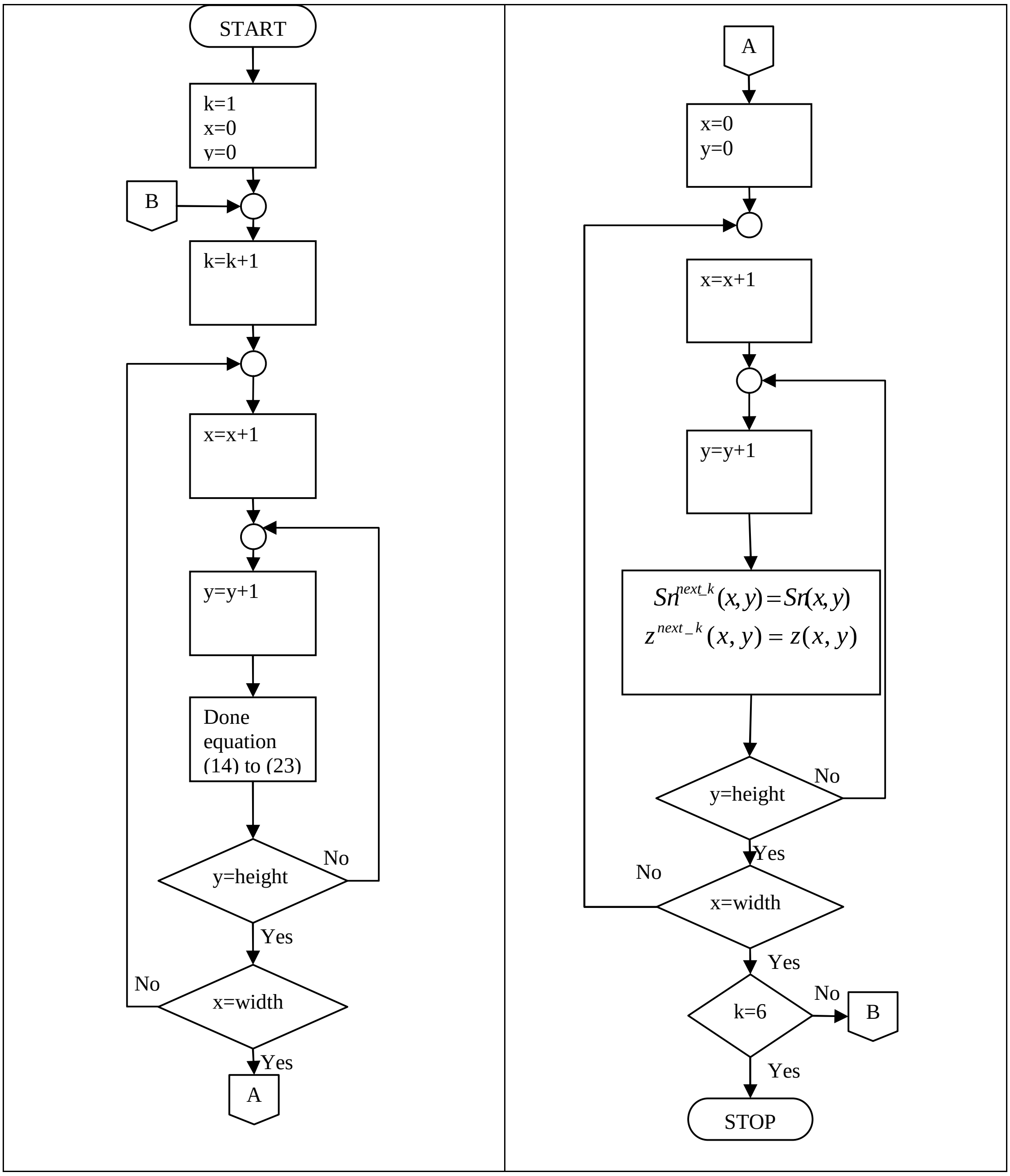

Figure 3.1 Flowchart presented the procedure of Tsi - Shah SFS

3.1.2.7 Seventh step concentrates on normalization as Shen&Yang (2005) pointe out process of normalization as follows:

- Compare each acquired value of $z(x, y)$ from the last set of calculation in order to find $z(\min), z(\max)$

- Approve minimum and maximun values of material, $o(\min), o(\max)$

- Start calculating normalization each point by using the equation below:

$$z^{norm}(x,y)=\left[\frac{z\ (x,y)-z(\min)}{z(\max)-z(\min)}\times o(\max)-o(\min)\right]+o(\min) \qquad (24)$$

After entirely completing the calculation, then $z(x,y)=z^{norm}(x,y)$

3.1.3 Coordinate Systems

In this work, it is important for every coordinate system relevant to SFS equation, Celestial object system, or VB, language software to be altogether connected and applied. In order to provide a better understanding, each of them is detailed as below.

3.1.3.1 Cartesian coordinate (This topic uses base information from Richard (2000)): The system is based on 3 identified positions of 3 axes which are X Y Z. Each axis provides 90 degree angle, and intersects at a original point. More importantly, X Y Z are quantified as **(**x, y, z). Note that to standardize this work, the direction of Cartesian coordinate system is totally considered to be on the right-handed side according to figure 3.2.

3.1.3.2 Stereographic Coordinate (This topic uses base information from Shen&Yang (2005)): The process is in the form of circle with function of (Sl, Tl, l) If Sl (Slant) is an angle between the direction of material against Z axis, Tl (Tilt) is an angle of the direction of material on to XY plane counterclockwise against X axis, and l represents the size of vector shown by figure 3.3. Compared to Cartesian coordinate system with right-handed regulation, it can be formed to metric as follows:

$$\begin{vmatrix} x \\ y \\ z \end{vmatrix} = \begin{vmatrix} l \sin\gamma \cos\tau \\ l \sin\gamma \sin\tau \\ l \cos\gamma \end{vmatrix} \tag{25}$$

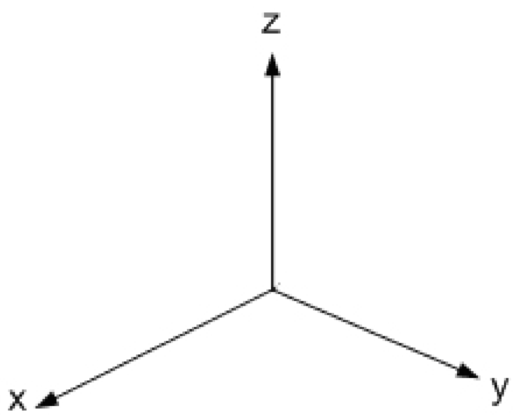

Figure 3.2 Cartesian coordinate

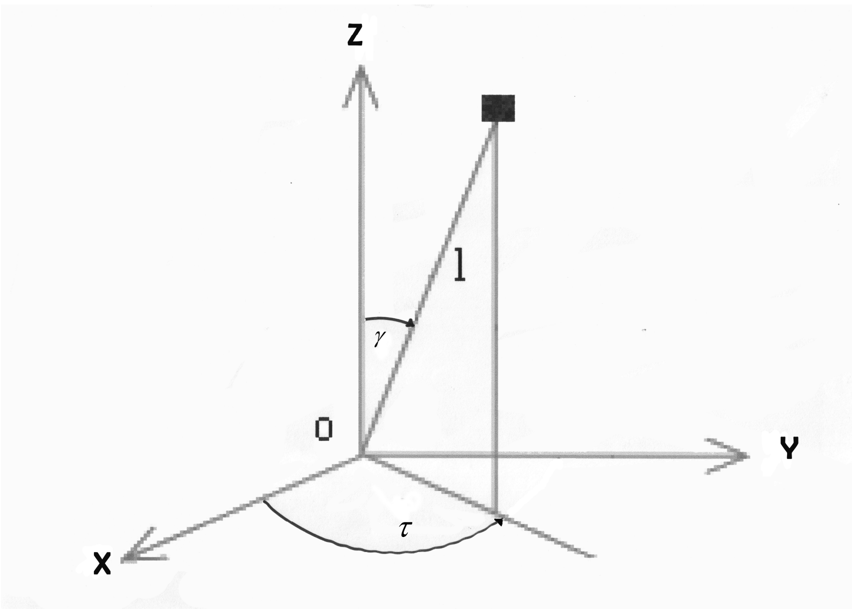

Figure 3.3 Stereographic Coordinate

3.1.3.3 Horizon system of Coordinate (This topic uses base information from Roj (1974) and Roderick (1992)): Its principle is similar to that of Stereographic Coordinate System. However, there are obviously just a few distinctions between these two systems. Horizon Coordinate System refers to the Northern axis and Zenith axis which is Z axis in the positive direction in Cartesian coordinate system. In Horizon Coordinate System, the northern direction of observer is positively X axis and the western direction of observer is positively Y axis. This system can be utilized for finding the position of Celestial object where the position of observer is situated at its center and seemingly smooth on observer's view. Moreover, a celestial object and an ending point of Zenith axis seemingly appears as a sphere no matter how far such object is located. On the other hand, celestial object within horizon and an ending point of Nadir also appears the same figure as that beyond horizon, but observer cannot view it. Horizon system of Coordinate notably mentions the celestial object to be seemingly centered by an observer to be a center and conversely the position of observer to be seemingly centered by celestial object. The overall characteristic of Horizon system of Coordinate is briefly drafted by figure3.4, the meaning of Zenith, Nadir and celestial object will be explained in topic3.1.14.

3.1.3.4 Celestial equator system of Coordinate (This topic uses base information from Roj (1974) and Roderick (1992)): is not only similar to Horizon system of Coordinate used for positioning celestial object according to figure3.5 but also relevant to Stereographic Coordinate system; however, its center or an intersection between axes of sphere is pointed at the center of earth. To specify the position will be handled on the basis of lengthening latitude and longitude towards celestial sphere called declination for latitude and Right Ascension for longitude. Definition of Astronomy vocabularies will provide in topic 3.1.4.

3.1.3.5 Coordinate System of Visual Basic (VB) (This topic uses base information from Bancha (2009) and Sittichoke (2007)): In graphically proceeding VB in the form of 2D, intersection between X and Y axis, $(x, y) = (0, 0)$ appears on the top-left corner of figure. Otherwise, X axis directs to the right-handed side of observer opposition to Y axis which heads to the bottom of figure. As a result, according to Cartesian coordinate, right-handed rule, if VB proceeds in 3D, Z axis will head away from observer presented by figure 3.6.

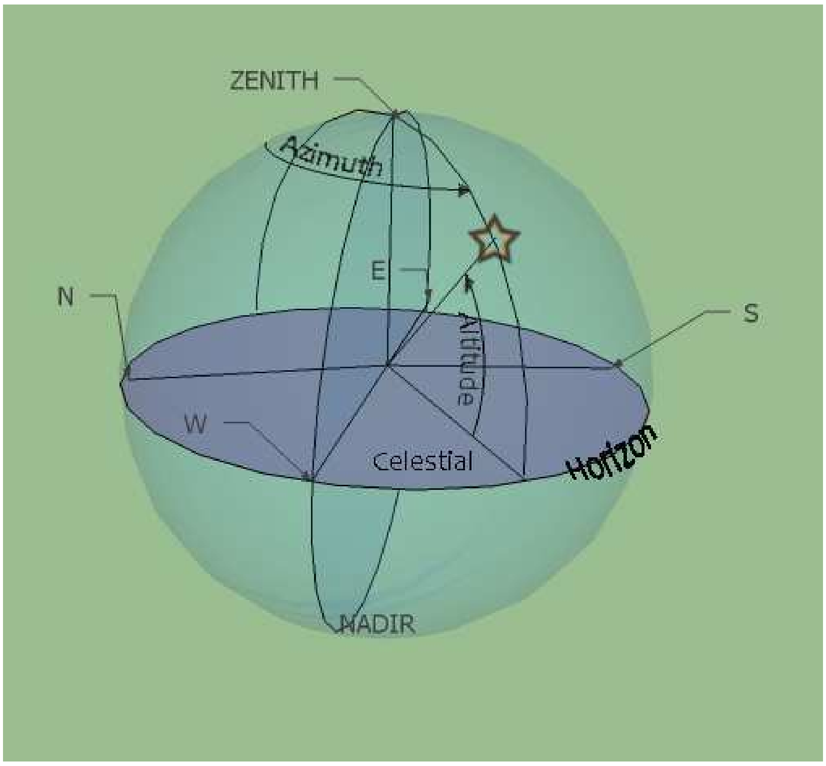

Figure 3.4 Horizon system of Coordinate

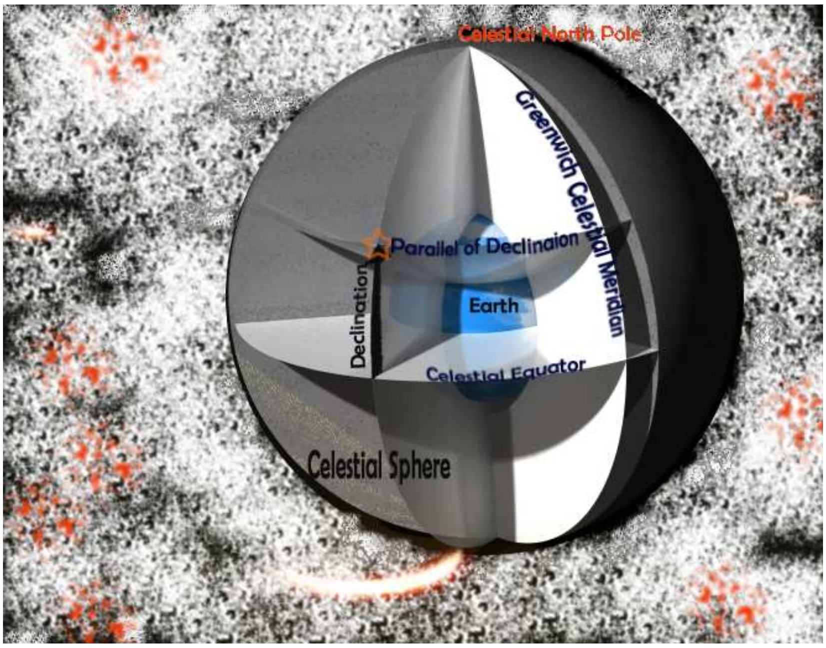

Figure 3.5 Celestial equator system of Coordinate

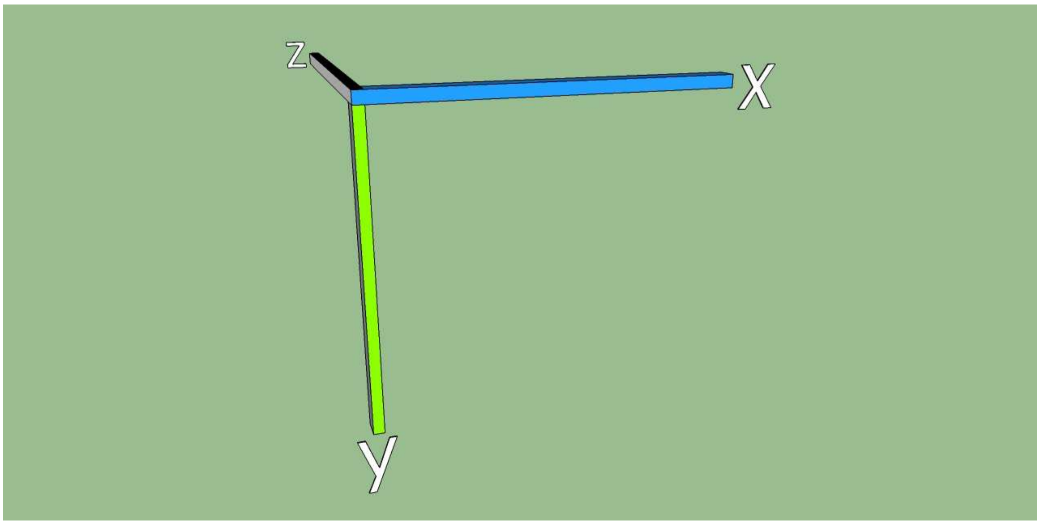

Figure 3.6 VB Coordinate System compared to Cartesian coordinate system

3.1.4 Astronomy Vocabulary and Astronomy knowledge base (This topic uses base information from Roj (1974), Roderick (1992) and Reda &Andreas (2004))

Since in terms of SPA calculation, a number of astronomy vocabularies including some preliminary data related to equation need to be realized as follows:

3.1.4.1 Astronomy Vocabulary

Latitude: generally means geographic latitude presented by figure 3.7, on the basis of an assumption that the earth shapes as a sphere opposed to a real fact that the earth is ellipsoid which its longest diameter, with the same length of radius is located at Equatorial plane. More importantly, Latitude is an angular distance from the center of earth to positions on the earth's surface and equatorial plane. If such position rather takes place onto the North Pole, such angel will be valued positively contrary to the South Pole where an angle will be valued negatively within the range between -90 to 90 degrees.

Longitude: is also geographic if compared to Stereographic Coordinate system, and angel θ starts from 0 degree at Greenwich towards the East, the angle will be positive and conversely towards the West the angle will be negative within the range between -180 to 80 degrees.

Geocentric: The system of substituting the shape of the Earth as oval which its longest radius is located at

Equatorial plane

Meridians: is the line on a surface of the Earth passing the point of parallel longitude angle.

Zenith: is the point on celestial sphere above observer's head, referred to Horizon system of Coordinate, the line starts at the centre of the Earth and passes an observer into the atmosphere, it will meet Zenith point presented by 3.8

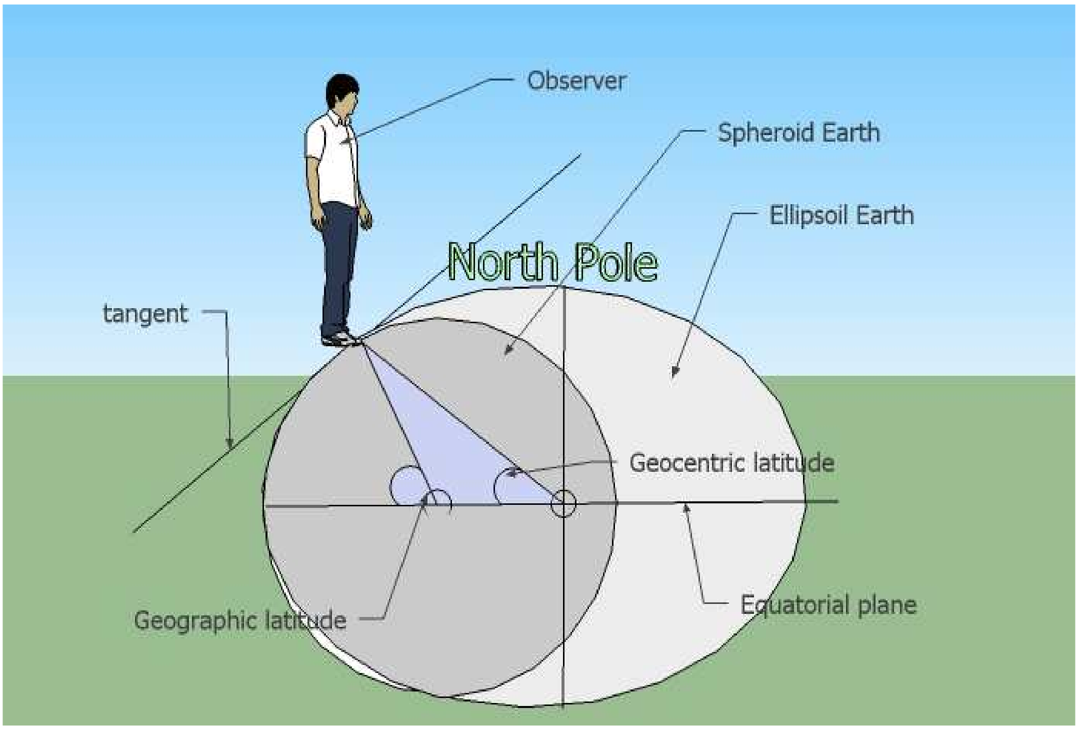

Figure 3.7 A comparison between Geocentric and Geographic

Nadir: is the point on celestial sphere under observer's foot referred to Horizon system of Coordinate, when the line starts at the centre of the Earth and passes an observer into the atmosphere, it will meet Nadir point. Nadir point, however, will not be entirely mentioned on this work, but it will only used for basically discussing Celestial sphere. This is due to the fact that Nadir is located under horizon where not only is invisible to be viewed by observer but also solar light cannot travel from the Equatorial plane.

Altitude: alternatively names Elevation Angle which is an angular distance for identifying celestial object according to Horizon system of

Coordinate**.** The angel takes place between the direction of celestial object and observer’s plane**,** “h” angel on figure 3.8.

Azimuth: is an angular distance travelling clockwise from the Northern direction of observer downwards Vertical circle of celestial object along the plane of observer, “A” angel figure 3.8.

Zenith Angle: is an angular distance between Zenith axis and celestial object, “Z” angel on figure 3.8.

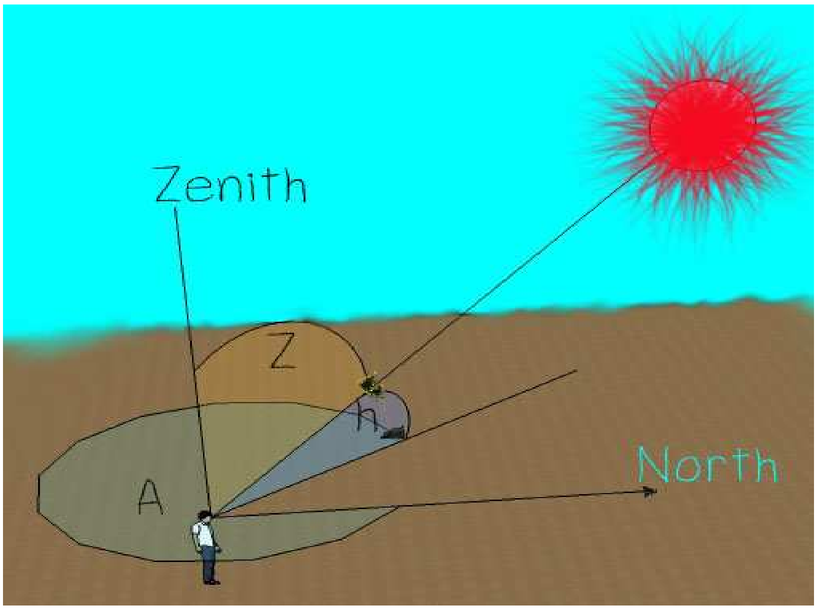

Figure 3.8 An identification of celestial object by based on the position of observer

Celestial sphere: is assumed to be unmeasured size by possessing its diameter on the Earth. More significantly, all celestial materials are supposed to be onto its surface.

Celestial Equator: is caused by extending equator plane of the Earth to Celestial sphere as can be seen in figure 3.5.

Celestial meridians: is to prolong meridians to Celestial sphere in Celestial equator system of Coordinate.

Declination: Like latitude, declination is an angular distance for pointing the position of celestial object. When the angular distance extends from latitude angel on the Earth’s surface to Celestial sphere, starting at Celestial Equator with 0 degree and reaching Celestial North Pole with the highest degree of 90 contrary to Celestial South Pole Declination with the lowest degree of -90 as can be seen in figure 3.5.

Astronomical Units (AU): is an astronomic unit of measurement which 1 unit represents an average distance between the Earth and the Sun equal to 9.463×10^{12} kilometer.

Parallax of the Sun: In spite of an estimated 9.463×10^{12} kilometer distance from the Sun to the Earth, it is not too far to cause two angles at the position of observer and the center of the Earth against the Sun to be different in astronomic calculation. Therefore, Parallax is set to balance such a different size of these two angles. As shown in figure 3.9, noticeably a angle is smaller than b angle.

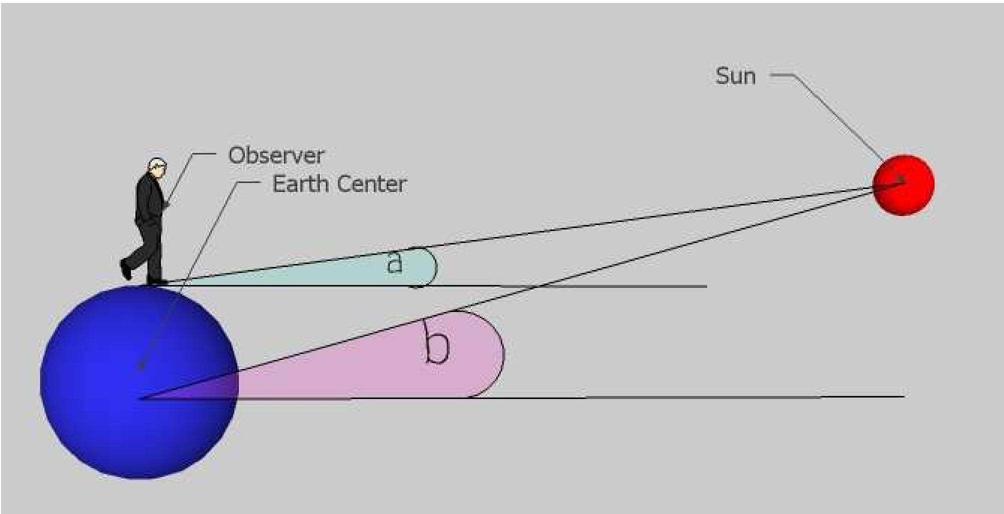

Figure 3.9 An effect of different size of two angle, the center of the Earth and observer, on the Sun

Greenwich Mean Time (GMT): Due to geographically different time, Greenwich Mean Time (GMT) has been formed and entitled by Greenwich city, located at meridian or 0 degree longitude. It is widely used as a standard of communication all over the world, hereby leading to a lot more convenience.

Local mean time (LMT): is the time of origin varying from the location. In Thailand if compared Local mean time (LMT) to the Greenwich Mean Time GMT, the standard time will be GMT+7.

Universal Time (UT): nowadays increasingly becomes to be used rather than GMT. It starts at 0 on the midnight and is counted by unit depending on mean solar day. Nevertheless, if there is a fluctuation of the Earth, its unit will sometimes be called as UT1 rather than UT.

International Atomic Time (TAI): is measured by vibration of cesium 133 in atomic clocks, and System International Second (SI-second) is referred as unit.

Terrestrial Time (TT): is to enable TAI to become an observative time, values at $TT = TAI + 32.184$ against International Atomic Time (TAI).

ΔT : arises form a distinction of TT by UT: $\Delta T = TT - UT$

ΔT has already quantified and is available not only in Astronomical Almanac but also on U.S. Naval Observatory (USNO) Website.

Julian Date: is a timing system used for an astronomic calculation by which the end of a day is terminated at the midday, and is measured on the basis of its initial use of January 1^{st}, 4712 B.C. To evaluate January 1^{st} 1995 at 18.00 o'clock, for example, is equal to 2,449,719.25 that means January 1^{st} 1995 at 18.00 o'clock has already passed by 2,449719.25 days from January 1^{st}, 4712 B.C.

Equinox: is an intersection point between Ecliptic and Celestial Equator according to Celestial equator system of Coordinate and results in equalization between day and night at the happening time and place. Equinox, in general, consists of two intersection points, Autumnal equinox and Vernal equinox approximately taken place on September 23 and March 21 respectively. By the way, Vernal equinox is mostly used as 0 degree of right Ascension presently relevant to Pisces presented by figure 3.10.

Sidereal Time: Owing to a dramatically long distance from the Earth and fixed stars, when compared to the Earth, it is seemingly untraveled, are used as referred point for calculating time of earth orbit. An angel of Sidereal Time is equal to 0 degree at Vernal Equinox, and if moving to the western direction, it will be in the range of 0-360.

Hour Angle: is an angle between celestial meridians of observer and celestial meridians of celestial object. When celestial object directs to the

West, Hour Angle will be in the range of 0-360 degrees or 0-24 hours presented by figure 3.10.

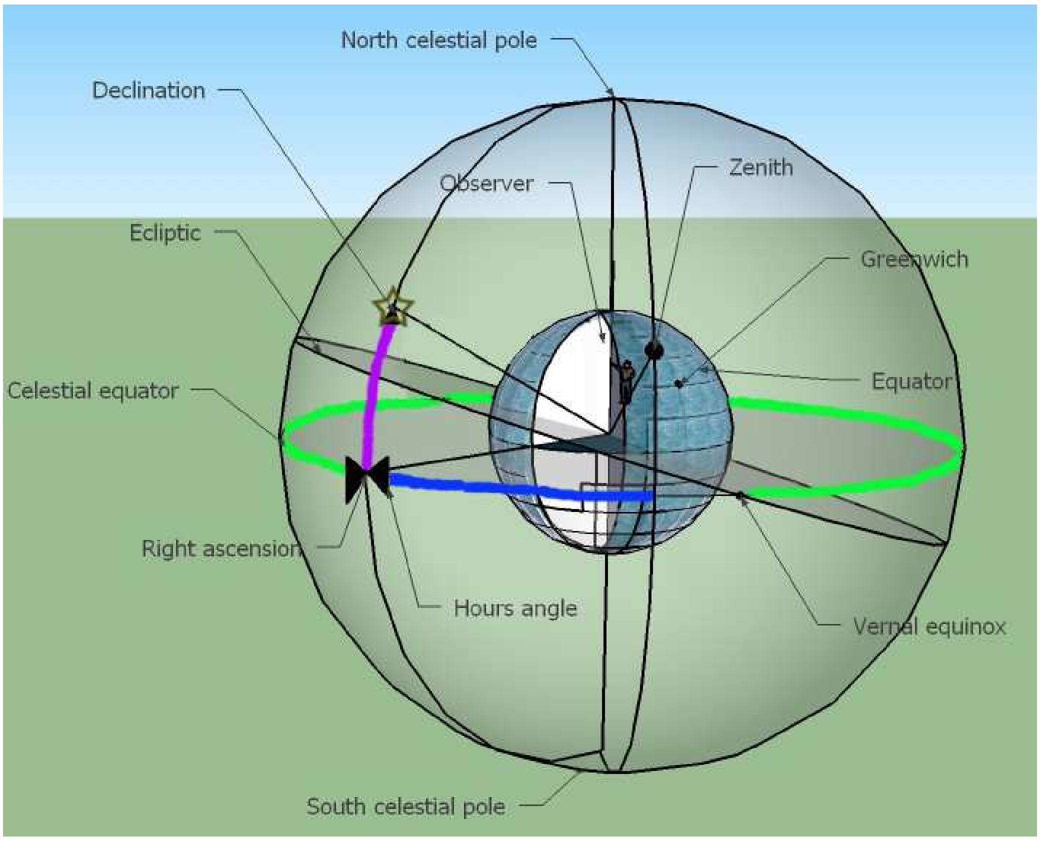

Figure 3.10 Relationship between Right Ascension and Hours angle

Right Ascension: is parallel to longitude, but different in terms of starting point where right ascension arises from Vernal Equinox rather than Greenwich City located in UK; furthermore, when directing to the East opposed to hours angle and Sidereal Time, it falls into the range of 0 to 360 degrees or 0 to 24 hours shown by figure3.10.

3.1.4.2 Astronomy knowledge base

An effect of earth orbit: as we know that the Earth's core is gradually rotating around itself all the time as funnel. In parallel with perpendicular to the Plane of orbit, celestial pole between North and South becomes more strikingly different resulting from which the shape of the Earth is not truly sphere. When affected by the gravity of the moon and the gravity of the Sun, such a funneled earth orbit causes the Earth's core to become changing. A declined angle between Celestial

Equator and Orbit Plane takes place. Additionally, this also causes Equinoxes to move backwards. As far as discussed above, the phenomenon is called as the Nutation presented in figure 3.11.

An effect of eye level: To view horizontal line relies on the eye level of observer. The higher eye level is taken, the lower horizontal line is more likely to be seen. This directly impacts on declination and parallax. However, there are other factors apart from the eye level also affecting this circumstance- funnel shape of the Earth and world radiance.

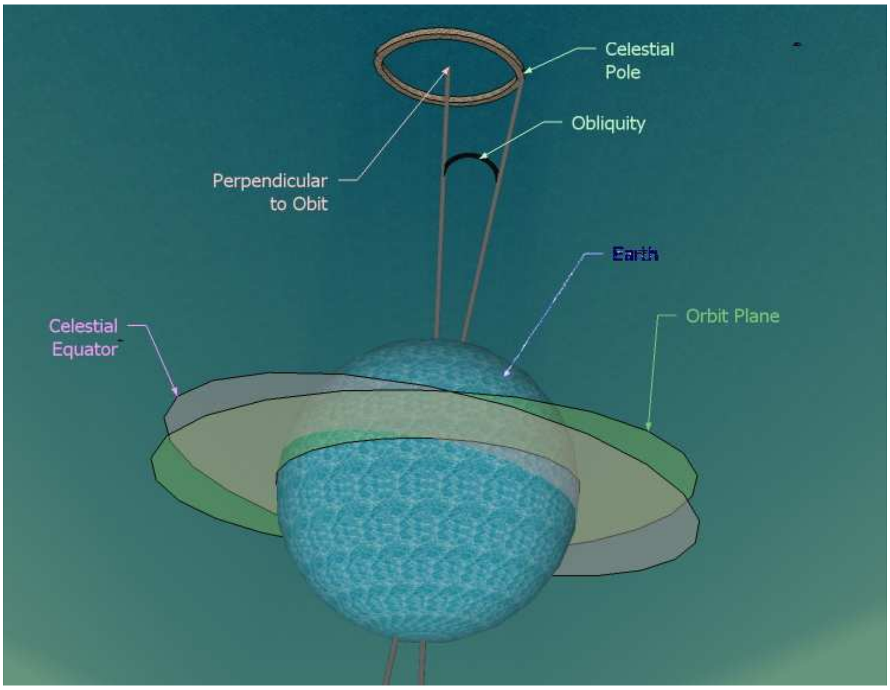

Figure3.11 Presentation of the Earth orbit

An effect of atmosphere: Atmosphere surrounding the Earth impacts on astronomic study in several terms. Lack of ability to view stars at the noon, for instance, is due to scattered light of the Sun caused by atmosphere around the Earth. In terms of calculating celestial object, the most significant factor is Refraction of Light due to density of atmosphere. Refraction, in general, causes observer to view celestial object at higher position than its real position. This also means the Zenith angle becomes smaller its real angle. Nonetheless, there is no impact of refraction on celestial material located at the Zenith axis or over observer’s head because such refraction varies from atmosphere where always becomes changing. It is important for conditions of atmosphere- air pressure and temperature to be taken into account in calculating the position of celestial object.

3.1.5 SPA, Solar Position Algorithm (This topic uses base information from Reda & Andreas(2004))

SPA developed by Ibrahim Reda and Afshin Andreas is a method of finding the position of the Sun. It has been entitles as the most effective method and possesses a wide range of using period. SPA was chosen to adopt into this work for a reason of the latter, not the former since this work does not require an up-to-0.0003 degree accuracy of light direction. Note that less than 5 degrees will not have an influence on the calculation.

3.1.5.1 Methodology for Covert Gregorian Times to Julian Times:

Julian Day: $JD = Int(365.25 \times (Y + 4716)) + Int(30.6001 \times (M + 1)) + D + B - 1524.5$ (26)

Julian Ephemeris Day: $JDE = JD + \dfrac{\Delta T}{86400}$ (27)

Julian Century: $JC = \dfrac{JD - 2451545}{36525}$ (28)

Julian Ephemeris Century: $JCE = \dfrac{JDE - 2451545}{362525}$ (29)

Julian Ephemeris Millennium: $JME = \dfrac{JCE}{10}$ (30)

3.1.5.2 Methodology for find Earth heliocentric:

Longitude (degrees):

$$L = \frac{(\mathrm{L0} + \mathrm{JME} \times (\mathrm{L1} + \mathrm{JME} \times (\mathrm{L2} + \mathrm{JME} \times (\mathrm{L3} + \mathrm{JME} \times (\mathrm{L4} + \mathrm{JME} \times \mathrm{L5})))))\times 180}{10000000\pi} \quad (31)$$

Where

$$Lj = \sum_{j=0}^{n} Lji \tag{32}$$

$$Lji = Ai \times \cos(Bi + Ci \times JME) \tag{33}$$

j = the number of term L , 0 to 5

i = the sequence of rows on each table, according to table A1.1-1.6 in Appendix A

n = the total number of rows on each table, according to table 1.1-1.6 in Appendix A

$Ai, Bi, AndCi$ = the value of A, B,C on row i , according to table A1.1 –1.6 in Appendix A

Latitude (degrees): $La = \dfrac{(\mathrm{La0} + \mathrm{La1} \times \mathrm{JME}) \times 180}{10000000\pi}$ (34)

Where

$$Laj = \sum_{j=0}^{n} Laji \tag{35}$$

$$Laji = Ai \times \cos(Bi + Ci \times JME) \tag{36}$$

j = the number of La term, 0 และ1

i = the sequence of rows on each table, according to A2.1-2.2 in Appendix A

n = the total number of rows on each table, according to A2.1-2.2 in Appendix A

$Ai, Bi, AndCi$ = the value of A,B,C on row i , according to A2.1-2.2 in Appendix A

Earth radius vector (AU):

$$R = \frac{(\mathrm{R0} + \mathrm{JME} \times (\mathrm{R1} + \mathrm{JME} \times (\mathrm{R2} + \mathrm{JME} \times (\mathrm{R3} + \mathrm{JME} \times \mathrm{R4}))))}{10000000} \quad (37)$$

Where

$$Rj = \sum_{j=0}^{n} Rji \quad (38)$$

$$Rji = Ai \times \cos(Bi + Ci \times JME) \quad (39)$$

j = the number of R term, 0 ถึง 4

i = the sequence of rows on each table, according A3.1-3.5 in Appendix A

n = the total number of rows on each table, according to A3.1-3.5 in Appendix A

$Ai, Bi, AndCi$ = the value of A,B,C on row i, according to A3.1-3.5 in Appendix A

3.1.5.3 Methodology for find Sun Position in Geocentric System:

Geocentric longitude: $\Theta = L + 180$ (40)

Geocentric latitude: $\beta = -La$ (41)

3.1.5.4 Methodology for find nutation in longitude และ obliquity:

nutation in longitude (degrees): $\Delta\psi = \frac{\sum_{i=0}^{n} \Delta\psi_i}{36000000}$ (42)

nutation in obliquity(degrees): $\Delta\varepsilon = \dfrac{\sum_{i=0}^{n} \Delta\varepsilon_i}{36000000}$ (43)

Where

$$\Delta\psi_i = (a_i + b_i \times JCE) \times \sin(\sum_{j=0}^{4} X_j \times Y_{i,j}) \tag{44}$$

$$\Delta\varepsilon_i = (c_i + d_i \times JCE) \times \sin(\sum_{j=0}^{4} X_j \times Y_{i,j}) \tag{45}$$

$$X_0 = 297.85036 + 445267.111480 \times JCE - 0.0019142 \times JCE^2 + \frac{JCE^3}{189474} \tag{46}$$

$$X_1 = 357.52772 + 35999.050340 \times JCE - 0.0001603 \times JCE^2 - \frac{JCE^3}{300000} \tag{47}$$

$$X_2 = 134.96298 + 477198.867398 \times JCE + 0.0086972 \times JCE^2 + \frac{JCE^3}{56250} \tag{48}$$

$$X_3 = 93.27191 + 483202.017538 \times JCE - 0.0036825 \times JCE^2 + \frac{JCE^3}{327270} \tag{49}$$

$$X_4 = 125.04452 - 1934.136261 \times JCE + 0.0020708 \times JCE^2 + \frac{JCE^3}{450000} \tag{50}$$

$a_i, b_i, c_i, and\ d_i$ = the value of $a, b, c, and\ d$ on row i, according to table A 4.1 in Appendix A

$Y_{i,j}$ = The value of Y on row i and column j according to table A 4.2 in Appendix A

i = 0 to 4

j = 0 to 62

n = 63

3.1.5.5 Methodology for find true obliquity of ecliptic:

True obliquity of ecliptic (degrees): $\varepsilon = \frac{\varepsilon_0}{3600} + \Delta\varepsilon$ (51)

Where

$$\varepsilon_0 = 84381.448 + \mathrm{U} \times (\text{-}4680.96 + \mathrm{U} \times (\text{-}1.55 + \mathrm{U} \times (1999.25 + \mathrm{U} \times (\text{-}51.38 + \mathrm{U} \times (\text{-}249.67 + \mathrm{U} \times (\text{-}39.05 + \mathrm{U} \times (7.12 + \mathrm{U} \times (27.87 + \mathrm{U} \times (5.79 + \mathrm{U} \times 2.45))))))))) \quad (52)$$

$$U = \frac{JME}{10} \quad (53)$$

3.1.5.6 Methodology for find aberration correction:

Aberration correction (degrees): $\Delta\tau = \frac{20.4898}{3600 \times R}$ (54)

3.1.5.7 Methodology for find apparent sun longitude:

Apparent sun longitude (degrees): $\lambda = \Theta + \Delta\psi + \Delta\tau$ (55)

3.1.5.8 Methodology for find local hour angle:

Local hour angle (degrees): $H = v + \sigma - \alpha$ (56)

Where

σ is observer or object geographical longitude

$$\delta = \frac{Arc\sin(\sin\beta \times \cos\varepsilon + \cos\beta \times \sin\varepsilon \times \sin\lambda) \times 180}{\pi} \quad (57)$$

$$\alpha = \frac{Arc\tan 2(\sin\lambda \times \cos\varepsilon - \tan\beta \times \sin\varepsilon, \cos\lambda) \times 180}{\pi} \quad (58)$$

$$v = v_0 + \Delta\psi \times \cos(\varepsilon) \quad (59)$$

$$v_0 = 280.46061837 + 360.98564736629 \times (JD - 2451545) + 0.000387933 \times JC^2 - \frac{JC^3}{38710000} \tag{60}$$

3.1.5.9 Methodology for finding topoccentric sun right ascension, topocentric sun declination and topocentric local hour angle: is to fix the number of solar position when viewed from the surface of the Earth.

topoccentric sun right ascension (degrees): $\alpha^{'} = \alpha + \Delta\alpha$ (61)

topocentric sun declination (degrees):

$$\delta^{'} = \frac{(Arc\tan 2((\sin\delta - y \times \sin\xi) \times \cos\Delta\alpha, \cos\delta - y \times \sin\xi \times \cos H)) \times 180}{\pi} \tag{62}$$

topocentric local hour angle (degrees): $H^{'} = H - \Delta\alpha$ (63)

Where

$$\Delta\alpha = \frac{(Arc\tan 2(-x \times \sin\xi \times \sin H, \cos\delta - x \times \sin\xi \times \cos H) \times 180}{\pi} \tag{64}$$

$$\xi = \frac{8.794}{3699 \times R} \tag{65}$$

$$x = \cos u + \frac{E}{6378140} \times \cos\varphi \tag{66}$$

$$y = 0.99664719 \times \sin u + \frac{E}{6378140} \times \sin\varphi \tag{67}$$

If you know distance from center of earth (ρ), then you can find x, y by

$$x = \rho \times \cos\varphi \tag{68}$$

$$y = \rho \times \sin\varphi \tag{69}$$

$$u = Arc\tan(0.99664719 \times \tan\varphi) \quad (70)$$

E is an observer or an object elevation

φ is an observer or an object geographical latitude

3.1.5.10 Methodology for finding zenith angle:

Zenith angle (degree): $\theta = 90 - e$ (71)

Where

$$e = e_0 + \Delta e \quad (72)$$

$$\Delta e = \frac{P}{1010} \times \frac{283}{273 \times T} \times \frac{1.02}{60 \times \tan(e_0 + \frac{10.3}{e_0 + 5.11})} \quad (73)$$

$$e_0 = \frac{(Arc\sin(\sin\varphi \times \sin\delta^{'} + \cos\varphi \times \cos\delta^{'} \cos H^{'}) \times 180}{\pi} \quad (74)$$

3.1.5.11 Methodology for finding topocentric azimuth angle:

topocentric azimuth angle (degree) : $\Phi = \Gamma + 180$ (75)

Where

$$\Gamma = \frac{(Arc\tan 2(\sin H^{'}, \cos H^{'} \times \sin\varphi - \tan\delta^{'} \times \cos\varphi) \times 180}{\pi} \quad (76)$$

Note

1. Equation (32), (41), (57), (59), (61), (75) and (76) need to constrain the degree from 0 to 360 degrees.

2 Equation (59), (63), (65) and (76) use the form of $Arc\tan 2(A,B)$, matching function by .net framework which means to calculate ArcTan(A/B), and the result must be an angle in a correct quadrant from 4 quadrants and values between π to $-\pi$. Otherwise, to perform the calculation has to consider the fact that term B is not equal to 0.

3.1.6 Transformation of Coordinates (This topic uses base information from Richard (2000))

Based on Cartesian coordinate system, X, Y, Z axis if change angular distance, will become $X^{'}, Y^{'}, Z^{'}$ with ($x^{'}, y^{'}, z^{'}$) values. In order to reach the most convenient calculation, axis orbit will be altered in to matrix type.

$$\begin{vmatrix} x^{'} \\ y^{'} \\ z^{'} \end{vmatrix} = |Aij| \bullet \begin{vmatrix} x \\ y \\ z \end{vmatrix} \tag{77}$$

$|Aij|$ depends on an orbit of X ,Y, Z axis and is calculated on the basis of counterclockwise rotation presented by figure 3.12. Calculating process is shown below:

- Calculation of X obit

$$|Aij| = \begin{vmatrix} 1 & 0 & 0 \\ 0 & \cos x^{\circ} & \sin x^{\circ} \\ 0 & -\sin x^{\circ} & \cos x^{\circ} \end{vmatrix} \tag{78}$$

if x° is an angle of X orbit

- Calculation of Y obit

$$|Aij| = \begin{vmatrix} \cos y^{\circ} & 0 & -\sin y^{\circ} \\ 0 & 1 & 0 \\ \sin y^{\circ} & 0 & \cos y^{\circ} \end{vmatrix} \tag{79}$$

If y° is an angle of Y orbit

- Calculation of Z obit

$$|Aij| = \begin{vmatrix} \cos z^\circ & \sin z^\circ & 0 \\ -\sin z^\circ & \cos z^\circ & 0 \\ 0 & 0 & 1 \end{vmatrix} \quad (80)$$

If z° is an angle of Z obit

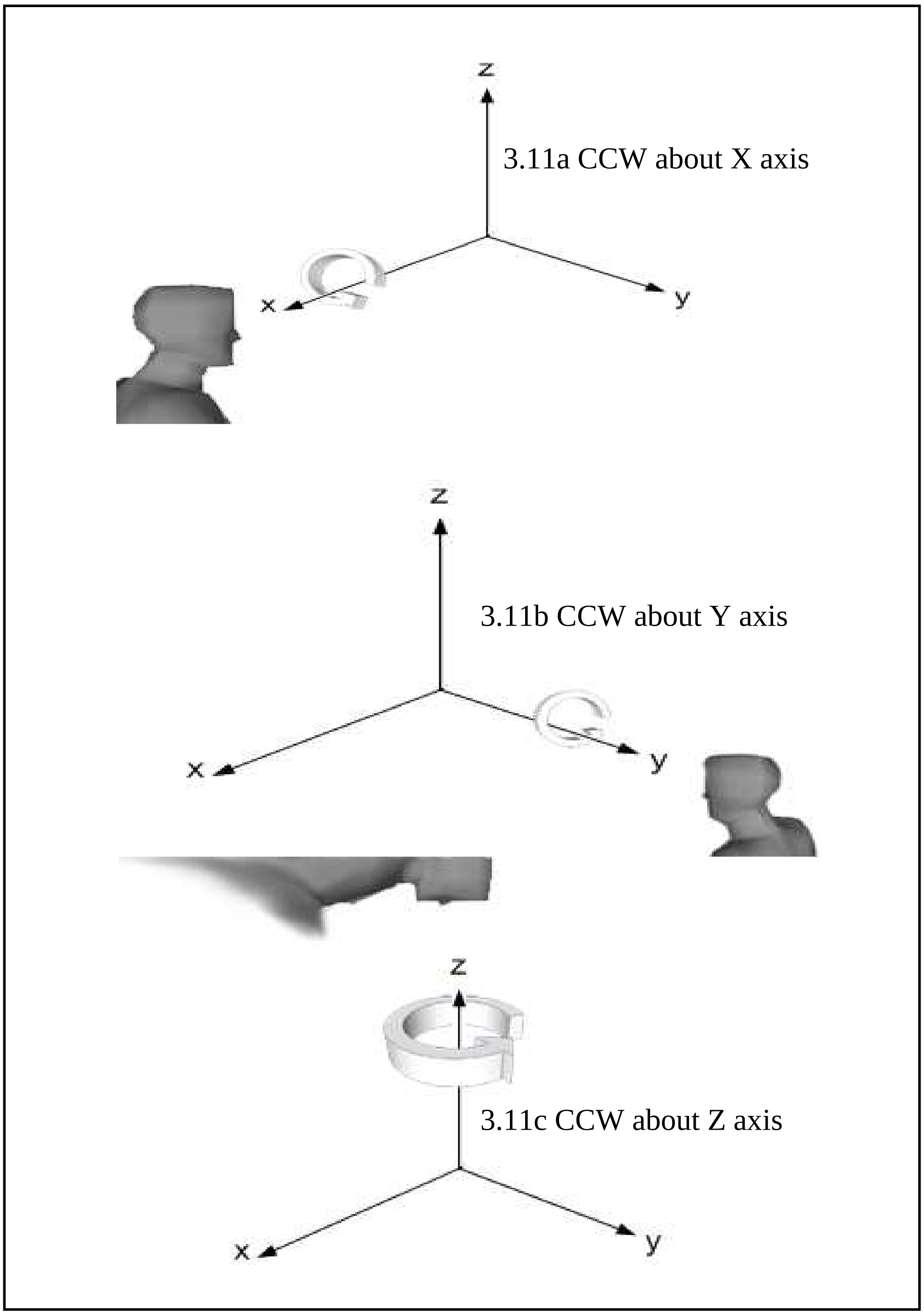

Figure 3.12 A counterclockwise orbit of X, Y, Z

3.1.7 Methodology for Covert Color Image to Gray Scale (This topic uses base information from Sittichoke(2007))

3.1.7.1 RGB Color System: RGB is the only one of a large number of color systems such as CMYK, HLS and etc., chosen to be used in this work because of ability to process with computer. RGB Color System is composed of three colors, primary colors -Red, Green, and Blue-. The level of color shade is in the range of 0 – 255, or the number of BIT of these three colors is quantified as 24 BIT.
This significantly a figure consists of three overlapping figures with three primary colors- Red, Green, and Blue-.

3.1.7.2 Gray Scale: With reference to topic 3.1.6.1, because of the composition of three primary colors, to convert figure into Gray Scale is to balance all of them with the same level of color shade. The easiest method is to assume all of them are occupied with the same level of light; as a result, a proportion of each color appears to be 1/3.

$$\left.\begin{aligned} R_G &= \frac{R+G+B}{3} \\ G_G &= \frac{R+G+B}{3} \\ B_G &= \frac{R+G+B}{3} \end{aligned}\right\} \qquad (81)$$

Based on the fact that a different level of light in those primary colors, the value representing such a different level must be used as a variable in calculating as shown in equation (81) below:

$$\left.\begin{aligned} R_G &= (R*0.299)+(G*0.587)+(B*0.114) \\ G_G &= (R*0.299)+(G*0.587)+(B*0.114) \\ B_G &= (R*0.299)+(G*0.587)+(B*0.114) \end{aligned}\right\} \qquad (82)$$

R_G , G_G และ B_G are values of the level of color shade, Red, Green, and Blue at Gray Scale level. Finally, after being converted, they are all equalized the same level of color shade in order to provide the result of RGB Color System.

3.2 TOOLS

3.2.1 Flowchart (This topic uses base information from Wacharaporn (2002))

Based on an application, flowchart is divided into two types, System flowchart and Programming Flowchart. Flowchart provides a variety of utilization. Software Development, for example, uses flowchart to draw concepts before writing programmed code, leading to a decrease in mistakes and an increase in a convenient inspection. More importantly, flowchart also provides a lot more understanding on the concept which developer intends to deliver to others. There are a number of standards relevant to drawing flowchart, but the most frequent used standards are American Nation Standard Institute (ANSI)-ANSI X3.6-1970- and International Standard Organizational (ISO) - ISO 5807-. However, ANSI X3.6-1970 was chosen to use for this work.

3.2.1.1 Considerate Principle in Using Flowchart: To gain the most effective in drawing flowchart, there are a few common principles as follow:

- Write from the top to the bottom or from the left to the right
- Avoid writing on a contradictory direction by planning systematically or symbolizing a connector
- Concise an explanation as much as possible, but remain meaningful
- categorize the same kind of work as only one flowchart within one page or use Off-Page Connecter to connect the pages.

3.2.1.2 Types of Flowchart Structure for Programming:

- Sequence is a structure for respectively running each step and classified as the simplest format shown by figure 3.13.

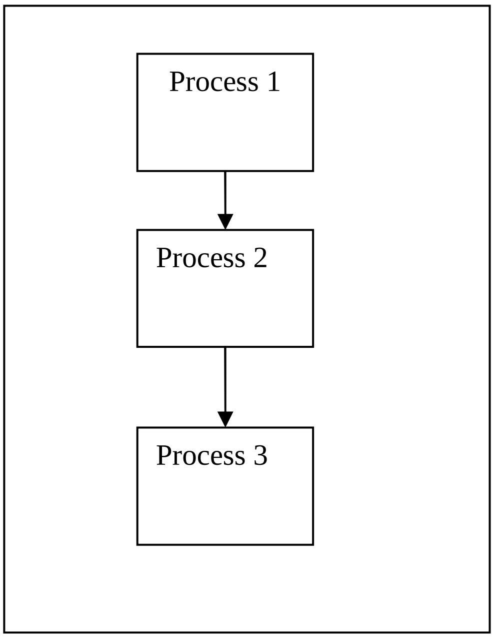

Figure 3.13 Flowchart of Sequence type

- Decision or Selection is adopted with a decision on which step will be appropriately used as a next work as its format is present in figure 3.14.

- Iteration or Loop is to write flowchart with a condition which the same steps may be written repeatedly till some of them will obviously exhibit whether they will become true or not. Consequently, the repeated process will be terminated as explained by figure 3.15.

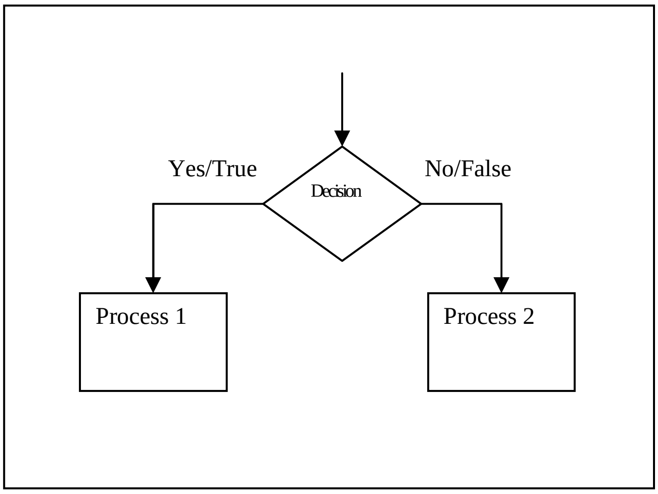

Figure 3.14 Flowchart of Decision or Selection type

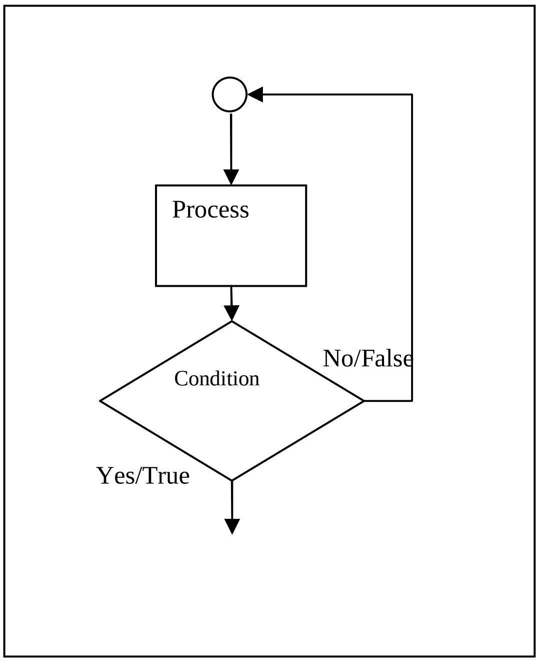

Figure3.15 Flowchart of Iteration or Loop

3.2.1.3 Flowchart Symbol: A large number of figures used as a symbol for this work presented on table 3.1.

Table 3.1 Flowchart Symbol

Flowchart Symbol	**Name**	**Description**
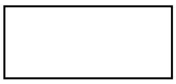	Process	An operation.
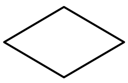	Decision	A yes/no question.
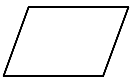	Data (I/O)	Indicates data inputs and outputs to/form a process.
	Terminator	A start or stop point.
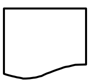	Document	A document report.

Table 3.1 Flowchart Symbol (cont.)

Flowchart Symbol	Name	Description
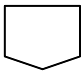	Off Page Connector	A connecter flow to another page.
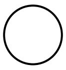	Connector	A connecter flow in a same page.
	Manual Input	User input data to a system.
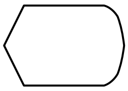	Display	Show result by monitor.
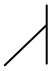	Callout	An explanation of flowchart (Callout has many kinds of symbol).
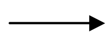	Flow Line	Indicates the direction of flow

3.2.2 Visual Basic 2008(VB 2008) (This topic uses base information from Bancha (2009) and Sittichoke(2007))

Visual Basic (VB), a lingual program, has been gradually developed from Basic (Beginners all Purpose Symbolic Instruction Code) by Microsoft. Visual Basic is, in general, compatible with Window operation. When Microsoft has already developed new platform leads VB step into an era of .NET Framework. A series of lingual program, available for any languages such as .NET, C# and C++ can support OOP (Object Oriented Programming). Additionally, according to an availability of Common Language Specification which allows every language to share all data together, VB 2008 is considered to be a tool for this work because its language is the most similar to human language. Moreover, to build Graphic User Interface (GUI) becomes less complicated. VB is hereby inevitable for a beginner of studying lingual program.

3.2.2.1 Stared with Project: To form a new program is composed of a set of composition. When each set of composition is combined altogether, it will become a project. If VB 2008 falls into the type of VB Express, it is unnecessary to select project. However, if it is acquired from Visual Studio, it is necessary to select the project as presented by figure 3.16.

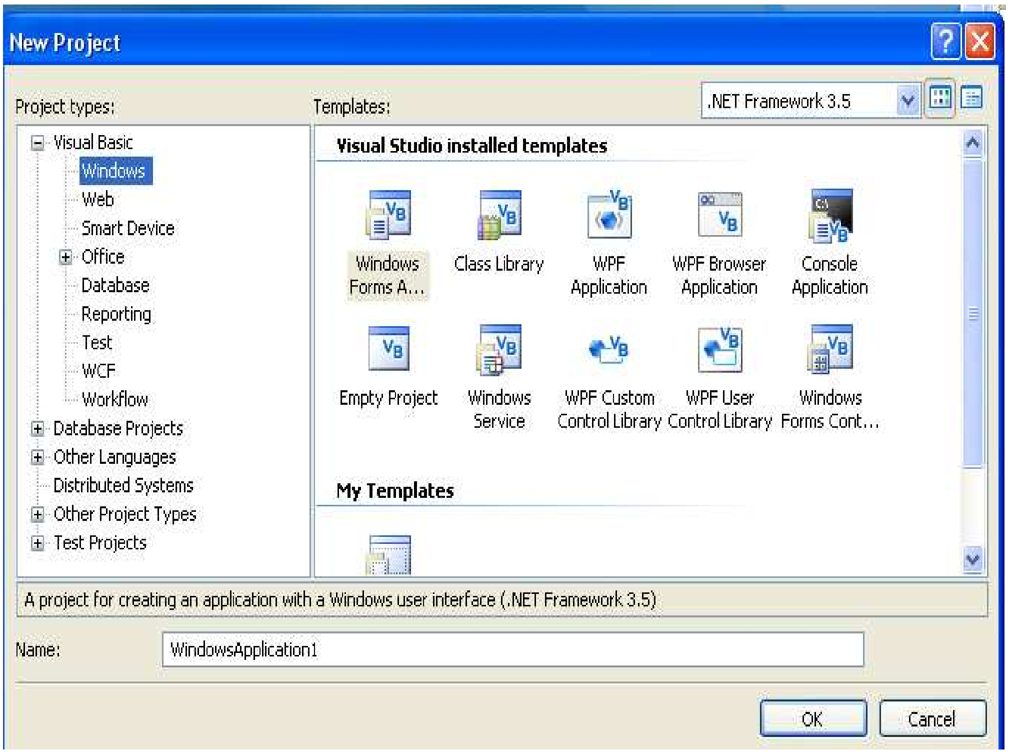

Figure 3.16 Window for building project of VB 2008

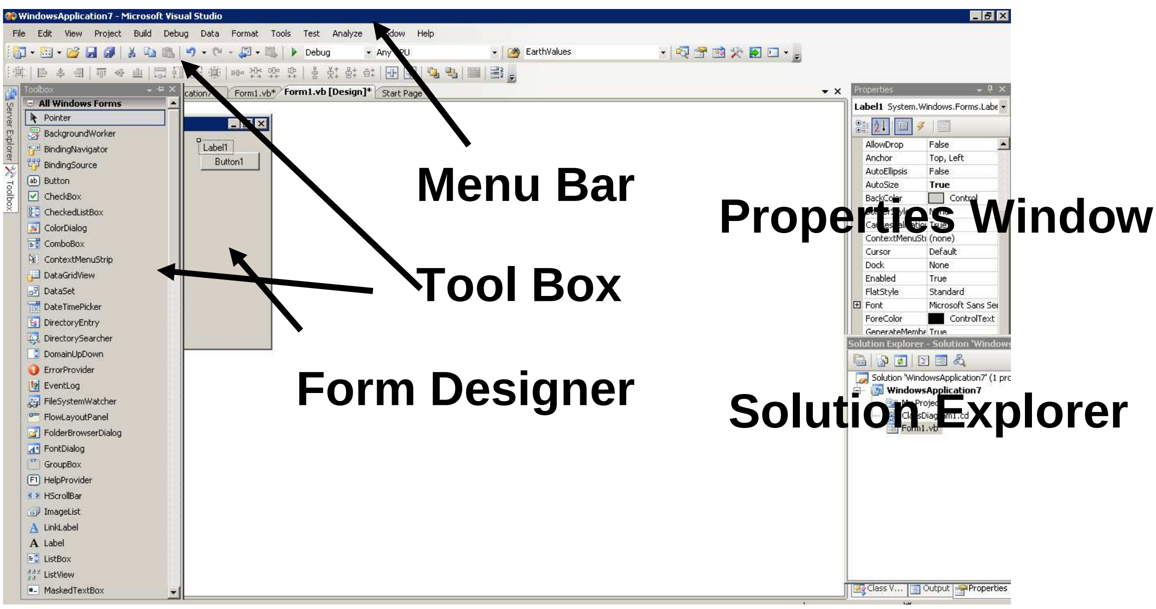

Figure 3.17 Window of VB 2008

According to figure 3.16, the project of VB 2008 appears to be as figure 3.17 when user enters the program by clicking on OK button; however, the project will vary from windows opened by user and controlled by View Menu.

3.2.2.2 File type of VB 2008 is categorized into types as follows:

- Visual studio solution: file extension = .sln for saving project detail in solution.
- Visual studio project: file extension = .vbprog for saving all items inside project.
- Class: file extension = .vb, for saving prototype of project.
- Module: file extension =.vb , for saving data of sub program
- HTML: file extension = .htm, .html, for being file html used in project.
- .NET XML Resource Template: file extension = .resx, for saving detail of resource XML.
- Assembly Information: file extension = AssemblyInfo.vb, for saving data of projects.

3.2.2.3 Variable and Data types in VB 2008 Variable: In every lingual program, it is important for variables to be valued in order to reserve the space in (RAM). However, user has to correctly and appropriately value all variables depending on type, size and capacity. Tables 3.2-3.5 present VB.2008 in the group of.NET Framework with capability of handling from one module to others which are different in the language.

Table 3.2 The type of integer data

type	Description	Memory (Byte)
Byte	Boundary value as 0 to 255	1
Short	Boundary value as -32,768 to 32,767	2
Integer	Boundary value as -2,147,483,648 to 2,147,483,647	4
Long	Boundary value as -9,223,372,036,854,775,808 to 9,223,372,036,854,775,808	8

Table 3.3 The type of real number data

type	Description	Memory (Byte)
Single	* Boundary value as (minus boundary) -3.4028235E+38 to -1.401298e-E-45 * Boundary value as (plus boundary) 1.401298e-E-45 to 3.4028235E+38	4
Double	* Boundary value as (minus boundary) -1.79769313486231570E+308 to -4.94065645841246544E-324 * Boundary value as (plus boundary) 4.94065645841246544E-324 to1.79769313486231570E+308	8

Table 3.4 The type of non numerical data

type	Description	Memory (Byte)
Char	This type is use for define alphabetic data Boundary value 1 alphabetic	2
String	This type is use for define alphabetic data Boundary value could be under a platform	0 to 2^{31}
Boolean	This type is use for define logical result data Boundary value As True or False Default Value As begin Could be false	2
Date	This type is use for define date and times Default Value As begin 12:00:00 AM	8

Table 3.5 The type of multi-type data

type	Description	Memory (Byte)
Decimal	This type can use foe all **numerical** type as integer and real number *Value As Integer 0 to $\pm$79,228,162,514,264,337,593,543,950,335 *Value As Real number 0 to $\pm$7.9228162514264337593543950335	16
Object	This type Can use for all types of data	4

3.2.2.4 Variable Announcement: User need to announce variable, before using a variable, by make name of the variable and define a type of data. Code order forms for an announcement are shown below text.

Dim <Variable name > As <Data type> (Note: this form for Local variable) / *Private <Variable name > As <Data type>* (Note: this form for Global variable)

If we want to define value of data use code order forms like this

<Variable name> = <Data value> or

Dim <Variable name > As <Data type> = <Data value> (Note: this form for Local variable)

Sometimes, data are form in group and have relationship among member of Group data, that we can announce data in form of array like this

Dim <Variable name (Upper boundary of array) > As <Data type> (Note: this form for one dimension array)

Dim <Variable name (Upper boundary of array 1^{st} *dimension, Upper boundary of array* 2^{nd} *dimension) > As <Data type>* (Note: this form for one dimension array)

3.2.2.5 Operators: Operators are sign for operate data or variables, get result to mathematics, logical, or string. Example of operators are plus minus, logical, more than etc. We can device operator into 4 main groups as follow.

- Arithmetic Operator
- String Manipulation Operator
- Logical Operator
- Comparison Operator

3.2.2.6 Conditional Statements: There are two types of controlling structures, Decision and Repetitive. The former falls into a condition which must be tested whether it becomes real. Such order is in the group of “If” possessing a variety of structures. An ordering structure, for instance, is:

IF<condition>Then

<thing to do if condition becomes true>

Else

< thing to do if condition becomes fault>

End If

The latter, Decision, is to repeat Loop, and its order is in the group of For, While or Do. An ordering structure, for instance, is:

For<Variable = Stated Value> To <Last Value>

<thing to do if in the loop>

Next

As discussed above, this is only an example of using some parts of Conditional Statements There are various types of usability depending on expected result. Occasionally, the use of a number of Conditional Statements must be taken in order to provide a same result.

3.2.2.7 Procedure: programming including several activities will be developed by dividing its procedure into small parts. Then, to further develop and to inspect are a lot more conveniently held. Additionally, a set of repeated order is also dwindled. To divide such procedure consists of 2 parts-Sub Program and function-.

3.2.2.8 Sub program: does not affected on other parts but can execute variables in the type of global announcement. With out global announcement, is unidentified its value. Sub program sometimes does not require the return of values, but will perform only one-way order.

An application of Sub Program requires its name as reference and has to define the type of data as Parameter. The type of parameters is classified by the same method as variables as below:

Private or Public or Protected or Friend Sub or "Nothing" < Sub Program Name> (Parameter)

<Order>

End Sub

And can be performed as

Sub Program Name (Argument)

which argument is parameter for feeding into Sub Program.

3.2.2.9 Function**:** arises from adherently being available from program and being crated by. In performing function, workable part can be revalued but occasionally it is unnecessary to do that relying on its use. Programming manually is shown as follows:

Private or Public or Protected or Friend or "Nothing" Function <Function Name> (Parameter)As <Type Of Result>

<Order>

Return <Result>

End Function

And can be used as:

<Variable> = <Function Name>(Argument)

3.2.3 Computer Aided Three-dimensional Interactive Application, CATIA (This topic uses icon figures and base information from CATIA documentation)

With a high potential, CAD CAM และ CAE are nowadays subject to DAUSSAUIL SYSTEM Inc., France. CATIA is composed of a large number of sub program named Workbench; however, Digital Shape Editor was picked up to be used for this research. When CATIA is opened, Digital Shape Editor Workbench will appear, and to get into this clicks on Start>Shape>Digtized Shape Editor respectively followed by figure 3.18. Afterwards, Cloud of point will be feeded intoCatia by clicking on Import 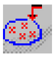 button available by two points presented by figure 3.19. Window will appear like figure 3.20 and then to choose file type clicks on “x##### y###### z#####” and OK button Note that Clound points is imported in the format of “x##### y###### z#####” for this work.

Figure 3.18 Staring to Digital Shape Editor Workbench

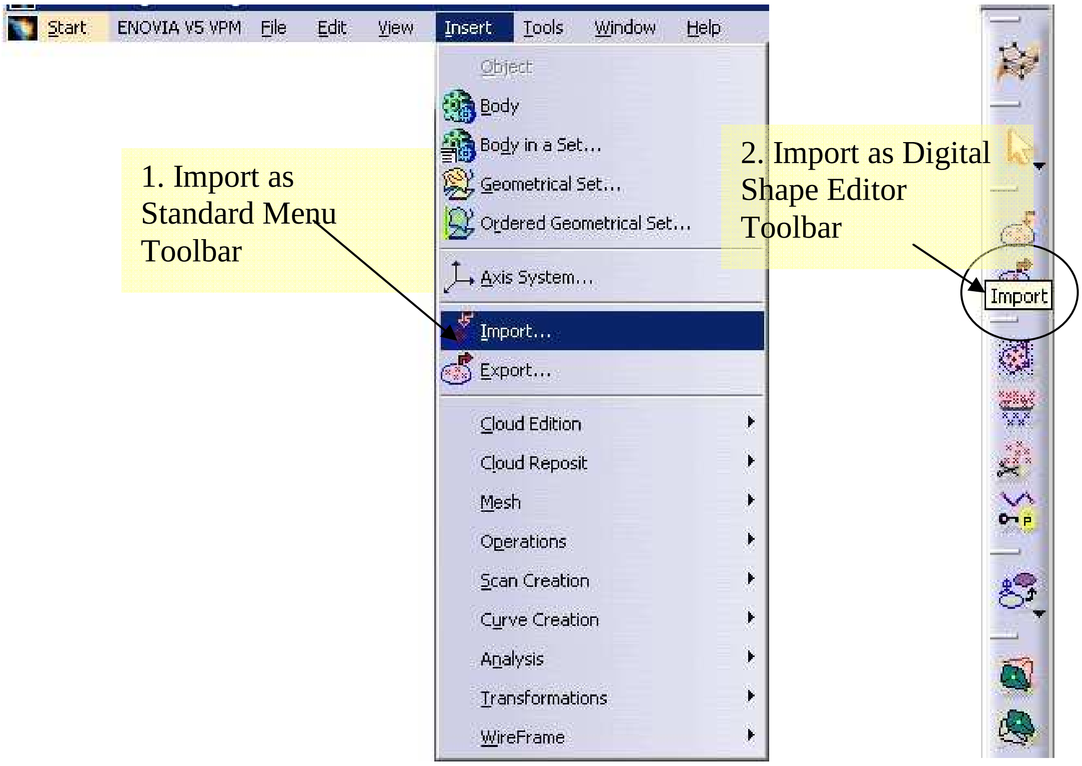

Figure 3.19 Import point data to CATIA

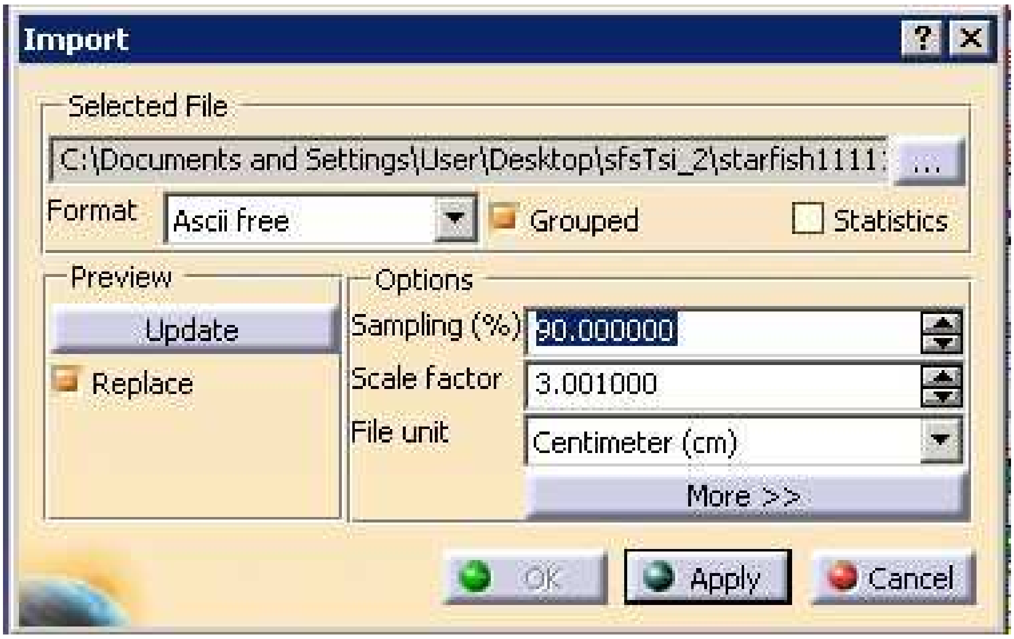

Figure 3.20 An Import window

3.2.3.1 To create 3D surface, like Import button when user clicks on Mesh Creation 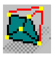 button available by two points, Mesh Creation will appear on the window shown by figure 3.21 and can be formed by selecting a format. A combination of meshes results in a formation of 3D surface which beforehand can view overall structure by clicking on Apply button in order to obtain the most required figure. Then, clicking OK button, we will finally secure 3D Bas-relief surface according to figure 3.32. In next subtopic will show management of point cloud with normalization that may be unsmooth surface in CATIA.

Figure 3.21 A Mesh Creation window

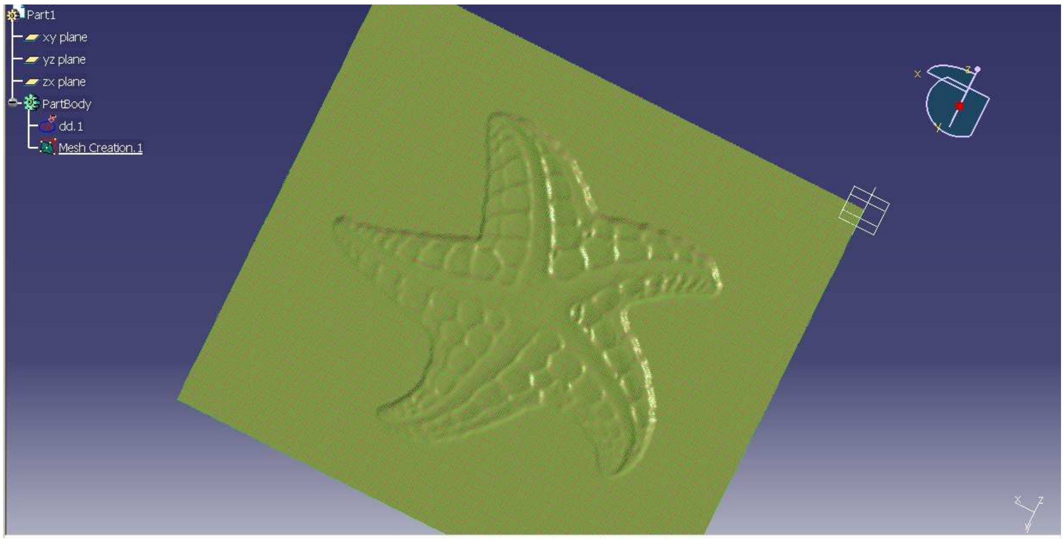

Figure 3D surface example was created by CATIA

3.2.2.2 Filter icon 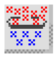 used for reducing the scatter points. When click this icon windows as same as figure 3.23 will appear. In this example used Adaptive function that adapt by rang setting of minimum and maximum.

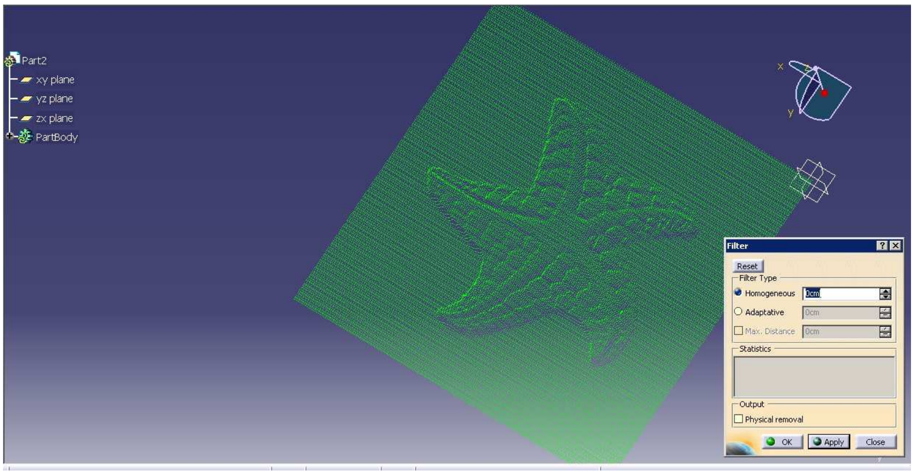

figure3.23 Filter window

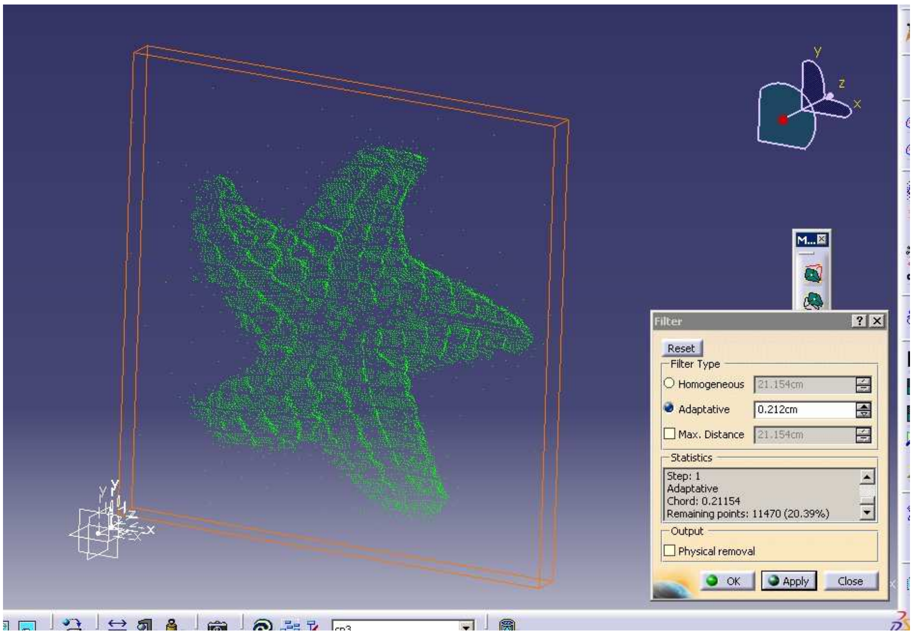

figure3.24 Filter window with used Adaptive function

2.2.2.3 Align by Best Fit icon 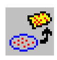 use when more point clound than one, for combine them needed to align. Use this icon for automaticly alignmaent respectively followed by figure 3.25-3.26.

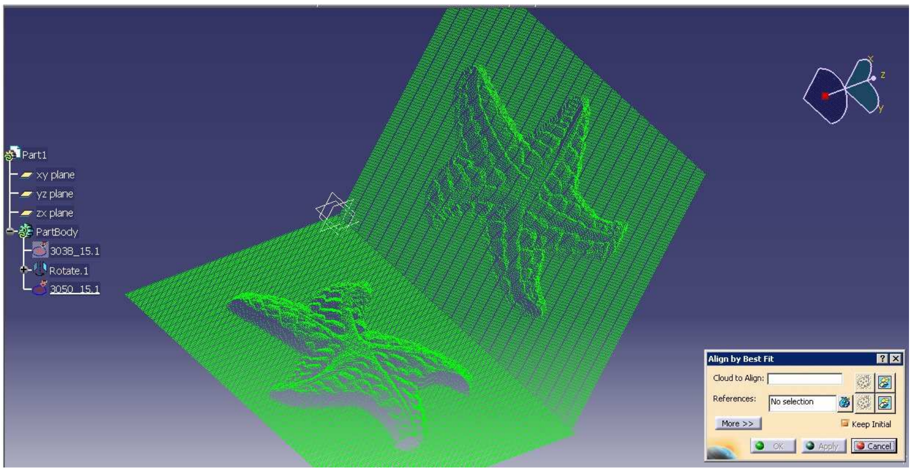

figure3.25 Align by Best Fit window

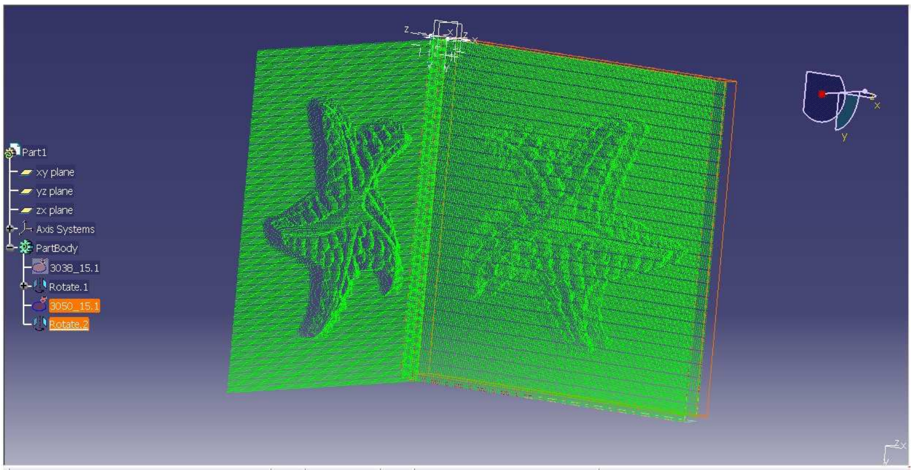

figure3.26 A fitted point cloud by used Align by Best

2.2.2.4 Activate icon 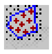 used for select only needed points for next operattion. According to figure3.27, Trap function and Inside Trap choise box was used to around needed points then figure3.27 is its result. And if needing to select points outside a cordon, thick in an Outside Trap choise box.

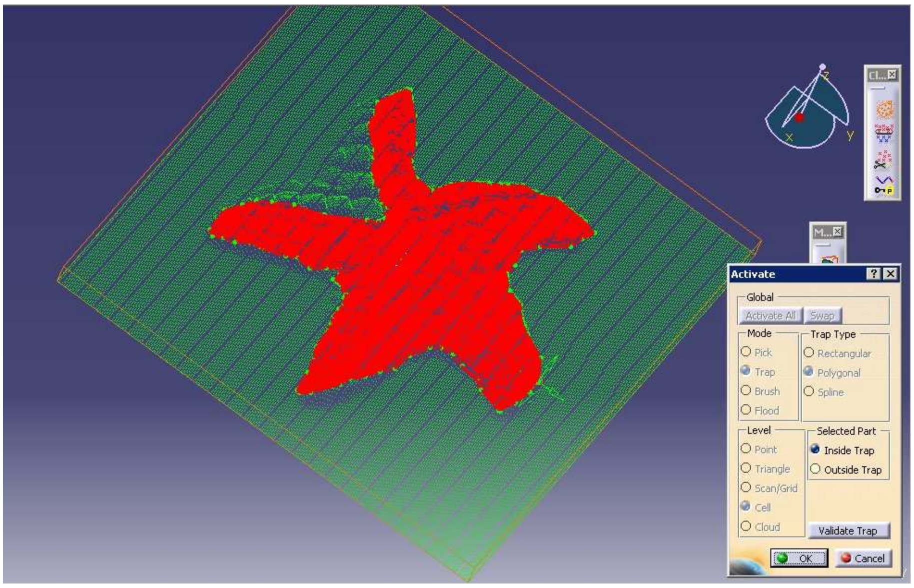

figure3.27 Activate window

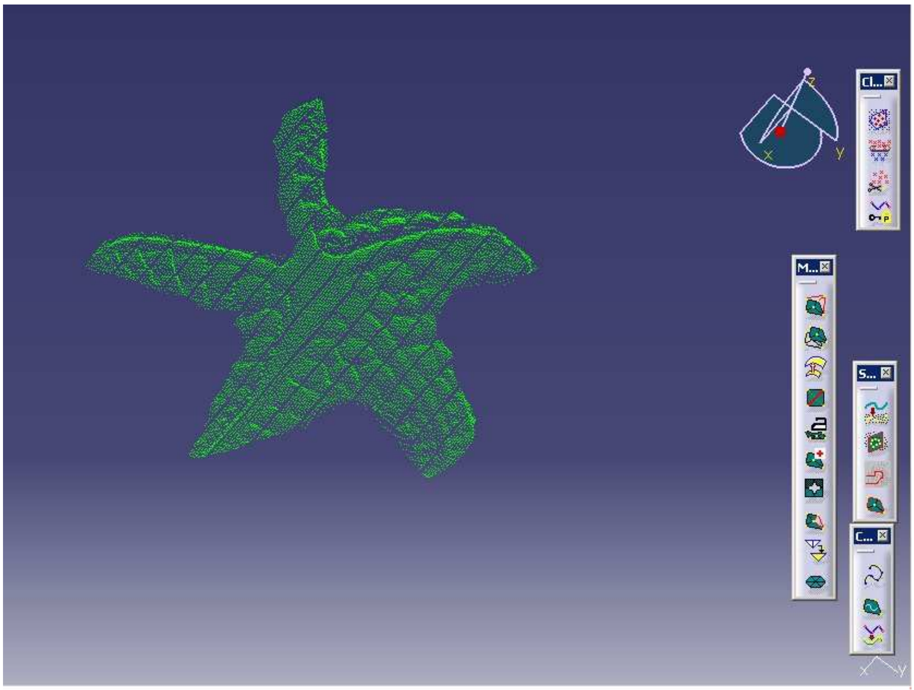

figure3.28 A selected points by used Activate

2.2.2.5 Mesh Cleaner icon  Used for elase meshes that efffect problem to fix surface, in next step work, for an example in figure 3.29 affter analisys found 31 non manifold vertices.

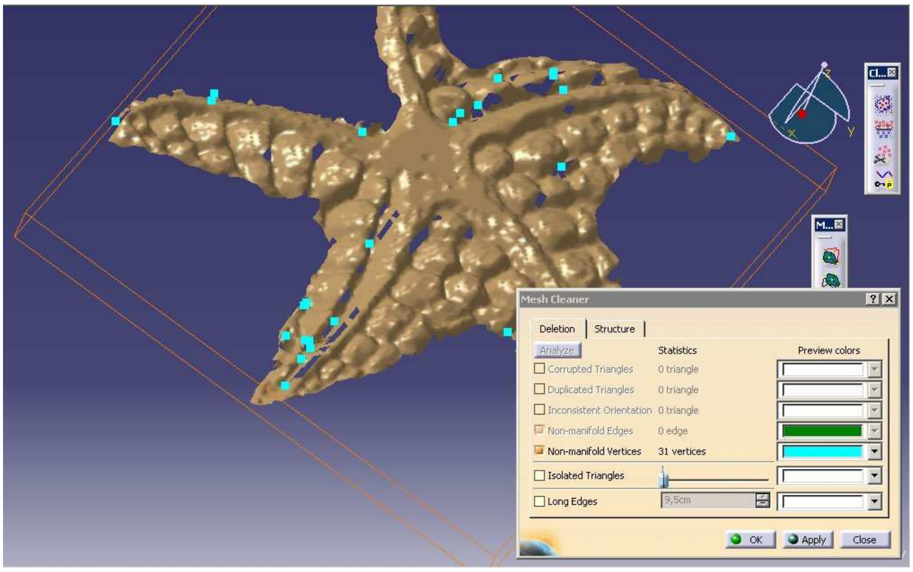

figure3.29 Mesh Cleaner window.

2.2.2.6 Fill Holes icon  used for fixing holes on surface. Acording in figure 3.30, holes will be fixed have green V othewise have red X, and chosen holes by click as letter X or set hole size in Hole size textbox.

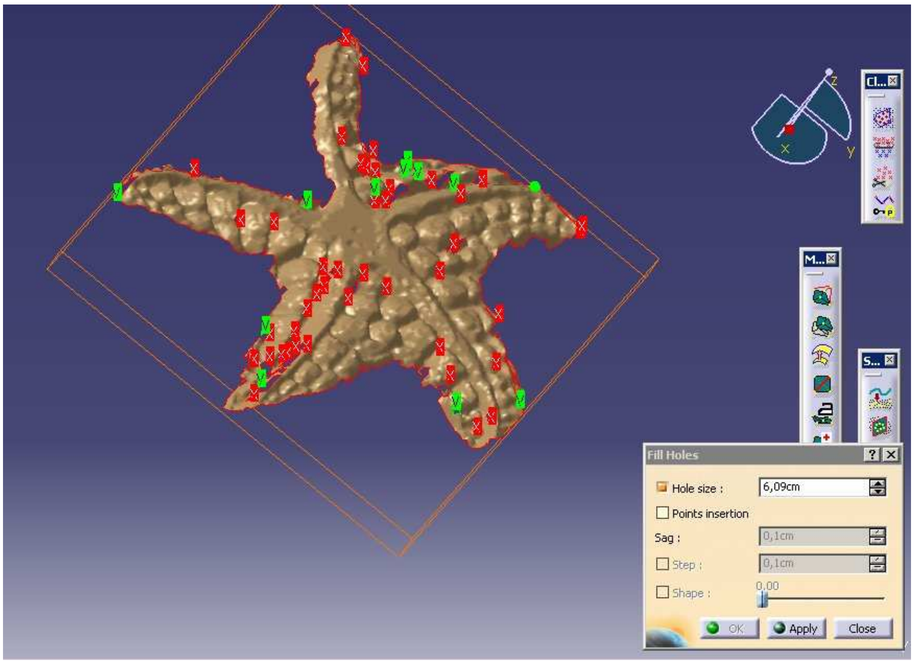

figure3.30 Fill Holes window.

2.2.2.7 Split a Mesh or a Cloud icon 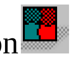 use for split unused meshes.It's function as same as the Activate icon. Acoording in figure3.31, used Brush function for direct cerection to meshes.

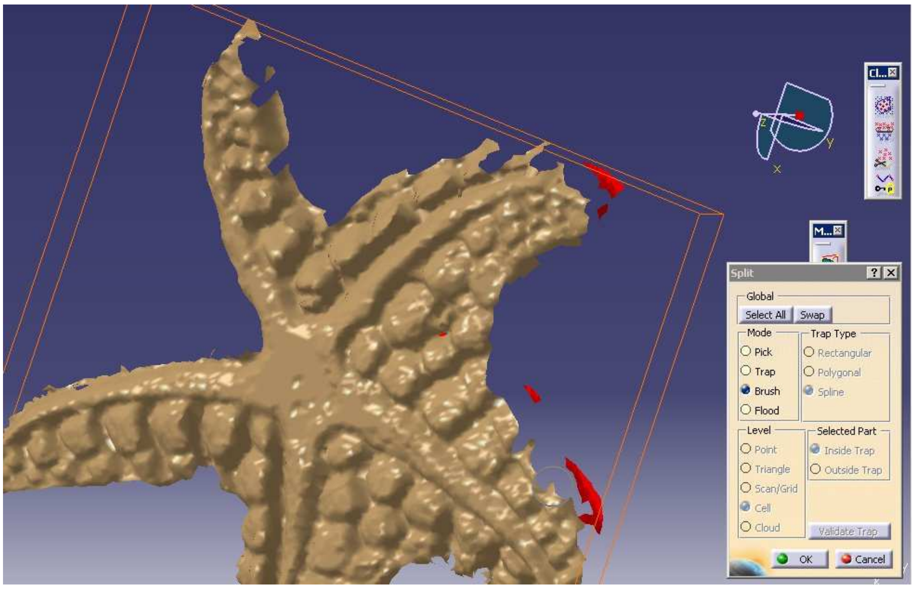

figure3.31 Split window.

2.2.2.8 Merge Clouds icon  used for combine surfaces, exsample sufaces as shown as figure3.32 and 3.33 and figure3.34 is result of conbination.

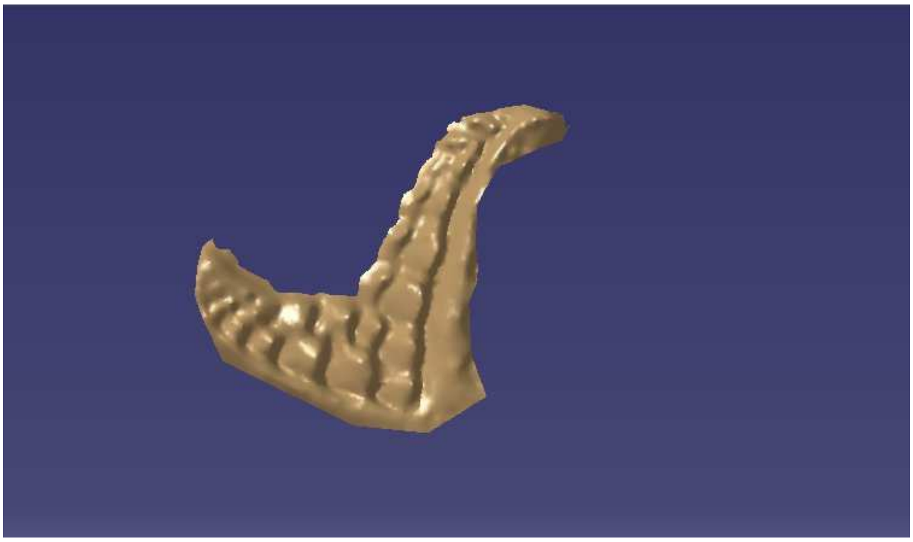
figure3.32 The first surface exxample for merge clouds.

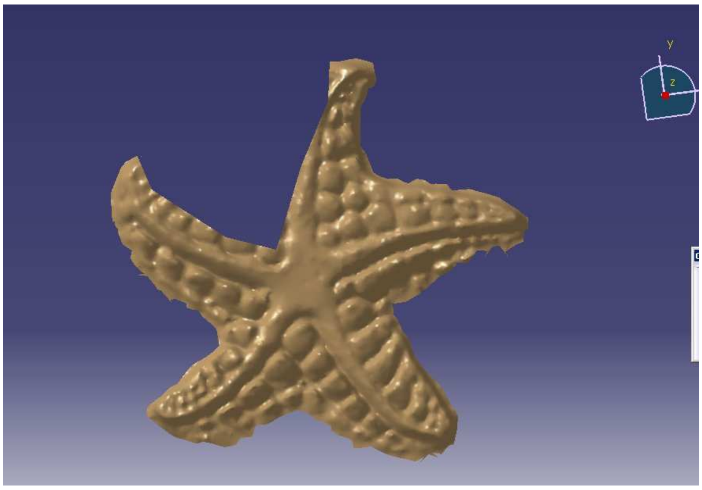

figure3.33 The second surface exxample for merge clouds.

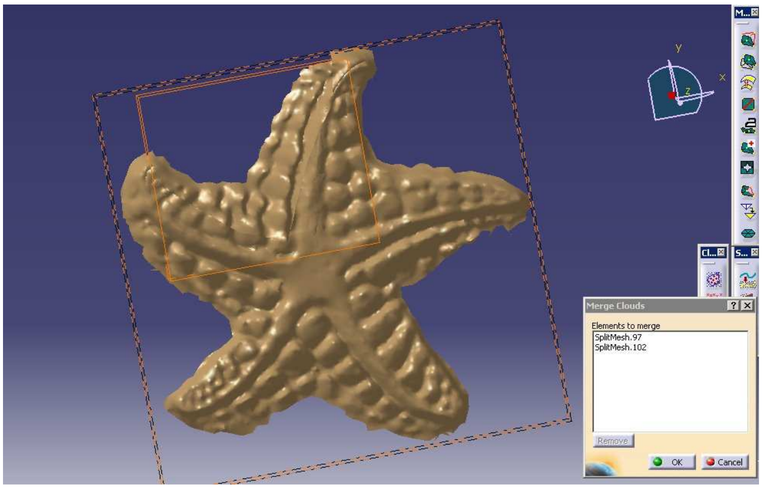

figure3.34 Merge Clouds window

3.2.4 Other tools

- GIMP 2.7.0 Spencer Kimball, Peter Mattis and the GIMP Development Team

- Digital camera / Canon power short A630

- Laptop / BenQ Intel core 2 duo CPU T8100 2.10 GHz 3 GB of RAM

- Compass

-Thermometer

-Rotating plane

- Lux meter

- Dimer

CHAPTER IV
SHAPE FROM SHADING WITH SOLAR LIGHT SOURCE CALCULATION

This chapter will present a use of simulation by means of assuming all parameters, in order to examine a series of calculating principles, used not only for SFS calculation but also for other related calculations. This may lead a lot more understanding in the process of this thesis.

4.1 Solar Position Algorithm (SPA) Calculation.

Example data for SPA calculation:

Date = 11/02/2010	*Time = 14:55:50*
Time zone (TZ) = +7 hours.	*Longitude =* $100^0\ 27'\ 51''$ *E*
Latitude = $13^0\ 45'\ 27''$ *N*	*Pressure = 1009.15 mbar.*
Elevation = 2.5 m.	*Temperature =* $36.5\ ^0$ *C.*
Surface slope = 0^0	ΔT *= 26 Seconds*

4.1.1 Julian Times Calculation: Follow to equation (26)-(30).

$$JD = Int(365.25\times(Y+4716)) + Int(30.6001\times(M+1)) + D + B - 1524.5$$

$$JD = Int(365.25\times(2010+4716)) + Int(30.6001\times(2+1)) + 3 + 0 - 1524.5$$

Julian Day = <u>2455238.8304398148 day</u>

$$JDE = JD + \frac{\Delta T}{86400}$$

$$JDE = 2455238.8304398148 + \frac{26}{86400}$$

Julian Ephemeris Day = 2455238.830740741 day

$$JC = \frac{JD - 2451545}{36525}$$

$$JC = \frac{2455238.8304398148 - 2451545}{36525}$$

Julian Century = 0.10113156577179554 century

$$JCE = \frac{JDE - 2451545}{362525}$$

$$JCE = \frac{2455238.830740741 - 2451545}{362525}$$

Julian Ephemeris Century = 0.10113157401070468 century

$$JME = \frac{JCE}{10}$$

$$JME = \frac{0.10113157401070468}{10}$$

Julian Ephemeris Millennium = 0.010113157401070468 millennium

4.1.2 Earth position Calculation: Follow to equation (31)-(36).

Earth heliocentric latitude simulator , because consists of just a few j terms and i values but still be sufficient to be used for calculating according to table A2.1-A2.2 in Appendix A, itself requires less calculating times than those of others as shown in subtopic 4.1.3 and 4.1.4, a full-step calculation.

$$Laji = Ai \times \cos(Bi + Ci \times JME)$$

$$La00 = A0 \times \cos(B0 + C0 \times JME)$$

$$La00 = 280 \times \cos(3.199 + 8433.4.662 \times 0.010113157401070468)$$

= -1.319654394535262

$$La01 = A1 \times \cos(B1 + C1 \times JME)$$

$$La01 = 102 \times \cos(50422 + 5507.553 \times 0.010113157401070468)$$

= -14.26434135256483

$$La02 = A2 \times \cos(B2 + C2 \times JME)$$

$$La02 = 80 \times \cos(3.88 + 5223.69 \times 0.010113157401070468)$$

= 78.986687079222510

$$La03 = A3 \times \cos(B3 + C3 \times JME)$$

$$La03 = 44 \times \cos(3.7 + 2352.87 \times 0.010113157401070468)$$

= -31.299089743960082

$$La04 = A4 \times \cos(B4 + C4 \times JME)$$

$$La04 = 32 \times \cos(4 + 1577.34 \times 0.010113157401070468)$$

= 10.448537497858992

$$La10 = A0 \times \cos(B0 + C0 \times JME)$$

$$La10 = 9 \times \cos(3.9 + 5507.55 \times 0.010113157401070468)$$

= - 8.962317944258693

$$La11 = A1 \times \cos(B1 + C1 \times JME)$$

$$La11 = 6 \times \cos(1.73 + 5223.69 \times 0.010113157401070468)$$

= -2.445862834479899

$$Laj = \sum_{j=0}^{n} Laji$$

La0 = -1.319654394535262 - 14.26434135256483 + 78.986687079222510 - 31.299089743960082+10.448537497858992

= <u>46.552139592029675</u>

La1 = - 8.962317944258693 -2.445862834479899

= <u>-11.408180778738592</u>

$$La = \frac{(\mathrm{La0} + \mathrm{La1} \times \mathrm{JME}) \times 180}{10000000\pi}$$

$$La = \frac{(46.552139592029675 + -11.408180778738592 \times 0.010113157401070468) \times 180}{10000000\pi}$$

Earth heliocentric latitude = <u>0.000026606307555489993 ^{o} or 0.00000046436766864154427 radian</u>

$$Lji = Ai \times \cos(Bi + Ci \times JME)$$

$$Lj = \sum_{j=0}^{n} Lji$$

After this, tables in Appendix A1.1-1.6 were used in the same process as subtopic 4.1.2 for finding heliocentric latitude which their results can be seen as follow.

L0 = 177437578.0725655

L1 = 628331764524.24609

L2 = 50910.03633610707

L3 = 329.81029394867375

L4 = -112.46204169325928

L5 = -0.9999987317275395

$$L = \frac{(\mathrm{L0} + \mathrm{JME} \times (\mathrm{L1} + \mathrm{JME} \times (\mathrm{L2} + \mathrm{JME} \times (\mathrm{L3} + \mathrm{JME} \times (\mathrm{L4} + \mathrm{JME} \times \mathrm{L5})))))\times 180}{10000000 \times \pi}$$

$$L = ((177437578.0725655 + 0.010113157401070468 \times (628331764524.24609 + 0.010113157401070468 \times (50910.03633610707 + 0.010113157401070468 \times (329.81029394867375 + 0.010113157401070468 \times (-112.46204169325928 + 0.010113157401070468 \times -0.9999987317275395))))) \times 180)/10000000 \times \pi$$

Earth heliocentric longitude = <u>142.47759300549779 ^{o} or 65.318556180058238 radian</u>

4.1.3 Earth radius Calculation: Follow to equation (37)-(39).

$$Rji = Ai \times \cos(Bi + Ci \times JME)$$

$$Rj = \sum_{j=0}^{n} Rji$$

After using tables in Appendix A3.1-3.5 in the same process as the calculation performed in subtopic 4.1.2, it provided results shown as follow.

R0 = 98700353.215089247

R1 = -27276.65651123615

R2 = 4339.0308818465874

R3 = 42.854212051209416

R4 = -3.96710734550197667

$$R = \frac{(\mathrm{R0} + \mathrm{JME} \times (\mathrm{R1} + \mathrm{JME} \times (\mathrm{R2} + \mathrm{JME} \times (\mathrm{R3} + \mathrm{JME} \times \mathrm{R4}))))}{10000000}$$

$$R = ((98700353.215089247 + 0.010113157401070468 \times$$
$$(-27276.65651123615 + 0.010113157401070468 \times$$
$$(4339.0308818465874 + 0.010113157401070468 \times$$
$$(42.854212051209416 + 0.010113157401070468 \times$$
$$-3.9671073455019767)))) / 10000000$$

Earth radius vector = <u>0.98700077805791375 AU</u>

4.1.4 Sun Position referent to Geocentric of the earth Calculation: Follow to equation (40)-(41).

$$\Theta = L + 180$$
$$\Theta = 142.47759300549779 + 180$$

Geocentric longitude = <u>3.22.477759300549779 °</u>

$$\beta = -La$$
$$\beta = -(0.000026606307555489993)$$

Geocentric latitude = <u>-0.000026606307555489993 °</u>

4.1.5 Nutation in longitude and obliquity Calculation: Follow to equation (42)-(50).

$$X_0 = 297.85036 + 445267.111480 \times JCE - 0.0019142 \times JCE^2 + \frac{JCE^3}{189474}$$

$$X_0 = 297.85036 + 445267.111480 \times 0.10113157401070468 -$$
$$0.0019142 \times JCE^2 + \frac{0.10113157401070468^3}{189474}$$
$$= \underline{45328.414179600106}$$

$$X_1 = 357.52772 + 35999.050340 \times JCE - 0.0001603 \times JCE^2 - \frac{JCE^3}{300000}$$

$$X_1 = 357.52772 + 35999.050340 \times 0.10113157401070468 -$$
$$0.0001603 \times 0.10113157401070468^2 - \frac{0.10113157401070468^3}{300000}$$
$$= \underline{3998.1683421318626}$$

$$X_2 = 134.96298 + 477198.867398 \times JCE + 0.0086972 \times JCE^2 + \frac{JCE^3}{56250}$$

$$X_2 = 134.96298 + 477198.867398 \times 0.10113157401070468$$
$$+ 0.0086972 \times 0.10113157401070468^2 + \frac{0.10113157401070468^3}{56250}$$
$$= \underline{48394.835645055107}$$

$$X_3 = 93.27191 + 483202.017538 \times JCE - 0.0036825 \times JCE^2 + \frac{JCE^3}{327270}$$

$$X_3 = 93.27191 + 483202.017538 \times 0.10113157401070468 -$$
$$0.0036825 \times \quad 0.10113157401070468^2 + \frac{0.10113157401070468^3}{327270}$$
$$= \underline{48960.252471106112}$$

$$X_4 = 125.04452 - 1934.136261 \times JCE + 0.0020708 \times JCE^2 + \frac{JCE^3}{450000}$$

$$X_4 = 125.04452 - 1934.136261 \times 0.10113157401070468 +$$
$$0.0020708 \times \quad 0.10113157401070468^2 +$$
$$\frac{0.10113157401070468^3}{450000}$$
$$= \underline{-70.557703244506642}$$

$$\Delta\psi_i = (a_i + b_i \times JCE) \times \sin\left(\sum_{j=0}^{4} X_j \times Y_{i,j}\right)$$

$$\Delta\psi_0 = (a_0 + b_0 \times JCE) \times \sin((X_0 \times Y_{0,1}) + (X_1 \times Y_{0,1}) + (X_2 \times Y_{0,2}) + (X_3 \times Y_{0,3}) + (X_4 \times Y_{0,4}))$$

$$\Delta\psi_0 = (-171996 + -174.2 \times 0.10113157401070468) \times \sin((45328.414179600106 \times 0) + (3998.1683421318626 \times 0) + (48394.835645055107 \times 0) + (48960.252471106112 \times 0) + (-70.557703244506642 \times 1))$$

$$= \underline{162204.91795863395}$$

$$\Delta\varepsilon_i = (c_i + d_i \times JCE) \times \cos(\sum_{j=0}^{4} X_j \times Y_{i,j})$$

$$\Delta\varepsilon_0 = (c_0 + d_0 \times JCE) \times \cos((X_0 \times Y_{0,1}) + (X_1 \times Y_{0,1}) + (X_2 \times Y_{0,2}) + (X_3 \times Y_{0,3}) + (X_4 \times Y_{0,4}))$$

$$\Delta\varepsilon_0 = (92025 + 8.9 \times 0.10113157401070468) \times \cos((45328.414179600106 \times 0) + (3998.1683421318626 \times 0) + (48394.835645055107 \times 0) + (48960.252471106112 \times 0) + (-70.557703244506642 \times 1))$$

$$= \underline{30631.496761765331}$$

$$\Delta\psi = \frac{\sum_{i=0}^{n} \Delta\psi_i}{36000000}$$

$$\Delta\psi = \frac{176980.2321259515}{36000000}$$

Nutation in longitude = $\underline{0.004916117559054208 5^{o}}$

$$\Delta\varepsilon = \frac{\sum_{i=0}^{n} \Delta\varepsilon_i}{36000000}$$

$$\Delta\varepsilon = \frac{32151.42306208576}{36000000}$$

Nutation in obliquity = $\underline{0.00089309508505793 78^{o}}$

4.1.6 True Obliquity of Ecliptic Calculation: Follow to equation (51)-(53).

$$U = \frac{JME}{10}$$

$$U = \frac{0.010113157401070468}{10}$$

$$= \underline{0.0010113157401070468}$$

$$\varepsilon_0 = 84381.448 + \mathrm{U} \times (\text{-}4680.96 + \mathrm{U} \times (\text{-}1.55 + \mathrm{U} \times (1999.25 + \mathrm{U} \times (\text{-}51.38 + \mathrm{U} \times (\text{-}249.67 + \mathrm{U} \times (\text{-}39.05 + \mathrm{U} \times (7.12 + \mathrm{U} \times (27.87 + \mathrm{U} \times (5.79 + \mathrm{U} \times 2.45)))))))))$$

$$\varepsilon_0 = 84381.448 + 0.0010113157401070468 \times (\text{-}4680.96 + 0.0010113157401070468 \times (\text{-}1.55 + 0.0010113157401070468 \times (1999.25 + 0.0010113157401070468 \times (\text{-}51.38 + 0.0010113157401070468 \times (\text{-}249.67 + 0.0010113157401070468 \times (\text{-}39.05 + 0.0010113157401070468 \times (7.12 + 0.0010113157401070468 \times (27.87 + 0.0010113157401070468 \times (5.79 + 0.0010113157401070468 \times 2.45)))))))))$$

$$= \underline{84376.71407195575}$$

$$\varepsilon = \frac{\varepsilon_0}{3600} + \Delta\varepsilon$$

$$\varepsilon = \frac{84376.71407195575}{3600} + 0.0008930950850579378$$

True obliquity of ecliptic **=** $\underline{23.438869226183876^{\circ}}$

4.1.7 Aberration Correction Calculation: Follow to equation (54).

$$\Delta\tau = -\frac{20.4898}{3600 \times R}$$

$$\Delta\tau = -\frac{20.4898}{3600 \times 0.98700077805791375}$$

Aberration correction = <u>-0.0057665720611794159 °</u>

4.1.8 Apparent Sun Longitude Calculation: Follow to equation (55).

$$\lambda = \Theta + \Delta\psi + \Delta\tau$$

$$\lambda = 322.477759300549779 + 0.049161175590542085 - 0.0057665720611794159$$

Apparent sun longitude = <u>322.47674255099565 °</u>

4.1.9 Local Hour Angle Calculation: Follow to equation (56)-(60).

Then covert unit's Longitude to degrees: σ = 100.59166666666667 °

$$\alpha = \frac{Arc\tan 2(\sin\lambda \times \cos\varepsilon - \tan\beta \times \sin\varepsilon, \cos\lambda) \times 180}{\pi}$$

$$\alpha = Arc\tan 2(\sin 322.47674255099565 \times \cos 23.438869226183876 - \tan\text{-}\,0.000026606307555489993 \times \sin 23.438869226183876\,, \cos\lambda) \times 180/\pi$$

= <u>324.83137400206277 °</u>

$$v_0 = 280.46061837 + 360.98564736629 \times (JD - 2451545) + 0.000387933 \times JC^2 - \frac{JC^3}{38710000}$$

$$v_0 = 280.46061837 + 360.98564736629 \times (2455238.8304398148 - 2451545) + 0.000387933 \times 0.10113156577179554^2 - \frac{0.10113156577179554^3}{38710000}$$

= <u>260.2332002052868 °</u>

$$v = v_0 + \Delta\psi \times \cos(\varepsilon)$$

$$v = 260.2332002052868 + 0.049161175590542085 \times \cos(23.438869226183876)$$

$$= \underline{260.23771033330305^{o}}$$

$$H = v + \sigma - \alpha$$

$$H = 260.23771033330305 + 100.59166666666667 - 324.83137400206277$$

Local hour angle = $\underline{35.998003331206917^{o}}$

4.1.10 Topoccentric Sun Right Ascension, Topocentric Sun Declination and Topocentric Local Hour Angle Calculation: Follow to equation (61)-(70).

$$\delta = \frac{Arc\sin(\sin\beta \times \cos\varepsilon + \cos\beta \times \sin\varepsilon \times \sin\lambda) \times 180}{\pi}$$

$$\begin{aligned}\delta = {} & Arc\sin(\sin\text{-}0.000026606307555489993 \times \\ & \cos 23.438869226183876 + \cos\text{-}0.000026606307555489993 \\ & \sin 23.438869226183876 \times \quad \sin 322.47674255099565) \times \\ & 180/\pi\end{aligned}$$

$$= \underline{-14.0208977724624^{o}}$$

Then covert unit's Latitude to degrees: $\varphi = 40.567476000000006^{o}$

$E = 2.5$ m.

$$u = Arc\tan(0.99664719 \times \tan\varphi)$$

$$u = Arc\tan(0.99664719 \times \tan 40.567476000000006)$$

= $\underline{0.70637729600250376 \text{ radians}}$

$$y = 0.99664719 \times \sin u + \frac{E}{6378140} \times \sin \varphi$$

$$y = 0.99664719 \times \sin 0.70637729600250376 + \frac{2.5}{6378140} \times$$
$$\sin 40.567476000000006$$
$$= \underline{0.64690617181611676}$$

$$x = \cos u + \frac{E}{6378140} \times \cos \varphi$$

$$x = \cos 0.70637729600250376 + \frac{2.5}{6378140} \times \cos 40.567476000000006$$
$$= \underline{0.76071859302572908}$$

$$\xi = \frac{8.794}{3699 \times R}$$

$$\xi = \frac{8.794}{3699 \times 0.98700077805791375}$$
$$= \underline{0.0024749502047853949}$$

$$\Delta\alpha = \frac{(Arc\tan 2(-x \times \sin \xi \times \sin H, \cos \delta - x \times \sin \xi \times \cos H) \times 180}{\pi}$$

$$\Delta\alpha = (Arc\tan 2(-0.76071859302572908 \times \sin 0.0024749502047853949 \times$$
$$\sin 35.998003331206917,$$
$$\cos(\text{-}14.0208977724624) - 0.76071859302572908 \times$$
$$\sin 0.0024749502047853949 \times \cos 35.998003331206917) \times 180 / \pi$$
$$= \underline{\text{-}0.0011406060133455616^{\circ}}$$

$$H' = H - \Delta\alpha$$

$$H' = 35.998003331206917 - \text{-}0.0011406060133455616$$

Topocentric local hour angle = $\underline{35.999143937220261^{\circ}}$

$$\alpha' = \alpha + \Delta\alpha$$

$$\alpha' = 324.83137400206277 + \text{-}0.00114060601334556 16$$

Topoccentric sun right ascension = <u>324.83023339604944 °</u>

$$\delta' = \frac{(Arc\tan 2((\sin\delta - y\times\sin\xi)\times\cos\Delta\alpha, \cos\delta - y\times\sin\xi\times\cos H))\times 180}{\pi}$$

$$\delta' = (Arc\tan 2((\sin(\text{-}14.0208977724624) - 0.64690617181611676\times \sin 0.0024749502047853949)\times\cos\text{-}\ 0.0011406060133455616, \cos(\text{-}14.0208977724624) - 0.64690617181611676\times \sin 0.0024749502047853949\times\cos 35.998003331206917))\times 180/\pi$$

Topocentric sun declination = <u>-14.022756224032634 °</u>

4.1.11 Zenith and Azimuth Angle Calculation: Follow to equation (71)-(76).

Asume: *Temparater: T= 36.5 ° C*

Pressure: P =1009.15 millibar

$$e_0 = \frac{(Arc\sin(\sin\varphi\times\sin\delta' + \cos\varphi\times\cos\delta'\cos H'))\times 180}{\pi}$$

$$e_0 = (Arc\sin(\sin 40.567476000000006\times\sin\text{-}14.022756224032634 + \cos 40.567476000000006\times\cos\text{-}14.022756224032634\times \cos 35.999143937220261))\times 180/\pi$$

= <u>26.019151827538703 °</u>

$$\Delta e = \frac{P}{1010}\times\frac{283}{273\times T}\times\frac{1.02}{60\times\tan(e_0 + \frac{10.3}{e_0 + 5.11})}$$

$$\Delta e = \frac{1009.15}{1010} \times \frac{283}{273 \times 36.5} \times$$

$$\frac{1.02}{60 \times \tan(26.019151827538703 + \frac{10.3}{26.019151827538703 + 5.11})}$$

$= \underline{0.031356324801866418^{\circ}}$

$e = e_0 + \Delta e$

$e = 26.019151827538703 + 0.031356324801866418$

$= 26.050508152340569^{\circ}$

$\theta = 90 - e$

$\theta = 90 - 26.050508152340569$

Zenith angle = $\underline{63.949491847659431^{\circ}}$

$$\Gamma = \frac{(Arc\tan 2(\sin H', \cos H' \times \sin\varphi - \tan\delta' \times \cos\varphi) \times 180}{\pi}$$

$\Gamma = (Arc\tan 2(\sin 35.999143937220261,$
$\cos 35.999143937220261 \times \sin 40.567476000000006 -$
$\tan\text{-}14.022756224032634 \times \cos 40.567476000000006) \times 180/\pi$

$= 39.88309573295^{\circ}$

$\Phi = \Gamma + 180$

$\Phi = 39.3883095732951 + 180$

Topocentric azimuth angle = $\underline{219.38830957325951^{\circ}}$

4.2 Transformation of Coordinates of Solar Light Calculation.

Example data for calculating transformation of coordinates.

Camera angle: Top view

Camera direction: South-East

Object turn = 30^{o}

4.2.1 Calculation for Convert Zenith Angle and Azimuth Angle to Stereographic Coordinate.

The Azimuth angle and the Zenith angle according to figure 3.8, to be calculated in SFS method must be transformed in comparison to Cartesian coordinate system or Stereographic Coordinate system.

For the former, Cartesian Coordinate system with consideration of VB Coordinate System, Zenith axis, if observer downwards directs camera to the object by following its axis, will become Z axis; at the same time, if observer turns camera towards the north, that will make the north be X axis. Then, when the coordination is transformed into the Stereographic coordinate system, Sl_s (slant of light) will equal to Z axis and Tl_s (tilt of light) will equal to 360- A, shown in figure 4.1.

Basically, no matter where direction of camera heads to or which angel photography is taken, the calculation must be taken by assuming all directions of cameras and all photographic angels to be as northern side and as top view angel accordingly, irrespective of those happened in reality. Consequently, now they will be calculated as follow.

X axis will be opposite to the northern side, so:

$$\begin{aligned} Tl_s &= 360 - \Phi \\ &= 360 - 219.38830957325951 \\ &= \underline{140.61169042674049^{o}}. \end{aligned}$$

Photography angle is Top view, so

$Sl_s = \theta$

$= \underline{63.949491847659431^{o}}.$

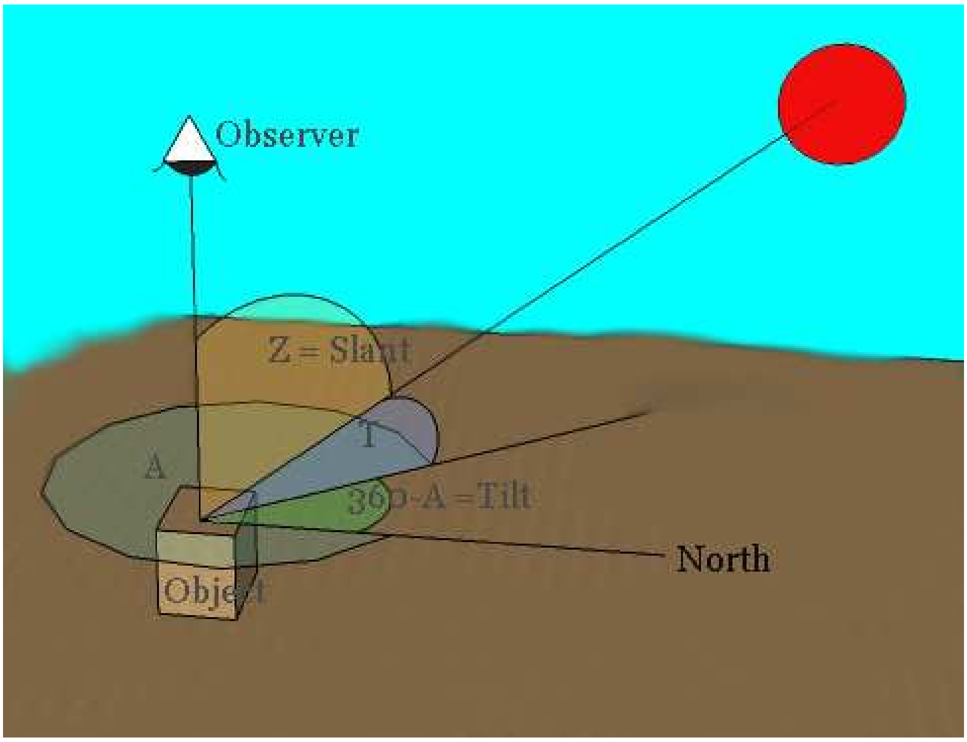

Figure 4.1 The azimuth and the zenith angle compare with the cartesian coordinate.

4.2.2 Calculation for Convert Light source from Stereographic Coordinate to Cartesian coordinate: Follow to equation (25).

This step is to relocate the position from (Sl, Tl, l) terms to (x, y, z) terms, leading to an easier calculating by transformation step. Then, since we require only the direction of light, amplitude will not be taken into account that means $l=1$, and direction of light becomes to be calculated as unit vector; therefore, according to equation (24), it can be calculated as:

$$\begin{vmatrix} x \\ y \\ z \end{vmatrix} = \begin{vmatrix} \sin Sl_s \times \cos Tl_s \\ \sin Sl_s \times \sin Tl_s \\ \cos Sl_s \end{vmatrix}$$

$$\begin{vmatrix} x \\ y \\ z \end{vmatrix} = \begin{vmatrix} \sin 63.949491847659431 \times \cos 140.61169042674049 \\ \sin 63.949491847659431 \times \sin 140.61169042674049 \\ \cos 63.949491847659431 \end{vmatrix}$$

$$\begin{vmatrix} x \\ y \\ z \end{vmatrix} = \begin{vmatrix} -0.69434578773306277 \\ 0.5701048011789764 \\ 0.439163293470093 \end{vmatrix}$$

4.2.3 Transformation Light source by Counter Clock Wise about Z axis Calculation: Follow to equation (77) and (80).

If observer views the object toward the north direction, Z axis will itself turn around. As far as Z axis is turning, it also creates any angels when turning along counter clock wise (CCW) direction, and such changing angels will be plus value. Conversely, when it is turning along opposite direction, any happened changing angels will be minus value in another way.

- Calculate for angle CCW about Z axis Z: z^o

z^o = Angle from north + Angle of turn object
= 225 + 30
=255 ^{o}

- Calculate for transformation CCW about Z axis.

$$|Aij| = \begin{vmatrix} \cos z^\circ & \sin z^\circ & 0 \\ -\sin z^\circ & \cos z^\circ & 0 \\ 0 & 0 & 1 \end{vmatrix}$$

$$|Aij| = \begin{vmatrix} \cos 255^o & \sin 255^o & 0 \\ -\sin 255^o & \cos 255^o & 0 \\ 0 & 0 & 1 \end{vmatrix}$$

$$\begin{vmatrix} x' \\ y' \\ z' \end{vmatrix} = |Aij| \bullet \begin{vmatrix} x \\ y \\ z \end{vmatrix}$$

$$\begin{vmatrix} x' \\ y' \\ z' \end{vmatrix} = \begin{vmatrix} \cos 255^o & \sin 255^o & 0 \\ -\sin 255^o & \cos 255^o & 0 \\ 0 & 0 & 1 \end{vmatrix} \bullet \begin{vmatrix} -0.69434578773306277 \\ 0.5701048011789764 \\ 0.439163293470093 \end{vmatrix}$$

$$\begin{vmatrix} x' \\ y' \\ z' \end{vmatrix} = \begin{vmatrix} 0.81824051907403206 \\ -0.37096907501024878 \\ 0.439163293470093 \end{vmatrix}$$

4.2.4 Transformation Light source by Counter Clock Wise about X axis Calculation: Follow to equation (77) and (78).

If observer converts photographic angle to be compatible with top view angle, turning X axis appears to be originated rather than turning Y axis, since according to VB coordinate, Y axis stays remain in the same level as observer’s head row. As far as X axis is turning along counter clock wise (CCW) direction or along Z axis toward Y axis direction, such changing angels will be plus. Conversely, when it is turning along opposite direction or along Z axis outward Y axis direction, any changing angels will be minus in another way.

- Find angle that CCW about X axis: x^o

x^o = Angular distance between top view to real sight

= 0^o

- Calculation for transformation CCW about X axis

In case of top view photography, the angel, turning around X axis is totally o degree. It is not necessary to be calculated for transformation, but calculation with zero degrees angle as shown below is only for an example of CCW about X axis calculation.

$$|Aij| = \begin{vmatrix} 1 & 0 & 0 \\ 0 & \cos x^\circ & \sin x^\circ \\ 0 & -\sin x^\circ & \cos x^\circ \end{vmatrix}$$

$$|Aij| = \begin{vmatrix} 1 & 0 & 0 \\ 0 & \cos 0^\circ & \sin 0^\circ \\ 0 & -\sin 0^\circ & \cos 0^\circ \end{vmatrix}$$

$$\begin{vmatrix} x' \\ y' \\ z' \end{vmatrix} = |Aij| \bullet \begin{vmatrix} x \\ y \\ z \end{vmatrix}$$

$$\begin{vmatrix} x' \\ y' \\ z' \end{vmatrix} = \begin{vmatrix} 1 & 0 & 0 \\ 0 & \cos 0^\circ & \sin 0^\circ \\ 0 & -\sin 0^\circ & \cos 0^\circ \end{vmatrix} \begin{vmatrix} 0.81824051907403206 \\ -0.37096907501024878 \\ 0.439163293470093 \end{vmatrix}$$

$$\begin{vmatrix} x' \\ y' \\ z' \end{vmatrix} = \begin{vmatrix} 0.81824051907403206 \\ -0.37096907501024878 \\ 0.439163293470093 \end{vmatrix}$$

4.2.5 Calculation for Convert Light source from Cartesian coordinate to Stereographic Coordinate: Follow to equation (25).

Tilt = $Arc\tan 2$ (y, x)

= $Arc\tan 2$ (0.370969075010248, 0.81824051907403206)

= -0.42565630104903213 radiens, -24.3888309573259537^{o}

$$\text{Slant} = Arccos(\, z \,)$$

$$= Arccos(\, 0.439163293470093 \,)$$

$$= \mathbf{1.116129187718929 \quad radiens, \quad 63.949491847659424\ ^{o}}$$

4.3 Transform and Make up Images.

From subtopic 3.1.3.5, we are known that Z axis of VB headed away against viewer's sight, and this may result in an error when images are matched with VB without transformation as shown in figure 4.2. Therefore, to precede SFS calculation, it is vital to transform images, for turning Z axis direction toward viewer's sight as figure 4.3 presents when images are matched with VB with transformation. Such transformation is to turn X axis into 180 degrees, and this problem is not able to be solved by use of equation transformation (2), but able to be solved by use of program for alternating coordinate's position by means of simply utilizing VB loop as presented by flowchart in figure 4.4. In developing software, this process itself relies on its procedure, to alter color shade into grayscale, which will combine all methods as one-step process, and will finally lead less CPU times.

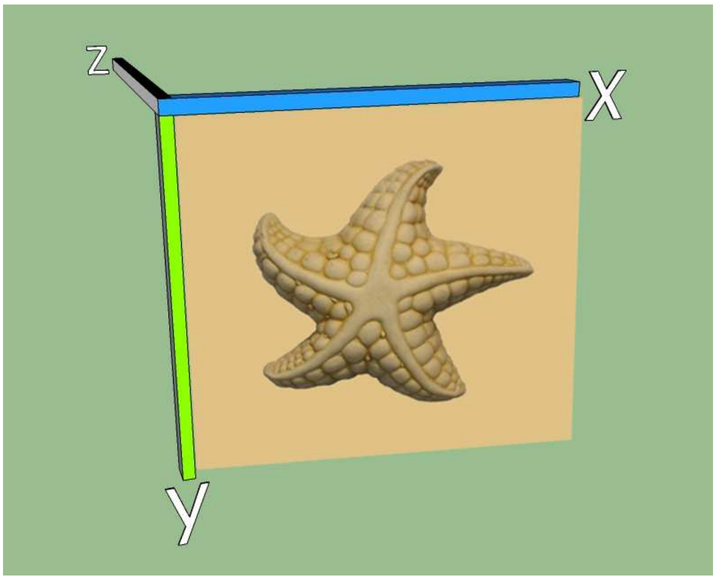

Figure 4.2 An image without transformation matching to VB.

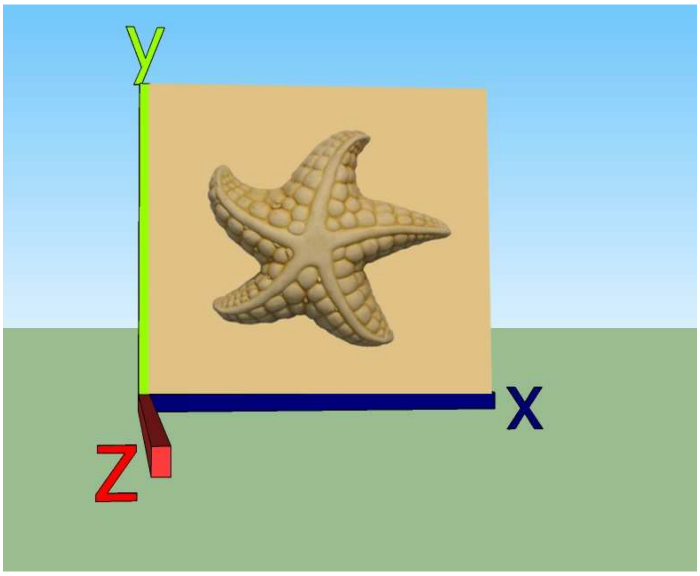

Figure 4.3 An image with transformation matching to VB.

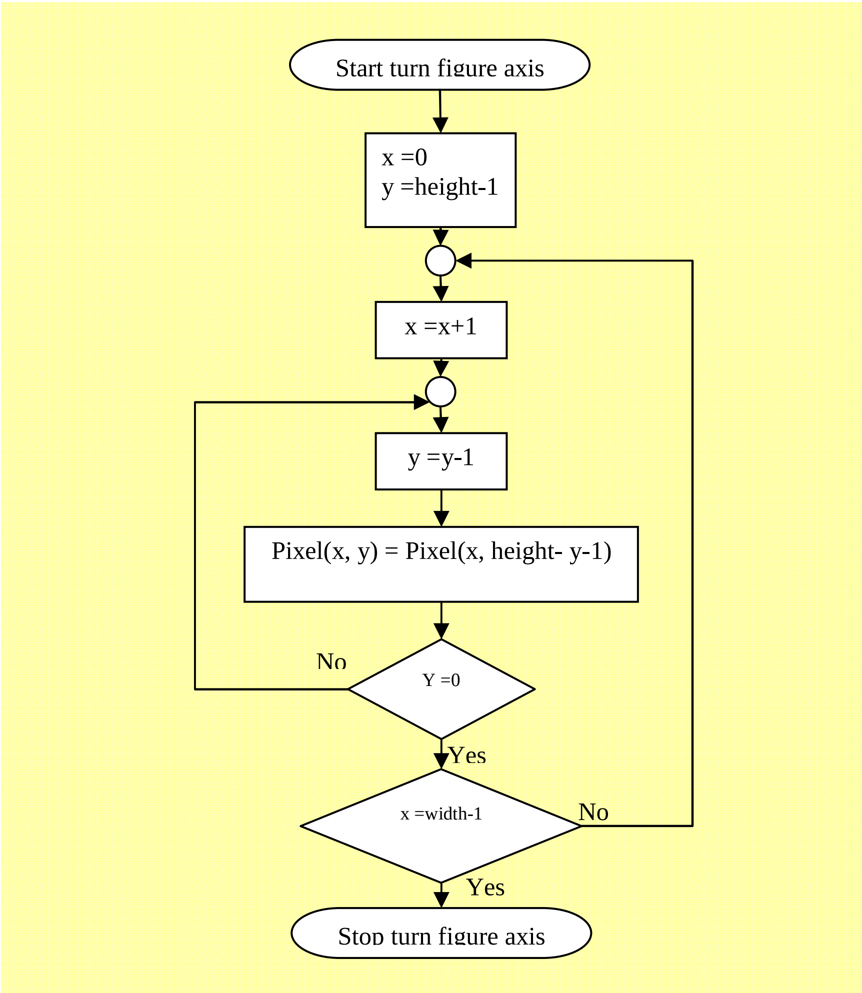

Figure 4.4 A schedule for figure transformation about X axis 180 degrees by programming.

4.4 Calculation for Converting Color Image to Gray Scale: Follow to equation (82).

This topic is related to a use of example images for calculating as the following figure 4.5 was synthetically formed with 5x5 pixel size. After finishing all process according to figure 4.4, it can be found that pixel (x, y) = (0, 0) was located at down-left corner of image and led x axis to be headed out, owing to avoiding any calculating mistakes from z values.

R160 G150 B149	R248 G237 B243	R255 G248 B255	R255 G245 B255	R255 G253 B141
R138 G129 B130	R216 G207 B212	R254 G242 B254	R255 G250 B252	R255 G255 B228
R174 G172 B173	R183 G179 B180	R180 G174 B176	R208 G201 B183	R245 G243 B186
R183 G184 B204	R175 G174 B190	R174 G171 B176	R210 G208 B187	R243 G244 B174
R163 G168 B223	R169 G171 B219	R186 G185 B216	R224 G224 B216	R246 G249 B82

Figure 4.5 An example image with Red Green Blue color level. Calculation by

equation (81) to find gray scale will show for example only in pixel (0, 0).

$$R_G, G_G, B_G = (R*0.299)+(G*0.587)+(B*0.114)$$

$$Grayscale(0,0) = (163\times 0.299)+(168\times 0.587)+(223\times 0.114)$$

$$=\underline{172.775}$$

For finding gray scale in all pixels, we need to solve equation (81). After acquiring the result of gray scale calculation as shown in figure 4.6, we will find the

Y

152.876	240.973	241.921	249.130	252.230
131.805	210.261	246.956	251.723	251.922
172.712	189.310	176.022	201.041	237.100
185.981	176.123	172.467	206.204	235.721
172.775	175.874	188.833	223.088	240.465

X

Figure 4.6 Gray scale result form example image.

Maximum color shade is in order to prepare a next calculation for SFS.

Maxshade = Gray scale at pixel(5,4) = 252.230

4.5 Tsi-Shah're Shape from Shading calculation.

For easily manual calculation, this calculation topic will be divided by using different criteria from calculation as shown in topic 3.1.2, emphasizing on writing program; however, the calculation will remain the same principle.

4.5.1 Calculation for Changing and Transformation Coordinates Light Source from SPA to Light gradient: Follow to equation (12) and (13).

$$q_s = \sin(Tl_s) \times \tan(Sl_s)$$

$$p_s = \cos(Tl_s) \times \tan(Sl_s)$$

$$q_s = \sin(\text{-24.388830.9573259537}) \times \tan(63.949491847659424)$$

$$p_s = \cos(\text{-24.388830.9573259537}) \times \tan(63.949491847659424)$$

$$q_s = \underline{-0.84471785444316}$$

$$p_s = \underline{1.8631805782505688}$$

4.5.2 Specification in starting calculate Tsi-Shah're SFS.

Specify height value z(x,y) equal 0 to all points of pixel.

$$z(x,y)_{start} = \begin{vmatrix} 0 & 0 & 0 & 0 & 0 \\ 0 & 0 & 0 & 0 & 0 \\ 0 & 0 & 0 & 0 & 0 \\ 0 & 0 & 0 & 0 & 0 \\ 0 & 0 & 0 & 0 & 0 \end{vmatrix}$$

Specify standard divation value Sn(x,y) equal 1 to all point of pixel.

$$(Sn(x,y))_{start} = \begin{vmatrix} 1 & 1 & 1 & 1 & 1 \\ 1 & 1 & 1 & 1 & 1 \\ 1 & 1 & 1 & 1 & 1 \\ 1 & 1 & 1 & 1 & 1 \\ 1 & 1 & 1 & 1 & 1 \end{vmatrix}$$

Specify a small value to Wn, this calculation equals 0.01:Wn =0.01.

4.5.3 Caluation example in 1st loop: Where (x, y) = (0, 0).

Find p,q value at (x,y) equal (0,0) as follow.

$x = 0 , p = 0$

$y = 0 ,q = 0$

Henceforth, calculation will be in line with equation (14)-(18).

$$pq = 1.0 + p^2 + q^2$$

$$pq = 1.0 + 0^2 + 0^2$$

$$= \underline{1.0}$$

$$pq_s = 1.0 + p_s^2 + q_s^2$$

$$pq_s = 1.0 + 1.8631805782505688^2 + \text{-}0.84471785444316^2$$

$$= \underline{5.18499012078518}$$

$$E_p(x, y) = \frac{shade(x, y)}{Maxshade}$$

$$E_p(0,0) = \frac{172.775}{252.230}$$

$$= \underline{0.68650793650793651}$$

$$R(x, y) = \frac{1 + p \times p_s + q \times q_s}{\sqrt{pq} \times \sqrt{pq_s}}$$

$$R(0,0) = \frac{1 + 0 \times 1.8631805782505688 + 0 \times \text{-}0.84471785444316}{\sqrt{1} \times \sqrt{5.18499012078518}}$$

$$= \underline{0.43916329347009292}$$

$$dfz = -1 \times \frac{p_s + q_s}{\sqrt{pq} \times \sqrt{pq_s}} - \frac{p + q \times (1.0 + p \times p_s + q \times q_s)}{\sqrt{pq^3} \times \sqrt{pq_s}}$$

$$dfz = -1 \times \frac{1.8631805782505688 + q_s}{\sqrt{1} \times \sqrt{5.18499012078518}} - \frac{0 + 0 \times (1.0 + 0 \times 1.8631805782505688 + 0 \times \text{-}0.84471785444316)}{\sqrt{1^3} \times \sqrt{5.18499012078518}}$$

$$= \underline{-0.4472714406378322}$$

$$k_d = \frac{Sn(x,y) \times dfz}{Wn + Sn(x,y) \times dfz^2}$$

$$k_d = \frac{1 \times \text{-}0.4472714406378322}{0.01 + 1 \times \text{-}0.4472714406378322^{\,2}}$$

$$= \underline{-2.12933934329385}$$

4.5.4 Calculation for find Gradient(p , q) that used in next-loop of x , y.

In the next loop $(x, y)^{next} = (0, 1)$

$x^{nextloop} = 0$, so

$p^{nextloop}$ will not equal z(x+1, y)- $z(x,y)$ but will equal 0: $p^{nextloop}$ **= 0**

$y^{nextloop} > 0$, so

$q^{nextloop}$ = z(x, y+1) - $z(x,y)$

$q^{nextloop}$ = 0- 0.52668067977345367

= $\underline{-0.52668067977345367}$

4.5.5 Calculation for find Z(x, y) and Sn(x, y) that used in next-loop of k .

The characteristic of k value is the number of round which can be assumed by researcher and must be valued more than 1. It was assumed to be equal 6 in this calculation.

$$Sn^{next-k}(x,y) = (1 - k_d \times dfz) \times Sn(x,y)$$

$$Sn^{next-k}(0,0) = (1 - \text{-}2.12933934329385 \times \text{-}0.4472714406378322\,) \times 1$$

$$= \underline{0.047607317023131812}$$

$$z^{next\_k}(x,y) = z(x,y) + k_d \times (R(x,y) - E_p(x,y))$$

$$z^{next\_k}(0,0) = z(x,y) + k_d \times (R(x,y) - 0.68650793\ 650793651$$

$$= \underline{0.52668067977345367}$$

The lastest calculation of k round, k = 6, $z^{next\_k}(x,y)$ will be $z(x,y)$. The results of the lastest k round, if not calculate the Normalization, will be Cloud of point in pattern as follow.

x0 y0 z1.31532264336715 : *x0 y1 z1.92089552509008*

x0 y2 z1.04015174203051 : *x0 y3 z0.08260119214291*

x0 y4 z1.62939891128292 : *x1 y0 z1.33349282828536*

x1 y1 z1.76535401334294 : *x1 y2 z1.14635756326588*

x1 y3 z0.72645505358669 : *x1 y4 z2.07916402510338*

x2 y0 z1.43174272457168 : *x2 y1 z1.48562672155279*

x2 y2 z1.30676870446686 : *x2 y3 z1.35274192595538*

x2 y4 z2.19883056980417 : *x3 y0 z1.74279575286074*

x3 y1 z1.46771960927611 : *x3 y2 z1.56335243393555*

x3 y3 z1.89719775807576 : *x3 y4 z2.28387319228941*

x4 y0 z2.08049616151646 : *x4 y1 z1.79859245469399*

x4 y2 z1.93459574976023 : *x4 y3 z2.71511964041032*

x4 y4 z2.6156890167323

4.6 Normalization Calculation: Follow to equation (24).

This step is to calculate normalization. There is an essential concern in this method, a comparison of dimension- between height or width of material and width, length, or width of figure in pixel unit. Height of figure unit can be found by multiple with ration between material dimension and pixel of material figure.

For example, figure 4.2 has its width $\times$ length equal 5 $\times$ 5 pixel, and material has its width $\times$length$\times$ height equal 10 $\times$ 10 $\times$ 8 then as follow.

Ratio = 5/10 = 1/2, so the highest z in pixel unit is 4 pixels.

From the calculation results in topic 4.5.5, it will be able to find z (min) and z (max) as follow.

z (min) = 0.08260119214291

z (max) = 2.71511964041032

o (min) = 0

o (max) = 4

$$z^{norm}(x,y) = \left[\frac{z\ \ (x,y) - z(\min)}{z(\max) - z(\min)} \times o(\max) - o(\min)\right] + o(\min)$$

$$z^{norm}(0,0) = \left[\frac{1.31532264336715 - 0.08260119214291}{2.71511964041032 - 0.08260119214291} \times 4 - 0\right] + 0$$

$$= \underline{1.87306790124955}$$

After all pixel calculations have done, the results are presented as follow.

x0 y0 z1.87306790124955 : *x0 y1 z2.79321018115872*

x0 y2 z1.45495740099039 : *x0 y3 z0*

x0 y4 z2.350293454023 : *x1 y0 z1.90067672568939*

x1 y1 z2.55687145867112 : *x1 y2 z1.61633263664014*

x1 y3 z0.97830860310595 : *x1 y4 z3.03369244652322*

x2 y0 z2.04996327120397 : *x2 y1 z2.13183771659155* *x2 y2 z1.86007055430838 : x2 y3 z1.92992491224275*

x2 y4 z3.21552067990871 : x3 y0 z2.5225951397385

x3 y1 z2.10462861985991 : x3 y2 z2.24993863616369

x3 y3 z2.75720243043633 : x3 y4 z3.34473933369054

x4 y0 z3.03571657123765 : x4 y1 z2.60737585893153

x4 y2 z2.81402709080532 : x4 y3 z4

x4 y4 z3.84891938934983

The cloud of points will be taken to create 3D surface by CATIA.

CHAPTER V
RESEARCH METHODOLOGY AND RESULT

5.1 Step of Research Methodology

5.1.1 A study of research and related theories

To analyze problem, other limitations and benefits of Image processing by comparing all of them with SFS, in order to properly meet the most profitability of this research.

To investigate groups of SFS methods in order to prepare properly SFS method for further researches.

To study a possibility to apply the solar light to being data for SFS calculation.

To study procedures and principles for calculating the direction of solar light.

To study research that adopts an application of SFS in order to assert the possibility of using SFS with the direction of solar light.

To find tools for solving the research’s problems.

5.1.2 Selection of SFS and solar position methods will be held on the basis of a comparison of previous result from topic 5.1.1 to expected result in order to gain the most appropriate SFS and Solar position methods for this research.

5.1.3 Tools creation, since the process of SFS and solar position concern with complicated calculating method, it is necessary to perform on the particular tools.

5.1.4 Tools examination and failure improvement focuses on these main issues as follow:

To select the figure for testing SFS procedure and to prepare data for testing the solar position.

To conclude occurring problems with the created tools, to solve them, and to retest such created tools.

5.1.5 Material Selection, because the light used in this research is in the form of solar light, not applicable for synthetic image, and otherwise photos taken with unidentified place, the direction, including the weather surrounding where they are taken cannot be adopted. It is necessary for researcher to discover the most proper materials in order to offset limitations of this research.

5.1.6 Data Input, figures already adjusted appropriately together with all data are taken to the developed calculating tools

5.1.7 Conclusion and Recommendation, all operation's result of the research will be summarized in terms of the quality of performing SFS based on the solar light's data, SFS application, problems or limitations as well as recommendations for further development.

5.1.8 Report Completion

5.2 Times of Research

Table 5.1 Table of research planner.

Item	**Research Plan**	**2009**			**2010**				
		Oct.	Nov.	Dec.	Jan.	Feb.	Mar.	Apr.	May
1	Study research and related theory								
2	Select properly SFS method and Solar position method								

Table 5.1 Table of research planner (cont.).

Item	Research Plan	2009			2010				
		Oct.	Nov.	Dec.	Jan.	Feb.	Mar.	Apr.	May
3	Create tools								
4	Examine tools and improve failure								
5	Select material for photography and bring it for this research								
6	Bring figure to research tools								
7	Conclude and recommend								
8	Complete the report								

5.3 Selecting properly SFS method and solar position method

5.3.1 SFS methods

There is a large number of existing SFS methods, for example, shown on table 5.2 and discussed in topic2.1. As far as they all have been concerned, it was rather hard to pick out one of them, so researcher decided to choose it from previously examined methods. Durou et al (2008) and Zhang et al (1999) did a survey, analyzed its result and extracted a small number of SFS methods as presented on table5.2:

Table 5.2 Example of SFS methods

SFS methods	Property
Pentland (1990)	Fourier transform
Tsi, Shah (1999)	Newton-Raphson

Table 5.2 Example of SFS methods (cont.)

SFS methods	Property
Chang et Al (2008)	Graph cut
Robles-Kelly &Hancock (2007)	Heat equation
Hsieh et Al (1995)	wavelet-based
Leclers&Bobick (1991)	Direct SFS
Cheung et Al (1997)	Direct SFS
Ahmed & Farag (2007)	Ward reflectance model
Volgel et al (2008)	Pong reflectance model
Zheng & Chellappa	Taylor series (minimize)
Bichsel & Pentland	Propagation Approache
Lee & Rosenfeld (1985)	Local Approache
Lee & Kuo (1991)	V-cycle multigrid scheme
Daniel & Durou (2000)	Minimize Approch
Falcone & Sagono (1997)	Local Approch (semi-Lagrangian approximation)
Durou et al (2008)	Surways
Zhang et al (1999)	

To meet the objectives of this research, an applicable of SFS to solar light must be focused on which needs only real images rather than synthetic images. As a result, there are a few SFS methods which are compatible with this principle as shown on table5.4:

Table 5.3 SFS methods in surveys of Durou et al and Zhang et al

SFS methods	Property
Pentland (1988)	Fourier transform
Tsi, Shah (1999)	Newton-Raphson
Zheng & Chellappa (1985)	Taylor series (minimize)

Table 5.3 SFS methods in surveys of Durou et al and Zhang et al (cont.)

SFS methods	Property
Bichsel & Pentland (1992)	Propagation Approache
Lee & Rosenfeld (1985)	Local Approache
lee & Kuo (1991)	V-cycle multigrid scheme
Daniel & Durou (2000)	Minimize Approch
Falcone & Sagono (1997)	Local Approch (semi-Lagrangian approximation)

Table 5.4 SFS method easy used with real image

SFS methods	Property
Tsi, Shah (1999)	Newton-Raphson
Daniel & Durou (2000)	Minimize Approch
Falcone & Sagono (1997)	Local Approch (semi-Lagrangian approximation)

Tsi-Shah method finally was chosen to be used for this research due to its shortest calculating time and suitability for personnel computer, mainly a processing tool. Specifications of Tsi-Shah method are listed as follow:

- Provided the least CPU times
- Does not need occluding boundary
- Does not need singular point
- Good in smooth surface
- But has much error in non smooth surface

5.3.2 Solar position method

For finding solar position, Reda and Andreas method has been selected from all available methods on table 5.5 on the basis of the longest adoptable time and the most accurate result measurement.

Table 5.5 Solar position method

Solar position methods	**Period / Error**
Michalsky (1988)	1950-2050 / 0.01 degrees
Blanco et al (2001)	1995 - 2015 / 0.008 degrees
Reda and Andreas , SPA (2004)	2000 BC.- 6000 /0.0003 degrees
Grena (2008)	2003 – 2022 / 0.0027 degrees.

5.4 Design concept explaining

Further explanations from topic 2.2 are provided in this topic in terms of Design concept - main idea developed by researcher. Its process appears on figure 5.1.

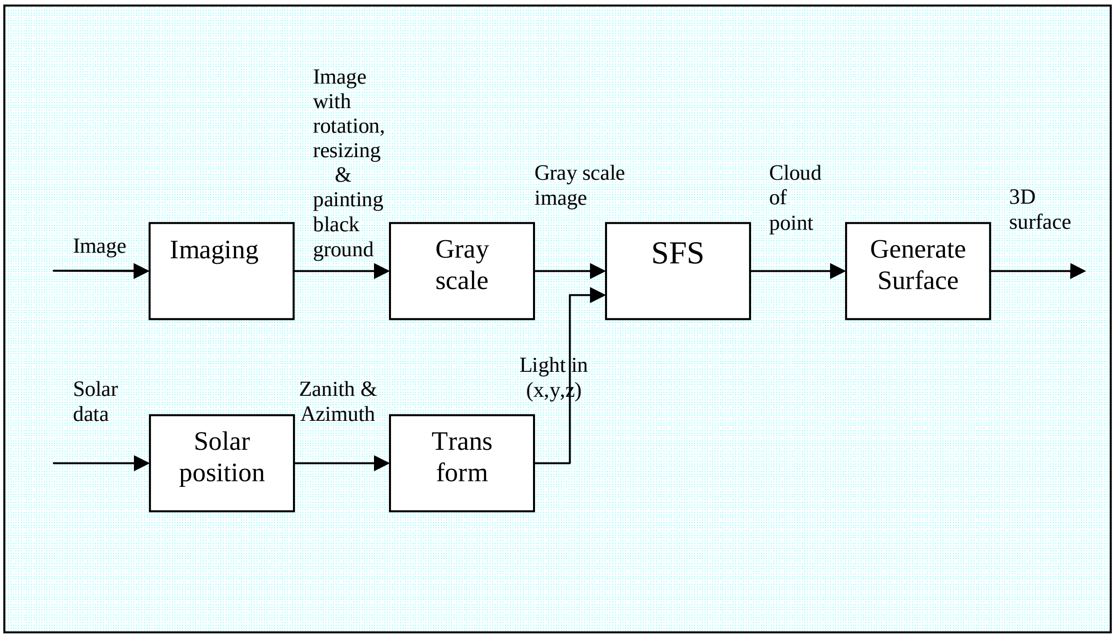

Figure 5.1 Black boxes for explain a design concept.

5.4.1 Imaging black box explaining

The process runs by means of utilizing Imaging program -GIMP 2.7 was specially selected for this research- and involves in pre-arranged input process. Firstly, the process begins with resizing image as it customized size, shown on figure 5.2a, and subsequently adjusting its background, shown on figure 5.2b. The final step is to rotate photo in order to alter light direction; however, it is subject to particular case, shown on figure 5.2 c which presented clockwise rotation with 90-degree angle. The rotation will happen in only two cases- for the use of combination point clouds and for acquiring the right direction of light leading to accuracy in Tsi-Shah SFS calculation.

5.2 a 5.2 b 5.2 c

Figure 5.2 Process in imaging black box

5.4.2 Gray scale black box explaining

This process is a part of software tool developed by researcher to calculate grey scale level. According to figure 5.3, for better understanding, the whole process can be divided into 3 sub processes- transformation from figure 5.3a to 5.3b in order to enable Z axis to stray away, Gray scale level's calculation, and maximum color shade's calculation-.

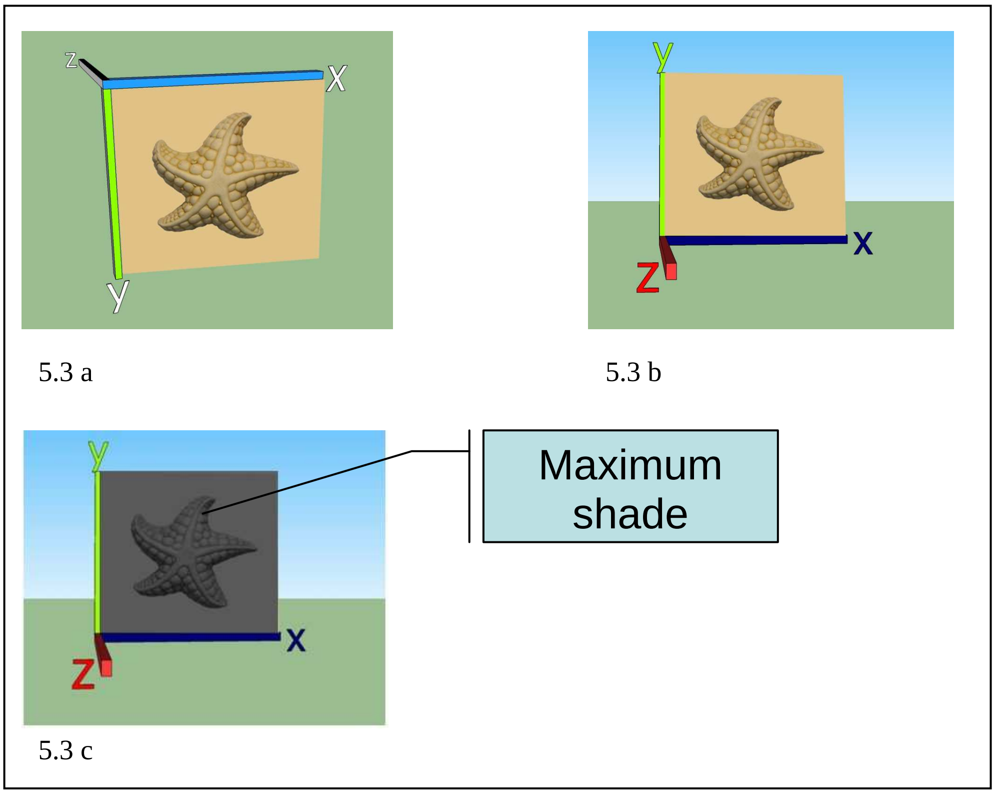

Figure 5.3 Process in gray scale black box

5.4.3 Solar position black box explaining

This process and aims to calculate Zenith angle and Azimuth angle based on the position of the sun, presented on figure 5.4. -The process lies in the developed software tool-.

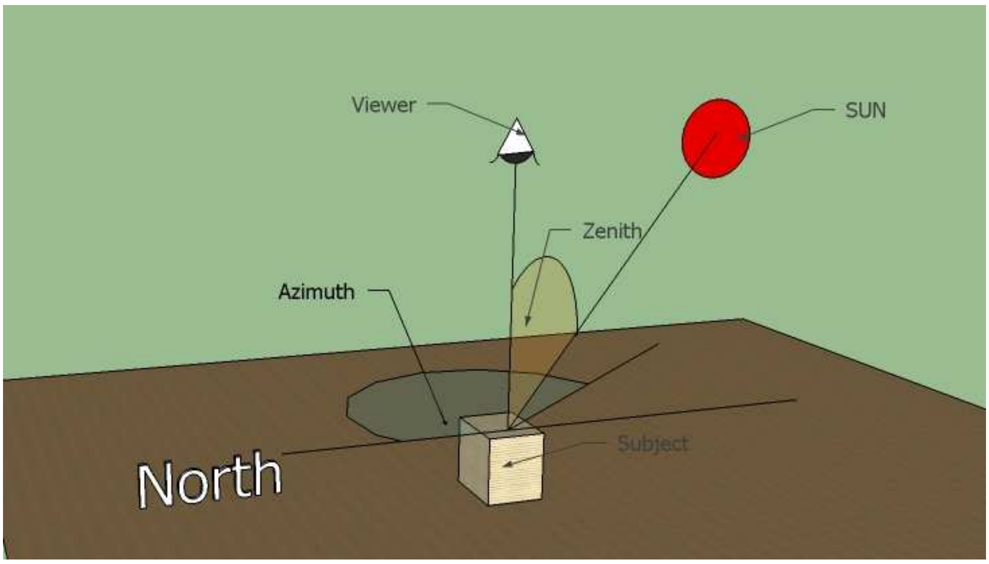

Figure 5.4 Azimuth and Zenith angle before transform

5.4.4 Transform black box explaining

Owing to an inconvenience for further calculation, it is necessary for Azimuth angle and Zenith angle to convert their values into Cartesian coordinate system. There is an alteration from figure 5.4 to figure 5.5. More importantly, when photo is rotated along clockwise direction with 90-degree angle according to figure 5.6, it will conversely cause Z axis to be rotated along anti-clockwise direction with 90-degree angle, from figure 5.5 to figure 5.7. -The process lies in the developed software tool -.

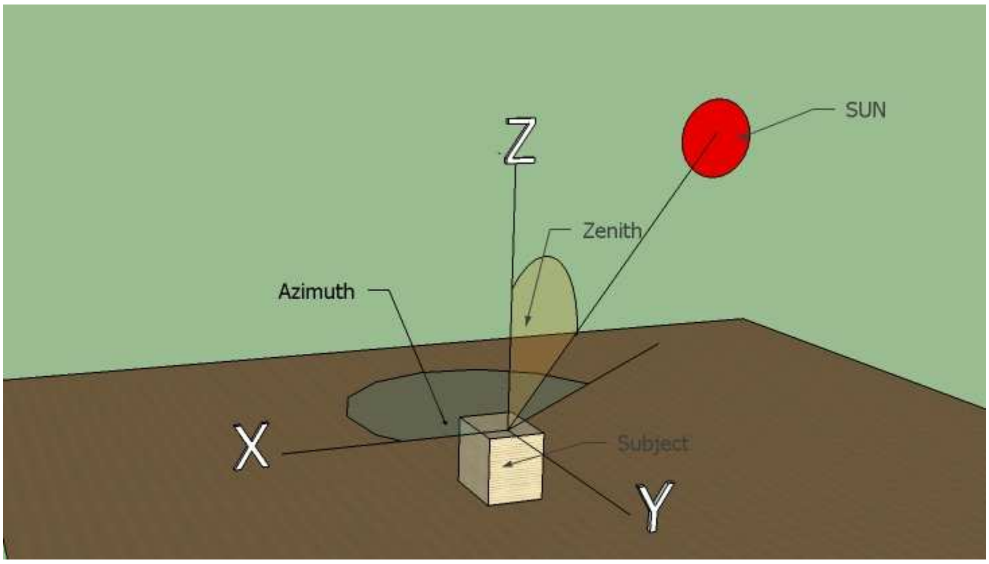

Figure 5.5 Transformation Azimuth and Zenith angle to the Cartesian coordinate system

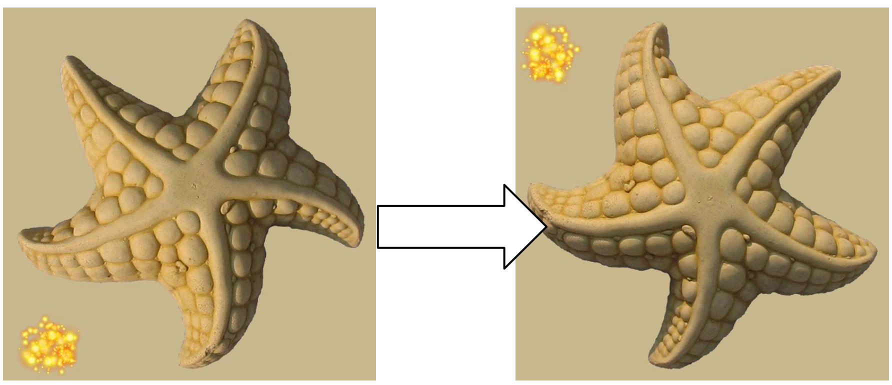

5.6 a 5.6 b

Figure 5.6 Turning image CW 90^0

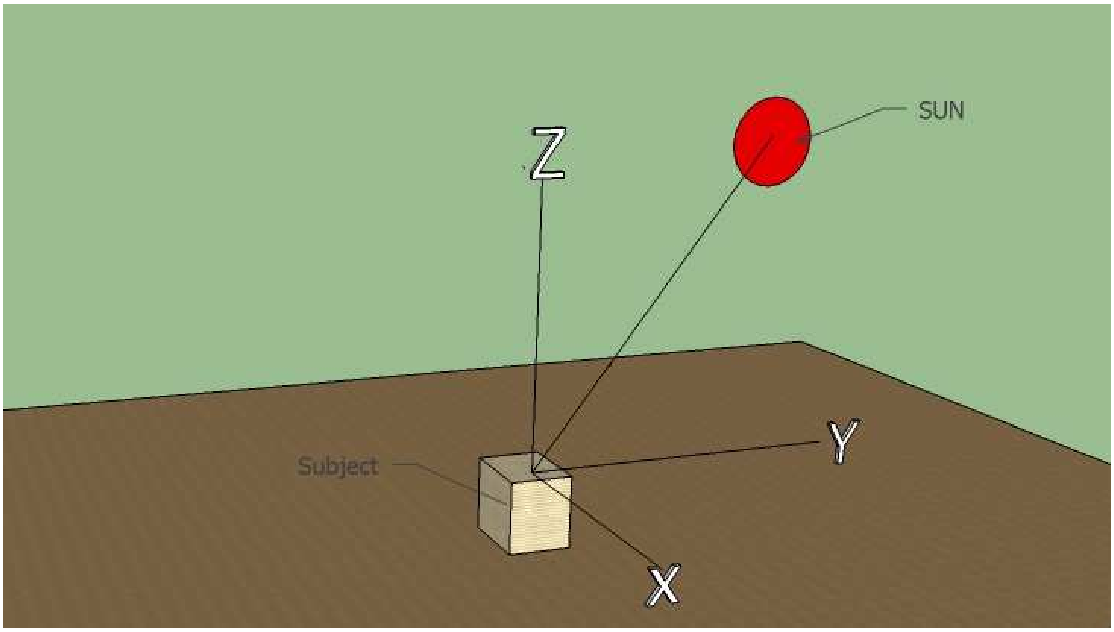

Figure 5.7 Result of transformation CCW Z axis 90^0 from figure 5.5

5.4.5 SFS black box explaining

When image and light direction data are available, they will be used for calculating Tsi-Shah's SFS and also for calculating normalization. The results will proceed in the form of point cloud with file type named .asc. The following examples include 4 points of cloud:

x0 y0 z6.313712311585
x0 y1 z5.31303319795297
x0 y2 z6.6573135046885
x0 y3 z7.84438874619771

2.2.6 Generate surface black box explaining

This process is to develop 3D surface from point cloud together with to improve 3D surface's perspective- subsequently to improve point cloud, to generate meshes and to improve meshes again-. Otherwise, the process may be classified as point cloud combination or surface combination.

5.5 Flowchart for system and program procedure

5.5.1 System procedure

In calculating the SFS with the direction of solar light, it consists of 3 procedures -the direction of solar light calculation, SFS calculation, light transformation calculation by matching coordinate of the direction between solar light and figure-. As shown on figure 5.8, system procedure begins with data for calculating the solar light direction such as sub-district, time, zone time, temperature, air pressure and delta T.

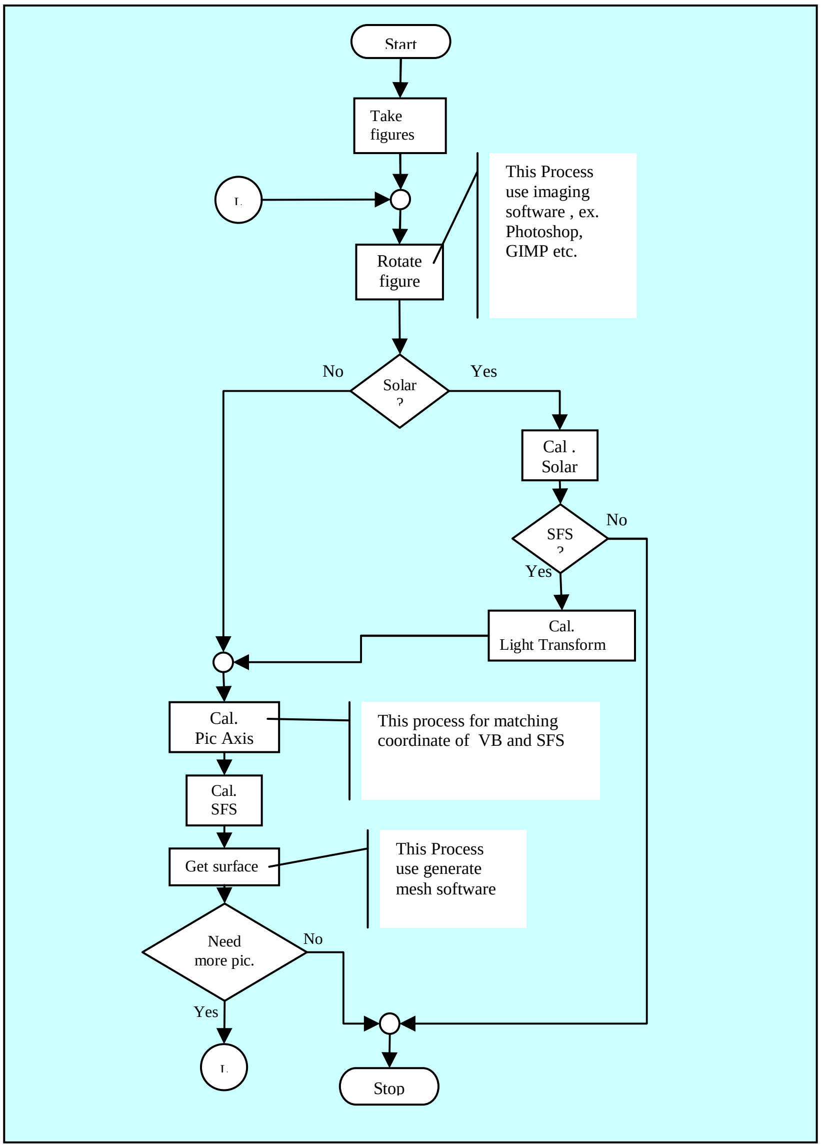

5.8 System procedure flowchart.

5.5.1.1 Take figures is a process of photography which location must be arranged by identifying sub-district place, selecting the smooth place examined by the water level together with determining the direction of place by using compass as a tool. While taking figures, some necessary data must be recorded, timing based on local standard time, temperature and air pressure which in case of being unable to be recorded, Thailand's average temperature and air pressure in 2008 can be substitute.

5.5.1.2 Rotate figure is a process for switching figure in case of more than 1 figure used for top view photography in order to adjust material of the figures into the same direction. In this step, the figure around the edge of material will be modified into material's boundary.

5.5.1.3 Cal. Solar is a calculating process to find the direction of solar light in which its results are the form of Azimuth angle and Zenith angle (Horizon system of Coordinate). Optionally, the procedure can be dwindled by remaining only the direction of light data collection.

5.5.1.4 Cal Pic Axis is a process for transforming the direction of figure's axis, Z axis, heading out of viewer for preparing SFS calculation.

5.5.1.5 Cal. SFS is a part of SFS calculation by Tsi-Shah, feeding data by which are in the form of figure and direction of light.

5.5.1.6 Cal. Transform is a process for changing the direction of light from Horizon system of Coordinate into Cartesian coordinate and enabling the direction of X Y Z axis to follow Cal. In handling SFS, the direction of solar light must be additionally calculated if the figure is previously rotated because rotating figure procedure seems to results in rotating the direction of light.

5.5.1.7 Get Surface is to create surface from x y z point and other positions resulting from SFS calculation in order to present overall view after all procedures have been done. More significantly, a combination of figure output to the same surface, by selecting the best of each figure measured by eye sight, will appear on this process.

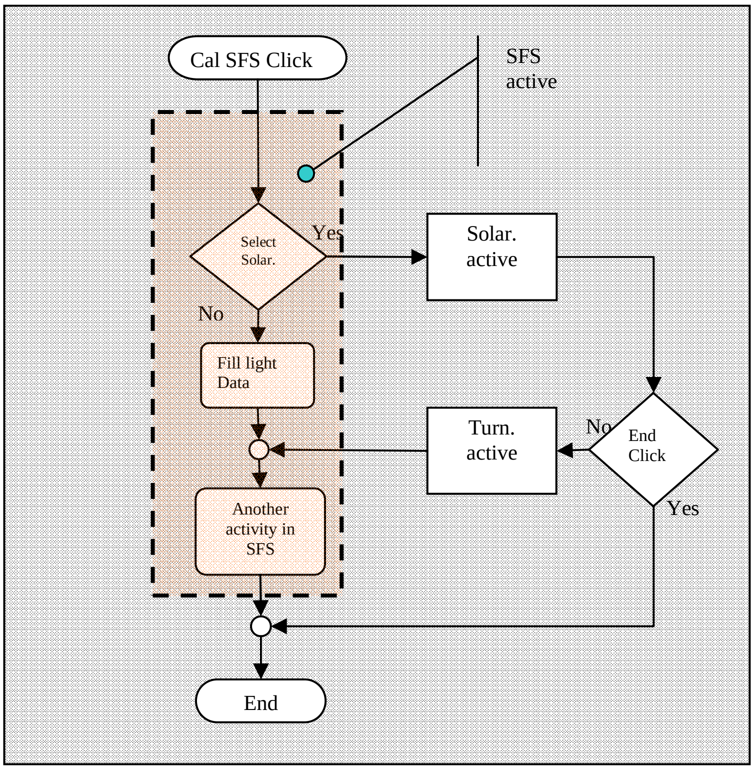

Figure 5.9 Flowchart when a Cal SFS button in the Main Form is clicked.

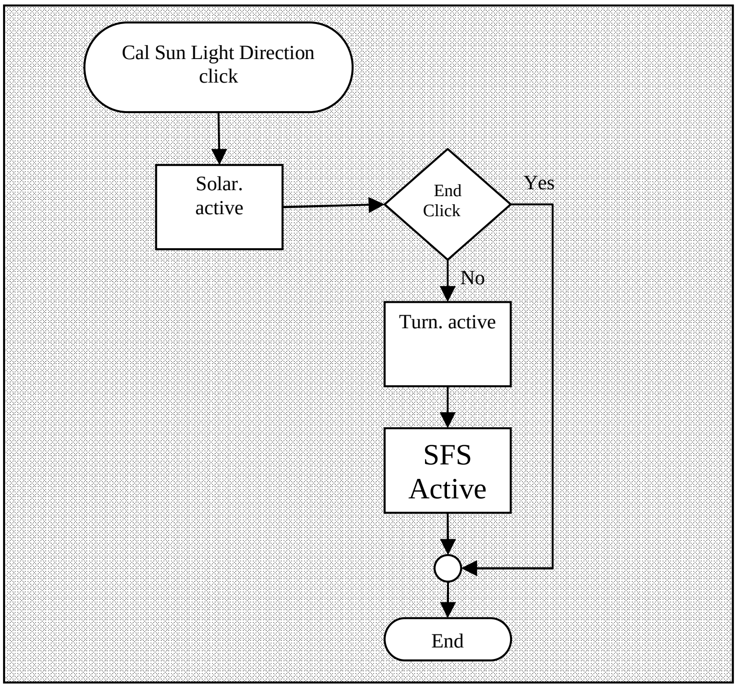

Figure 5.10 Flowchart when a Cal Sun Light Direction button in the Main Form is clicked.

5.5.2 Program procedure

To create tools, there are four forms of VB 2008, used for writing code and creating GUI as follows:

- Main Form is a main form to control all sub-forms.
- SFS Form is a sub-form to calculate SFS
- Calculate Solar Light Form is a sub-form for calculating the direction of sun light.
- Calculate Angle Turn is a sub-form for enabling the coordinate light to be calculated in SFS Form

A manual of developing program tools is in Appendix B and explains the concept in figure 5.9-5.13

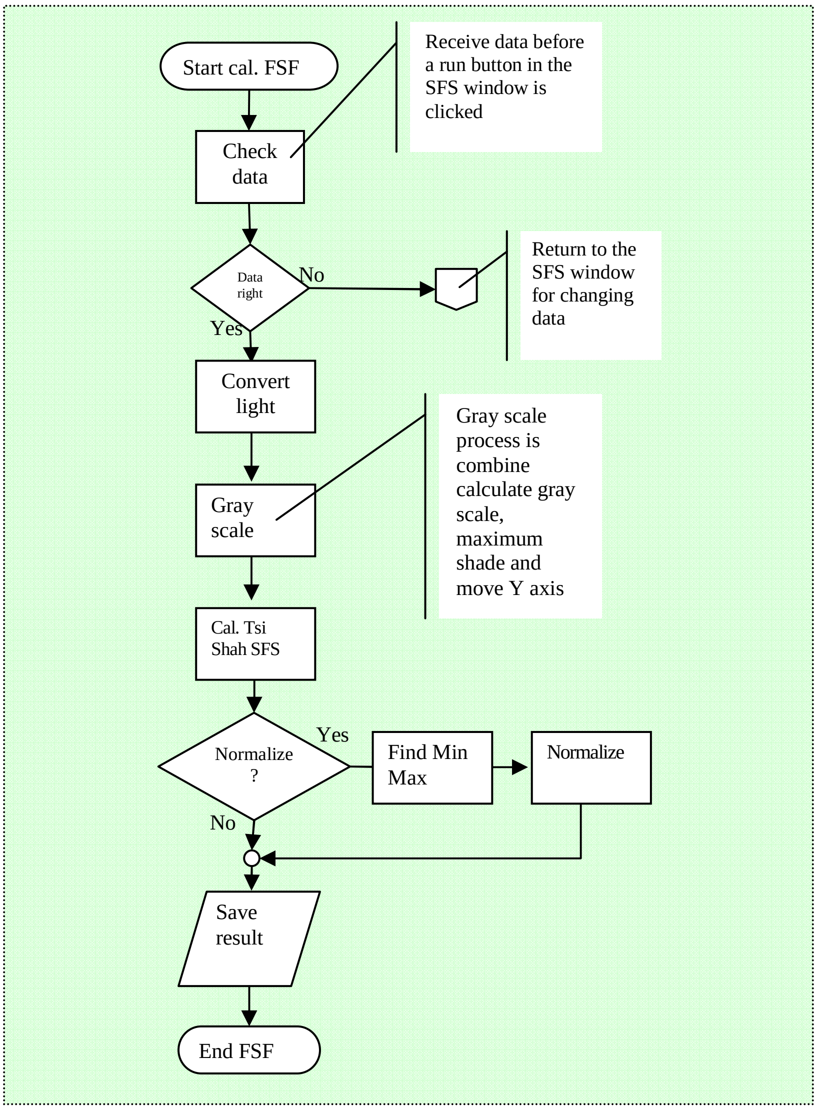

Figure 5.11 Flowchart when a Run button in the FSF Form is clicked.

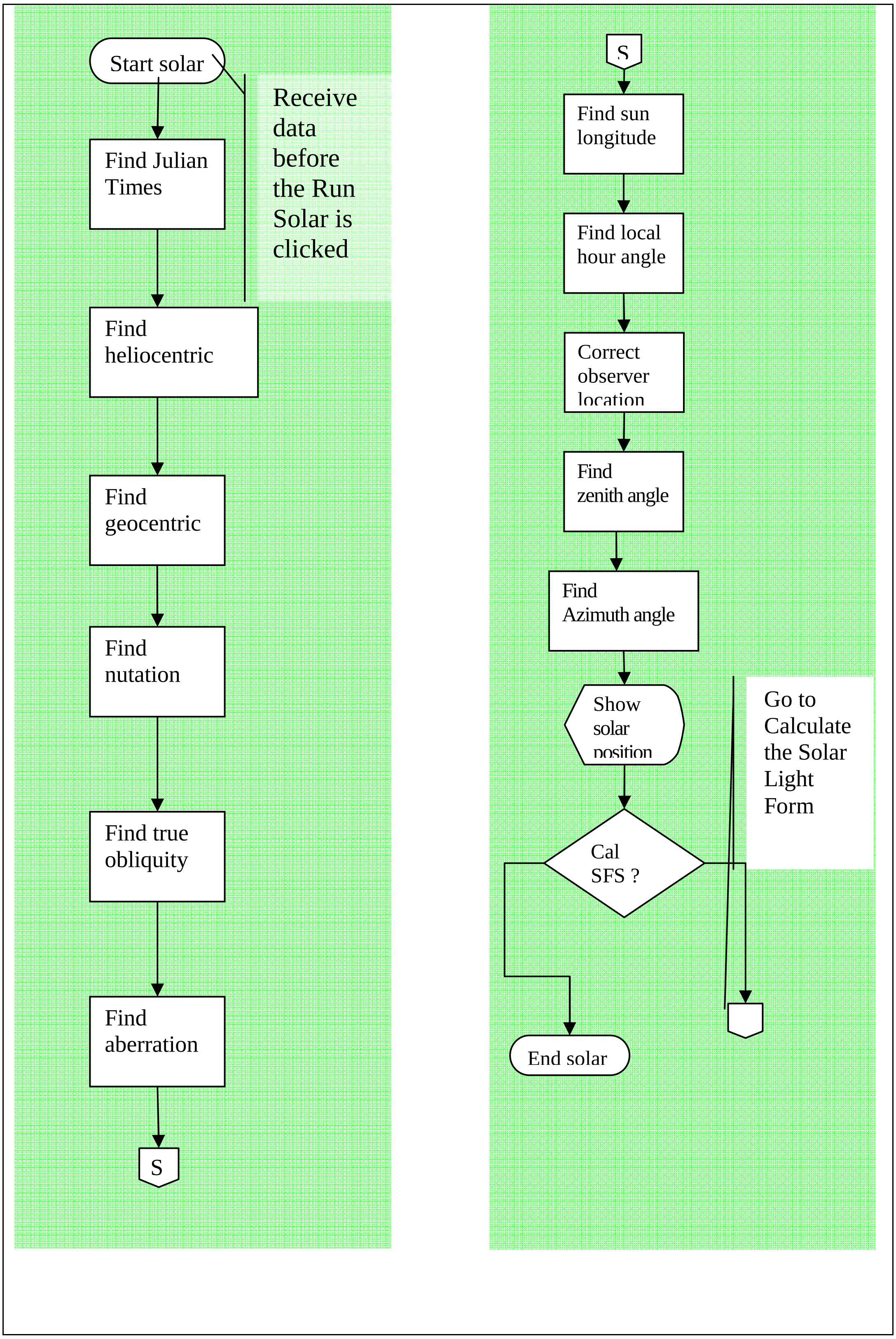

Figure 5.12 Flowchart when a Run Solar button in the Calculate Solar Light Form is clicked.

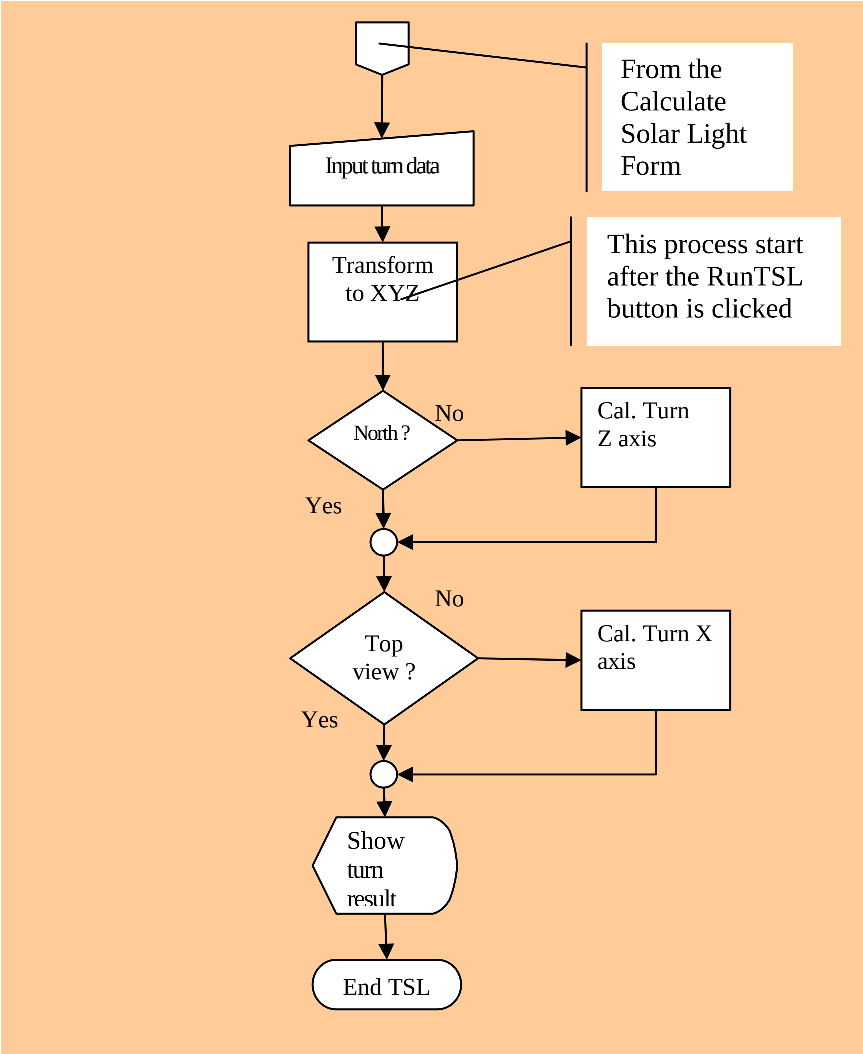

Figure 5.13 Flowchart when click Ok button in massage box of the Calculate Solar Light Form is clicked, final time.

5.6 Chosen Objects

Because this research emphasizes on the use of sun as a light source for calculating the SFS, to reveal the procedure and the quality of solar light, synthetic figure, figure taken beyond the solar light, and even figure taken under the solar light without identified time, place or unknown direction of photography will not be taken into account. However, it is difficult to completely find such a customized figure from existing popular figures which are normally used for image processing test. It is important to take real figures by selecting 3 materials- Can, Button and Starfish - based on different level of their features and surface shown on figure 5.14, respectively starting from minimum to maximum complication of their surface on the basis of 3 following principles:

5.6.1 Can

According to its feature, Geometry type (cylinder). can will be used as substitute for simply shape material.

5.6.2 Bottle

Since button possesses a bit more curves on its surface, it will be used as substitute for non-basic Geometry type.

5.6.3 Star fish

Star fish is classified as the most complicated surface in the group of testing materials; therefore, it will be used as substitute for freeform type.

5.14a 5.14b 5.14c

Figure 5.14 The objects for testing 5.14 a Can, 5.14b Bottle, 5.14c Starfish.

5.7 Photograph place with adjustment

Based on preliminary criteria, place for taking photo must be located at outdoor area which is uncovered from any shadow, non-slope and easy for an arrangement. As a result, a chosen place is on Latitude $13^{0}\ 45^{'}\ 27^{''}$ Longitude $100^{0}\ 27^{'}\ 51^{''}$. Then, place must add a bit more preparation by laying the marking of direction and camera distance presented by figure 5.15. Otherwise, the direction of turning material must be known by means of increasing the number of rotating plates. As shown by figure 5.16, location and rotating plates used for indicating object's turning angle are provided.

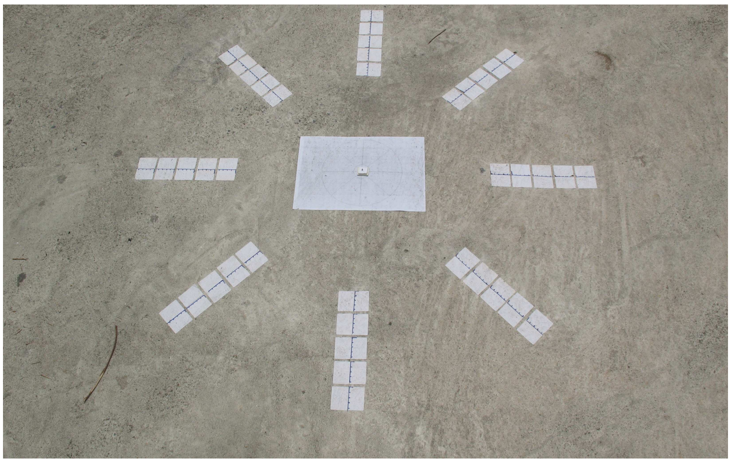

Figure 5.15 Photograph place with adjustment.

Figure 5.16 A rotating plate on photograph place.

5.8 A test of Tsi-Shah, programming with VB

For testing Image Processing, the most popular real images namely Lena and Pepper are used. Then, the figures will be feed in the developed program with the direction of light source as (0, 1, 1). When cloud points' result is shown, 3D surface will be generated by CATIA. Final results are presented by figure 5.17 and 5.18

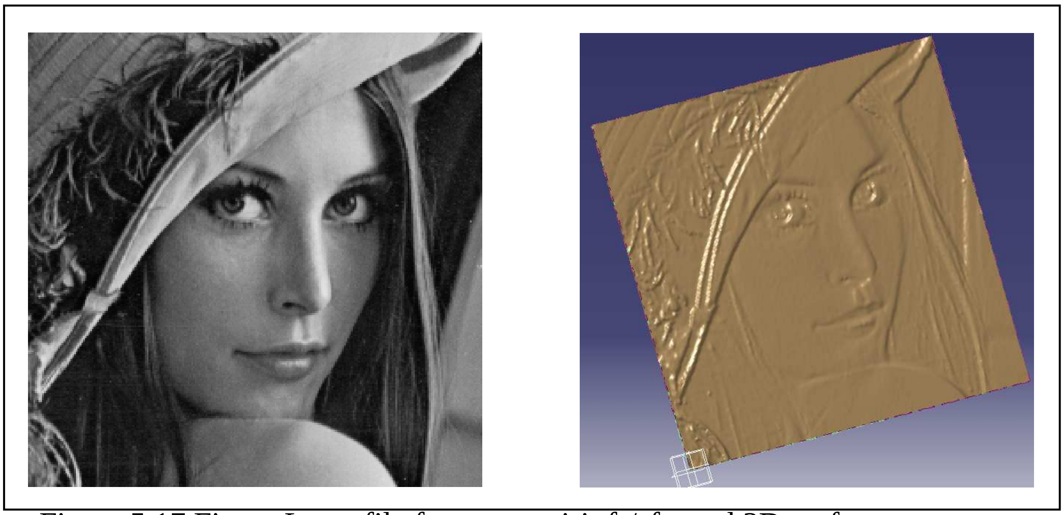

Figure 5.17 Figure Lena, file form www.irit.fr/sfs, and 3D surface was reconstruction by CATIA.

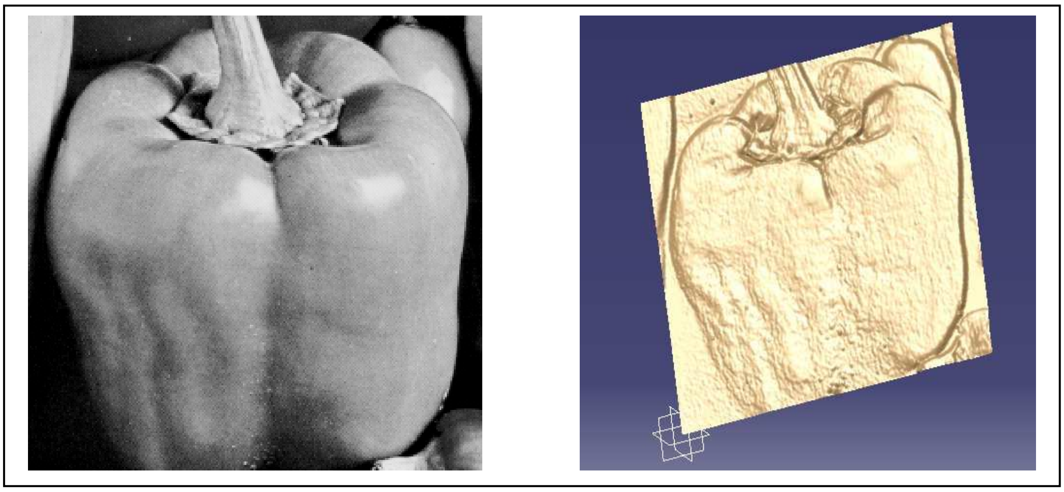

Figure 5.18 Figure Pepper, file form www.irit.fr/sfs, and 3D surface was reconstruction by CATIA.

5.9 A test of SPA, programming with VB

Using test data from Reda & Andreas (2005) as follow**.**

- Date = 17/10/2003.	*- Time = 12:30:30*
- Time zone = -7 hours.	*- Longitude = 105.1786 ^{o} West*
- Latitude = 39.742476 ^{o} North	*- Pressure = 820 mbar.*
- Elevation = 1830.14 m.	*- Temperature = 11 ^{o} C.*
- Zenith Angle = 50.11162 ^{o}	*- Azimuth = 194.34024 ^{o}*

After SPA test, results were shown as follow.

Zenith Angle = $\underline{50.1115705435261^{o}}$

Azimuth = $\underline{194.340251457843^{o}}$

Calculation’s results of SPA test were different from those of suggested test by Reda & Andeeas (2005), not more than 0.0001 degrees. This may caused by the different number of decimal positions that accumulated error from all calculating methods in SPA calculation. Nevertheless, this error was in the extent of its standard; therefore, SPA test by VB can be finally adopted in this research.

5.10 Tasting developed software in part of SPA

Since SPA calculation requires a large amount of data such as temperature, air pressure or elevation, they sometimes can be estimated in order to have a lot more convenient use, but such estimation must be subject to just a few impacts on the calculation. The result obtained from topic 5.10.1-5.10.4 presented that temperature, air pressure and elevation hardly affected on calculating the position of the sun, so if there are no data available, they can seemingly be estimated average values which already existed in this software.

5.10.1 An examination of a difference among changing temperature was held, whereas values of other data remained unchanging as follows:

Date =29/04/2010	*Time = 08:00:00*
Time zone (TZ) = +7 hours.	*Longitude =* $100^{0}\ 27^{'}\ 51^{''}$ *E*
Latitude = $13^{0}\ 45^{'}\ 27^{''}$ *N*	*Pressure = 1009.15 mbar.*
Elevation = 2.5 m.	*Surface slope =* 0^{0}
ΔT *= 26 Seconds*	

Table 5.6 Difference of solar position when changing only temperature

Item	Temperature (^{0} C)	Zenith (degrees)	Azimuth (degrees)
1	7	60.8423895089355	95.9089186536306
2	8	60.8424978111402	95.9089186536306
3	9	60.8426053452441	95.9089186536306
4	10	60.8427121193897	95.9089186536306
5	15	60.8432348678109	95.9089186536306
6	20	60.843739774989	95.9089186536306
7	40	60.845598091504	95.9089186536306

From table 5.6, it can be inferred that changing temperature did not affect on Azimuth angle, but caused 33-degree-difference of Zenith angle to change by 0.003208582569 degree.

5.10.2 An examination of a difference among changing air pressure was held, whereas values of other data remained unchanging as follows:

Date =29/04/2010 *Time = 08:00:00*

Time zone (TZ) = +7 hours. *Longitude = 100^0 $27'$ $51''$ E*

Latitude = 13^0 $45'$ $27''$ N *Elevation = 2.5 m.*

Temperature = 27.9 ^{0} C. *Surface slope = 0^0*

ΔT *= 26 Seconds*

Table 5.7 Difference of solar position when changing only pressure

Item	Pressure (mbar)	Zenith (degrees)	Azimuth (degrees)
1	1001	60.8447320355334	95.9089186536306
2	1002	60.8447039732028	95.9089186536306

Table 5.7 Difference of solar position when changing only pressure (cont.)

Item	Pressure (mbar)	Zenith (degrees)	Azimuth (degrees)
3	1003	60.8446759108722	95.9089186536306
4	1009	60.8445075368887	95.9089186536306
5	1016	60.8443111005746	95.9089186536306

From table 5.7, it can be inferred that changing air-pressure did not affect on Azimuth angle, but caused 15-mbar-difference of Zenith angle to change by 0.002244986447 degree.

5.10.3 An examination of a difference among changing temperature and changing air pressure was held, whereas values of other data remained unchanging as follows:

Date =29/04/2010	*Time = 08:00:00*
Time zone (TZ) = +7 hours.	*Longitude = $100^{0}\ 27^{'}\ 51^{''}$ E*
Latitude = $13^{0}\ 45^{'}\ 27^{''}$ N	*Elevation = 2.5 m.*
Surface slope = 0^{0}	*ΔT = 26 Seconds*

Table 5.8 Difference of solar position when changing temperature and pressure

Item	Pressure (mbar)	Temperature (^{0}C)	Zenith (degrees)	Azimuth (degrees)
1	1001	7	60.8426352883479	95.9089186536306
2	1001	40	60.845817958071	95.9089186536306
3	1016	7	60.8421829336012	95.9089186536306
4	1016	40	60.8454132956778	95.9089186536306
5	1009.15	27.9	60.8445033275392	95.9089186536306

From table 5.8, it can be inferred that there is a different angle of 0.00363502447 degree between the highest Zenith angle at 1001-mbar air-pressure with 40-degree temperature and the lowest Zenith angle at 1016-mbar air pressure with 7-degree temperature.

5.10.4 An examination of a different elevation among changing areas was held, whereas values of other data remained unchanging as follows:

Date =29/04/2010	*Time = 08:00:00*
Time zone (TZ) = +7 hours.	*Longitude =* $100^{0}\ 27^{'}\ 51^{''}$ *E*
Latitude = $13^{0}\ 45^{'}\ 27^{''}$ *N*	*Pressure = 1009.15 mbar.*
Elevation = 2.5 m.	*Temperature =* $27.9\ ^{0}$ *C.*
ΔT *= 26 Seconds*	

Table 5.9 Difference of solar position when changing only elevation

Item	Elevation (meter)	Zenith (degrees)	Azimuth (degrees)
1	0	60.8445033266925	95.9089186536063
2	1	60.8445033273698	95.9089186536275
3	5	60.8445033283858	95.9089186536548
4	10	60.8445033300792	95.9089186537032
5	20	60.8445033334659	95.9089186538002
6	40	60.8445033402394	95.9089186539941
7	80	60.8445033537864	95.9089186543818
8	160	60.8445033808803	95.9089186551574
9	320	60.8445034350681	95.9089186567085
10	640	60.8445035434439	95.9089186598108
11	2565	60.8445041953931	95.9089186784747

From table 5.9, it can be inferred that changing elevation of 2565 meters caused Zenith angle to change by 0.000008687006 degree and Azimuth angle to change by 0.0000000248684 degree.

5.11 Testing effect of light intensity

This is to examine an effect of light intensity on material surface’s quality from photos taken by Canon power short A630 and cell phone camera.

Table 5.10 Testing effect of light intensity with Digital camera ,- Canon power short A630-

Item	Figure name	Light intensity (lux.)	Normalization	Light direction (degrees)
1	IMG 0024	40	0-10	Sl 45, Tl 45
2	IMG 0025	50	0-10	Sl 45, Tl 45
3	IMG 0026	60	0-10	Sl 45, Tl 45
4	IMG 0027	70	0-10	Sl 45, Tl 45
5	IMG 0028	80	0-10	Sl 45, Tl 45
6	IMG 0029	90	0-10	Sl 45, Tl 45
7	IMG 0030	100	0-10	Sl 45, Tl 45
8	IMG 0031	110	0-10	Sl 45, Tl 45
9	IMG 0032	120	0-10	Sl 45, Tl 45

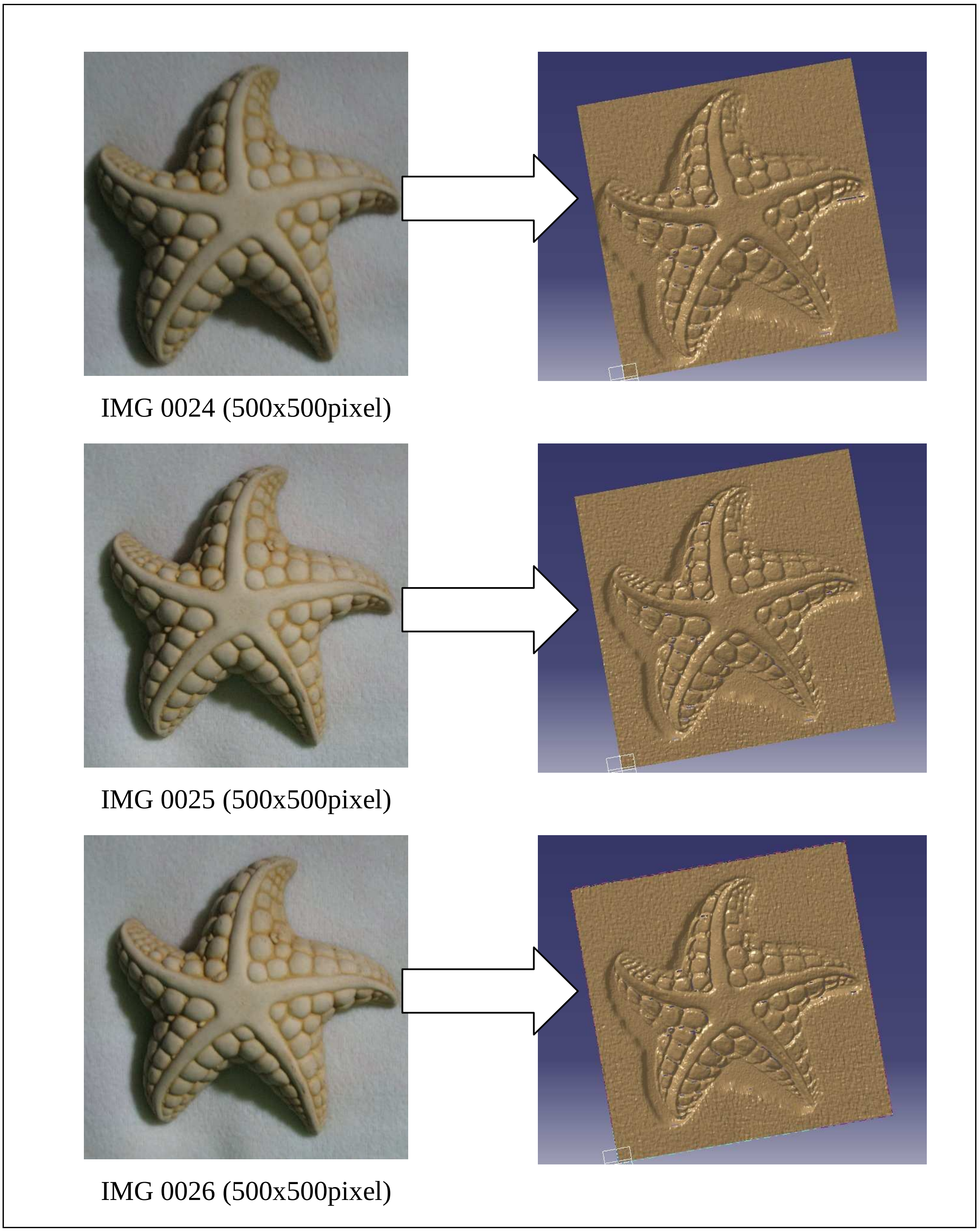

Figure 5.19a Results of light intensity effect when use Canon power short A630, Figure name IMG_0024, IMG_0025, IMG_0026

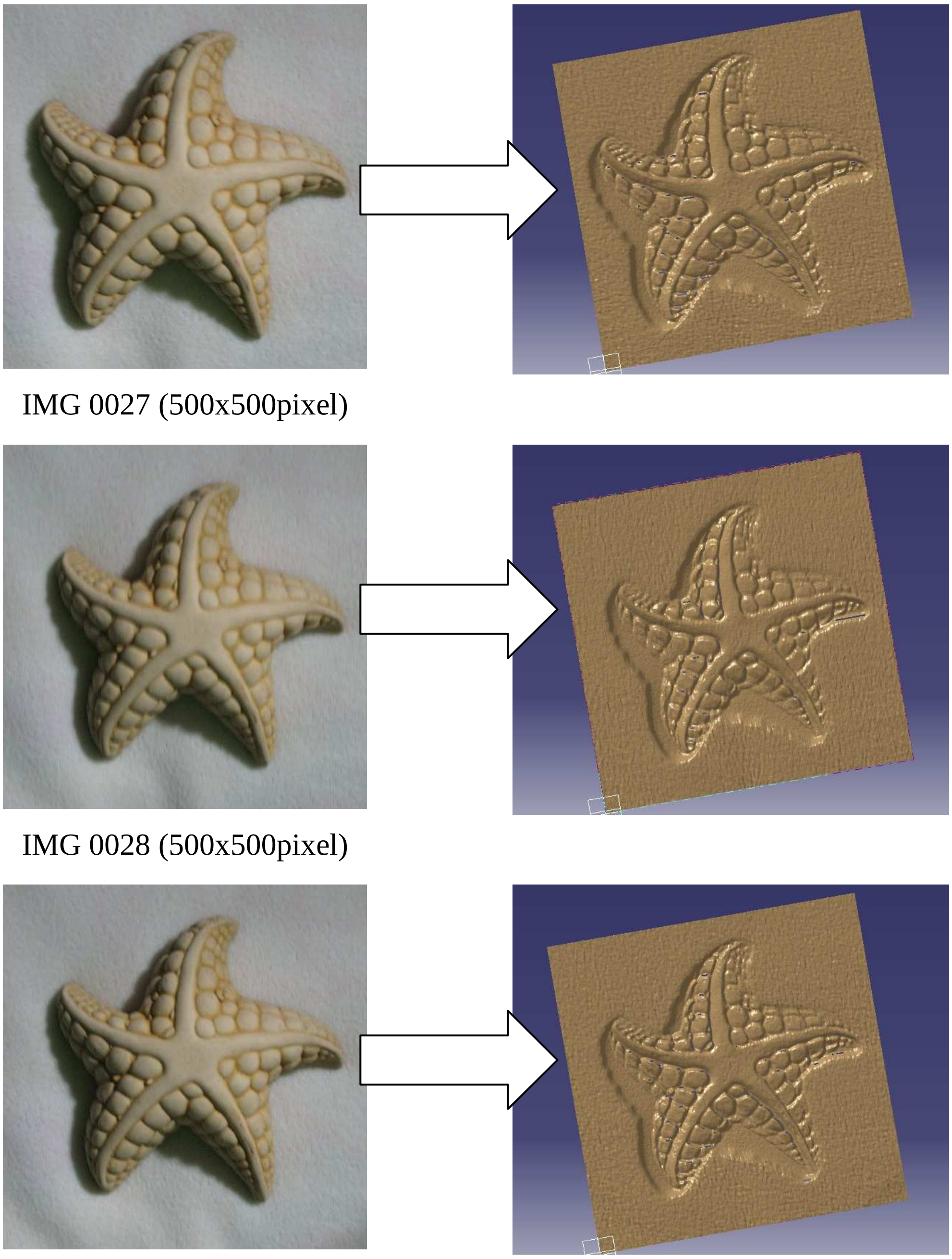

IMG 0027 (500x500pixel)

IMG 0028 (500x500pixel)

IMG 0029 (500x500pixel)

Figure 5.19b Results of light intensity effect when use Canon power short A630, Figure name IMG 0027, IMG 0028, IMG 0029

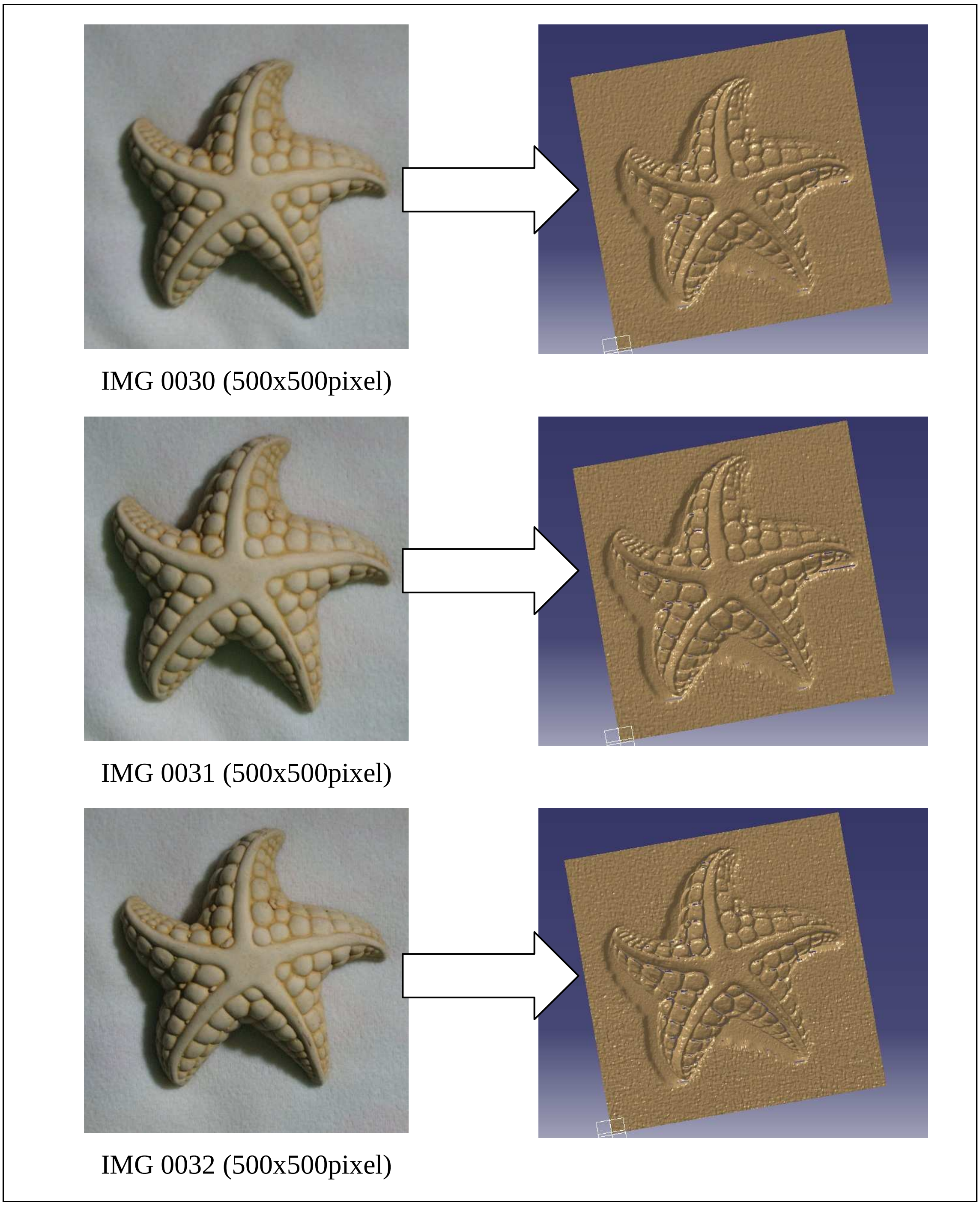

Figure 5.19c Results of light intensity effect when use Canon power short A630, Figure name IMG 0030, IMG 0031, IMG 0032

From figure 5.19, there is no effect of light intensity on a reconstucted material surface. This may be caused by automatic shutter sensitivity built in a camera which is measured by ISO rating. As a result, cell phone camera, without automatic shutter sensitivity is taken into account instead. Table 5.10 presents details of an examination as follows:

Table 5.11 Testing effect of light intensity with cell phone camera

Item	Figure name	Light intensity (lux.)	Normalization	Light direction (degrees)
1	IMG 003A	160	0-15	Sl 30, Tl 45
2	IMG 004A	100	0-15	Sl 30, Tl 45
3	IMG 006A	70	0-15	Sl 30, Tl 45
4	IMG 007A	40	0-15	Sl 30, Tl 45
5	IMG 009B	30	0-15	Sl 30, Tl 45
6	IMG 010B	10	0-15	Sl 30, Tl 45
7	IMG 008A	7	0-15	Sl 30, Tl 45

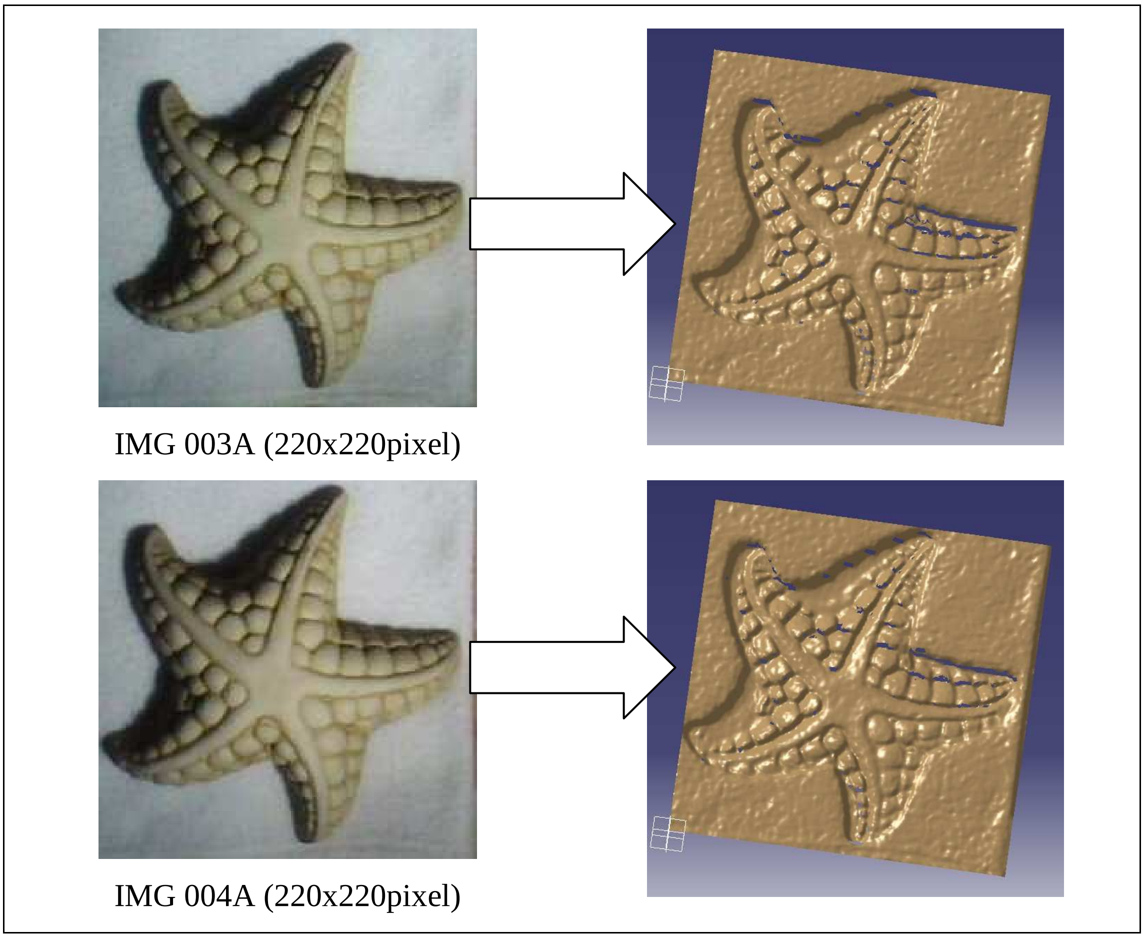

Figure 5.20a Figure show results of light intensity effect when use cell phone camara, Figure name IMG 003A, IMG004A

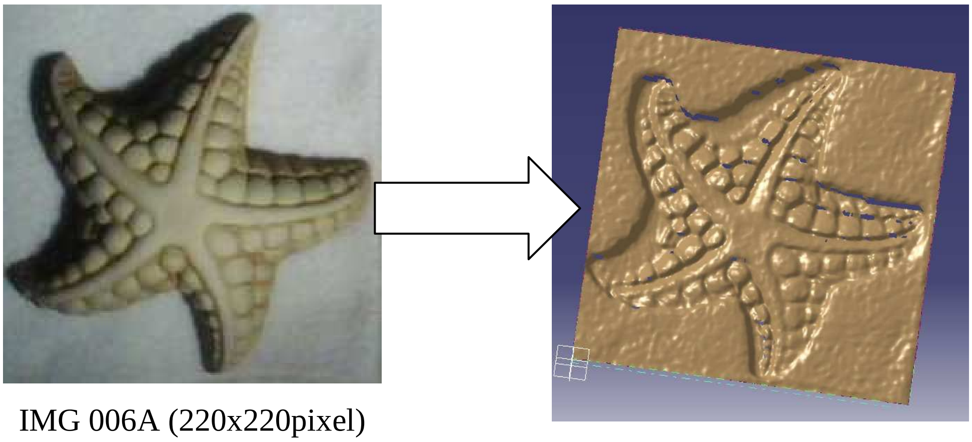

IMG 006A (220x220pixel)

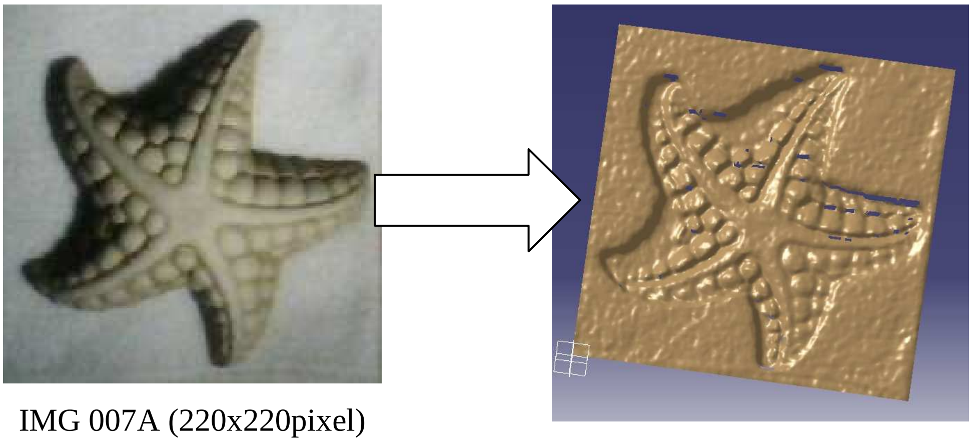

IMG 007A (220x220pixel)

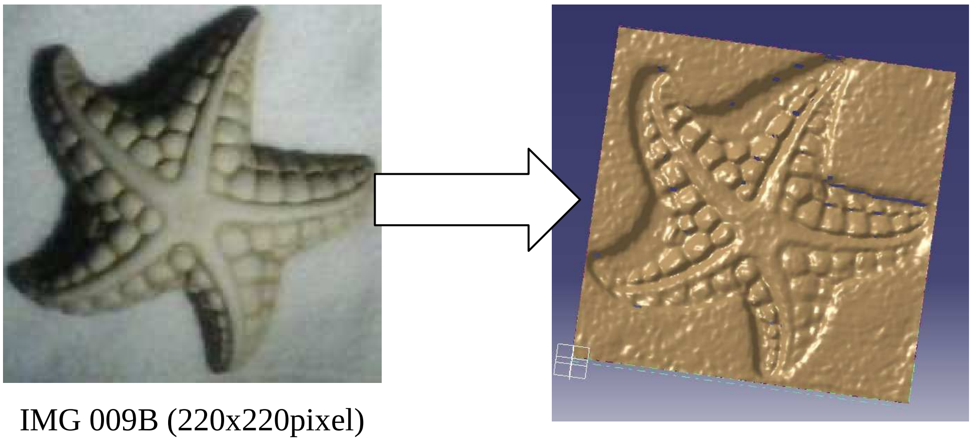

IMG 009B (220x220pixel)

Figure 5.20b Figure show results of light intensity effect when use cell phone camara, Figure name IMG 006A, IMG 007A,IMG 009B

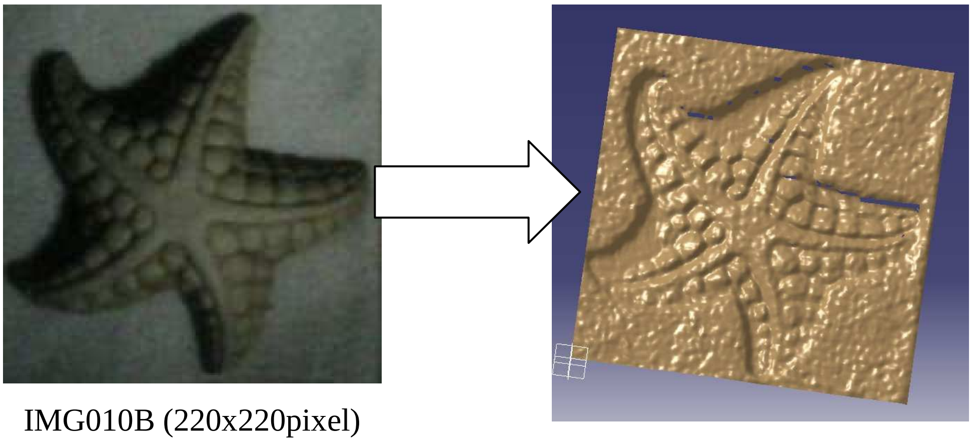

IMG010B (220x220pixel)

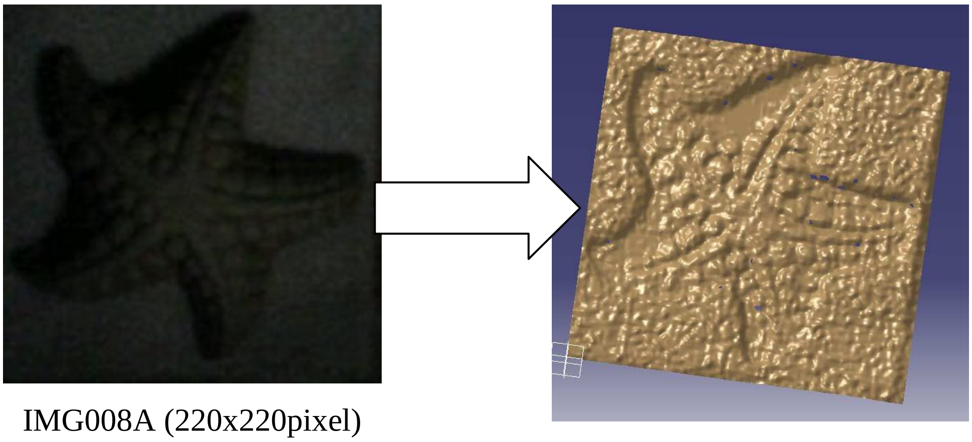

IMG008A (220x220pixel)

Figure 5.20c Figure show results of light intensity effect when use cell phone camara , Figure name IMG 010B, IMG 008A

From figure 5.20, contrary to digital camera, cell phone camera noticeably increased photo's sharpness which continuously affects on a quality of reconstructed material surface.

5.12 Testing effect of light direction

This is to observe an effect of light direction on Tsi-Shah SFS's calculation. Its details appear on table 5.12 as follows:

Table 5.12 Testing effect of light direction, test day 11/02/2010

Item	Figure name	Time	Azimuth Zenith (degrees)	Normalization	Turn (degrees)	Tilt (degrees)
1	IMG 3038	14:40:18	Z= 62.1591 A=215.6715	0-25	0	54.3285
2	IMG 3039	14:41:04	Z=62.2439 A=215.8585	0-25	30	24.1415
3	IMG 3040	14:41:45	Z=62.3198 A=216.0248	0-25	60	6.0248
4	IMG 3041	14:42:35	Z=62.4128 A=216.2272	0-25	90	-36.2272
5	IMG 3042	14:43:25	Z=62.5063 A=216.4292	0-25	120	-66.4292
6	IMG 3043	14:44:10	Z=62.5908 A=216.6107	0-25	150	-96.6107
7	IMG 3044	14:51:15	Z=63.4064 A=218.3067	0-25	180	-128.3067
8	IMG 3045	14:52:05	Z=63.5044 A=218.5042	0-25	210	-158.5042
9	IMG 3046	14:53:47	Z=63.7057 A=218.9057	0-25	240	171.0941
10	IMG 3047	14:54:43	Z=63.8170 A=219.1254	0-25	270	140.8746
11	IMG 3048	14:55:50	Z=63.9507 A=219.3874	0-25	300	110.6126
12	IMG 3050	14:57:07	Z=64.1054 A=219.6877	0-25	330	80.3123

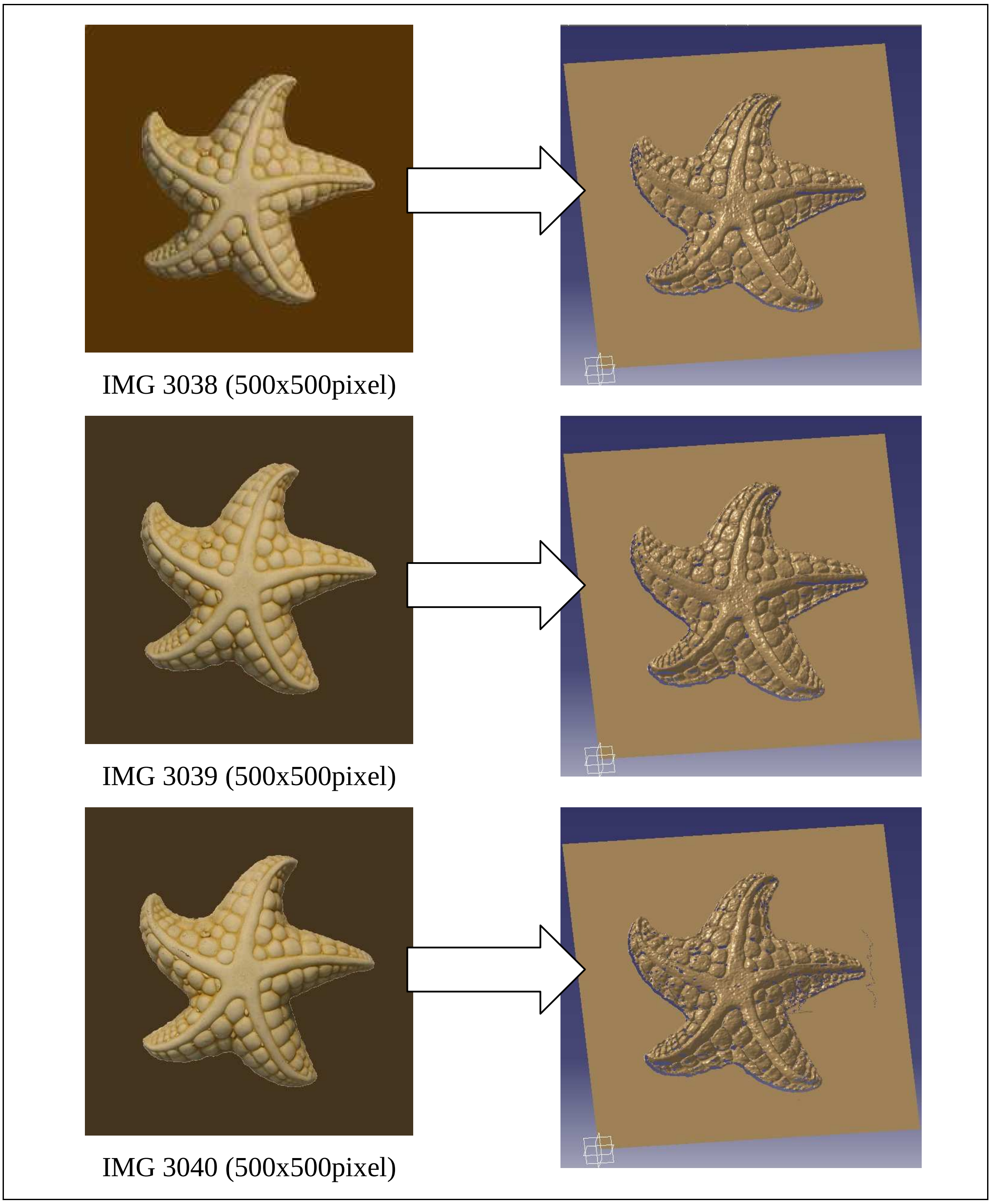

Figure 5.21a Result of light direction effect, Figure name IMG 3038, IMG 3039, IMG 3040

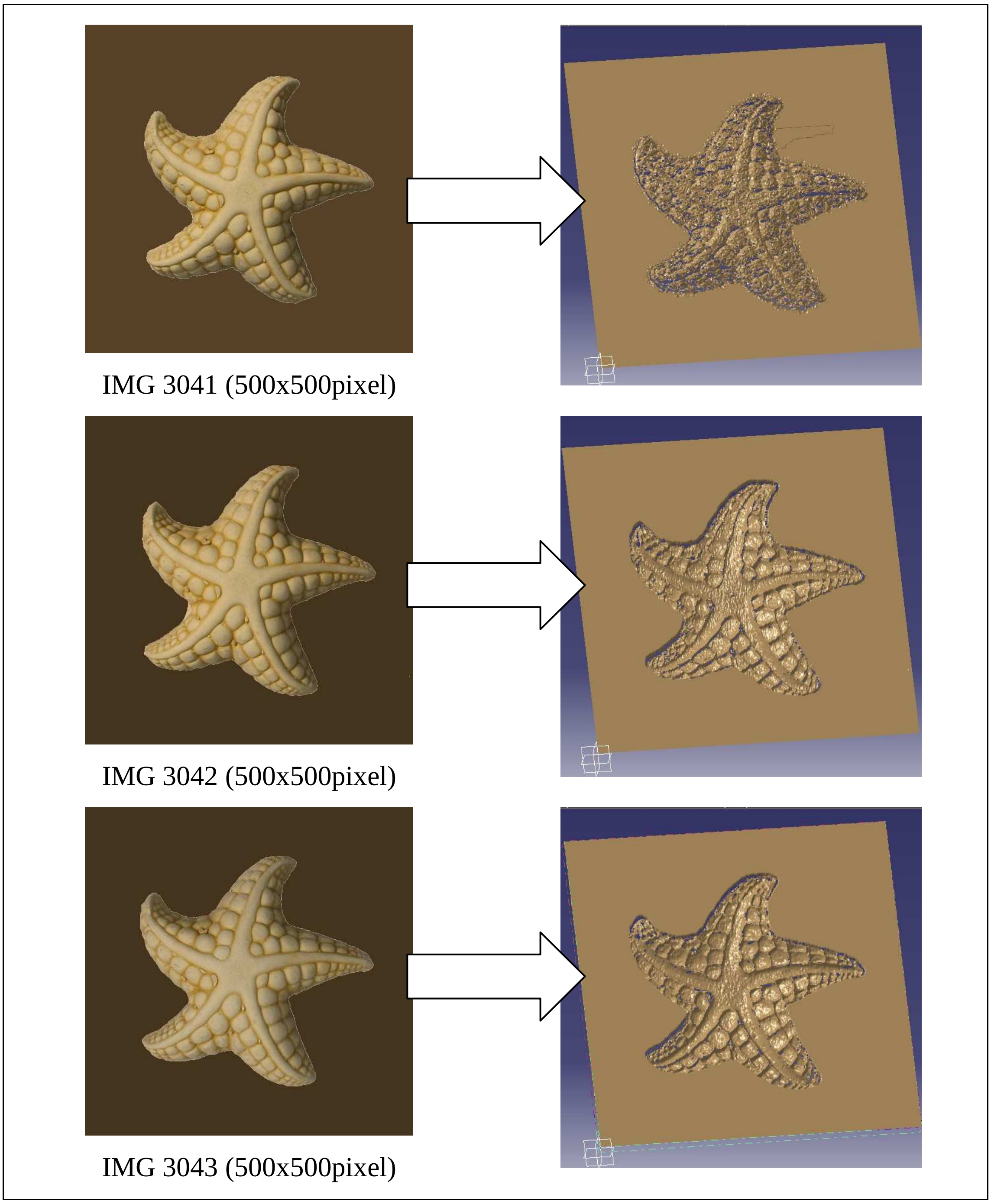

Figure 5.21b Result of light direction effect, Figure name IMG 3041, IMG 3042, IMG 3043

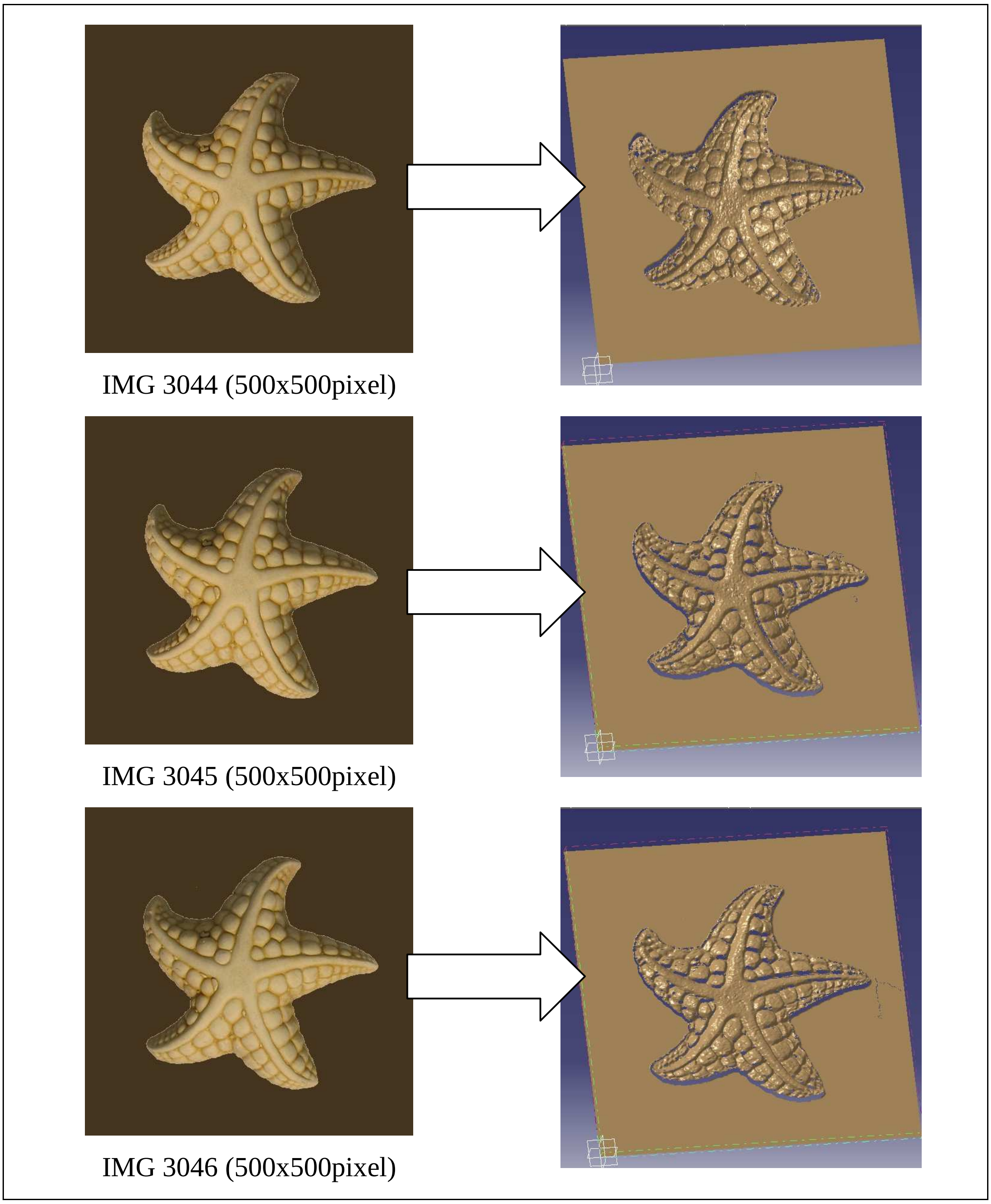

Figure 5.21c Result of light direction effect, Figure name IMG 3044, IMG 3045, IMG 3046

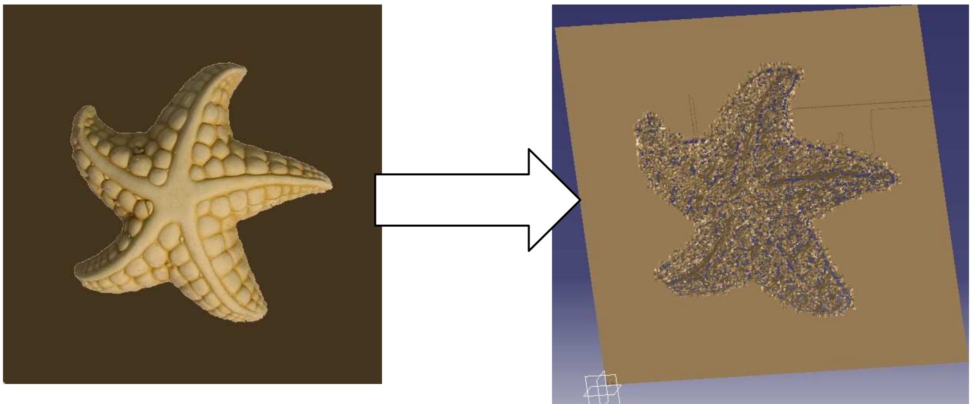

IMG 3047 (500x500pixel)

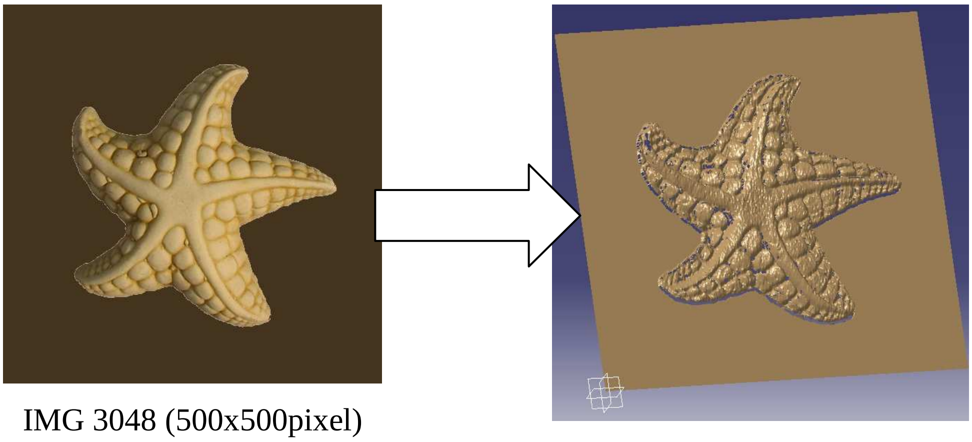

IMG 3048 (500x500pixel)

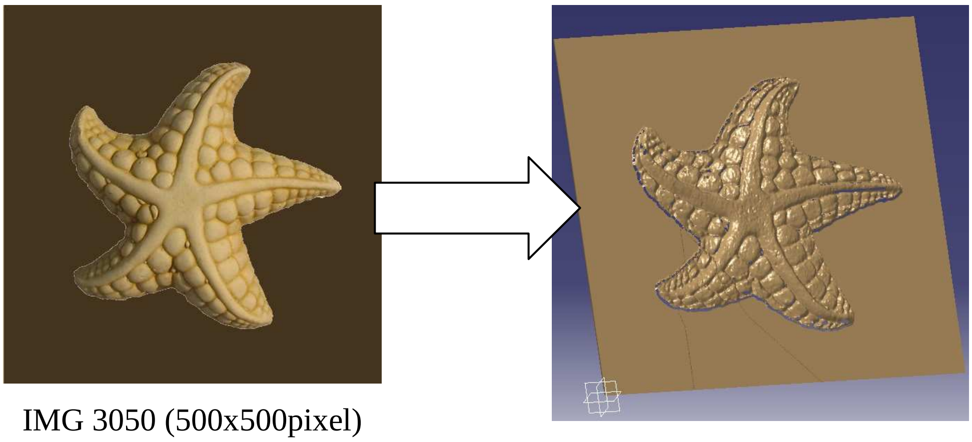

IMG 3050 (500x500pixel)

Figure 5.21d Result of light direction effect, Figure name IMG 3047, IMG 3048, IMG 3050

As can be seen on figure 5.21, the light direction at tilt 135 degrees and –45 degrees was more likely to cause the most problematic surface, significantly supposed that within a range of tilt 125 to 145 and tilt -35 to-55, divergence failure seems to occur. Additionally, an effect of shadow also results in a failure.

5.13 Testing effect of background

Figure 5.22a presented a created surface without background painting. There were a number of holes on the surface. Unlike figure 5.22a, figure 5.22b was created after already painted its background; as a result, the amount of its holes was lesser than those of figure 5.22a. However, an impact of background painting on a created surface additionally relies on background's characteristic and background's color. Figure 5.23 presented that material surface appeared to curve out on darkened background and appeared to cave in on brightened background.

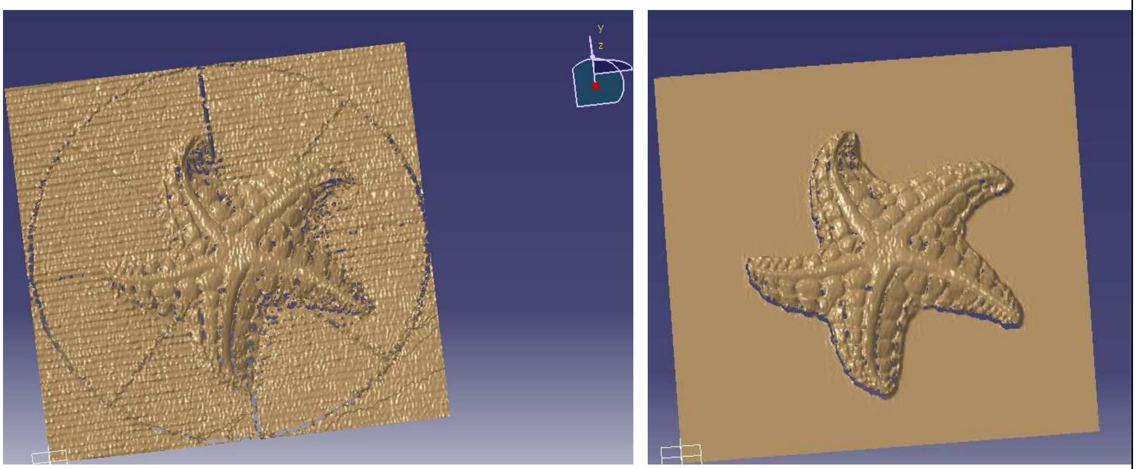

5.22a without painting background 5.22b with painting background

Figure 5.22 Reconstruction expanding height 3D surface without painting background and reconstruction expanding height 3D surface with painting background

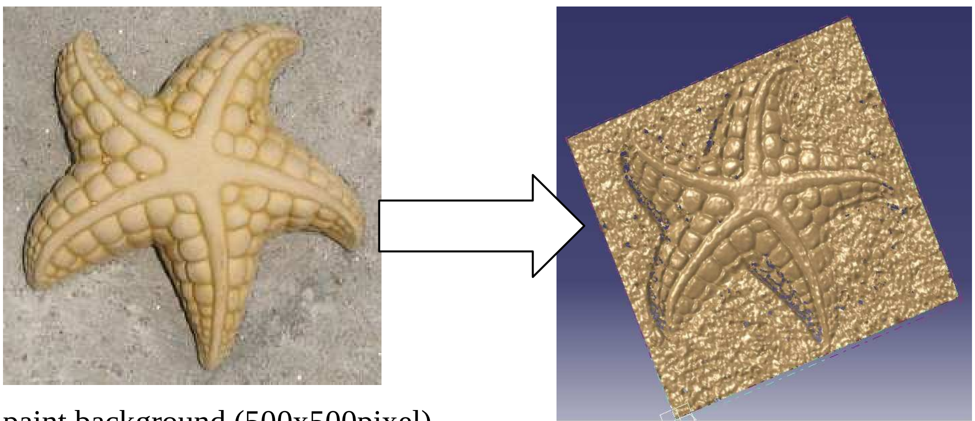

Un-paint background (500x500pixel)

Figure 5.23a Result of background color effect, un-paint background

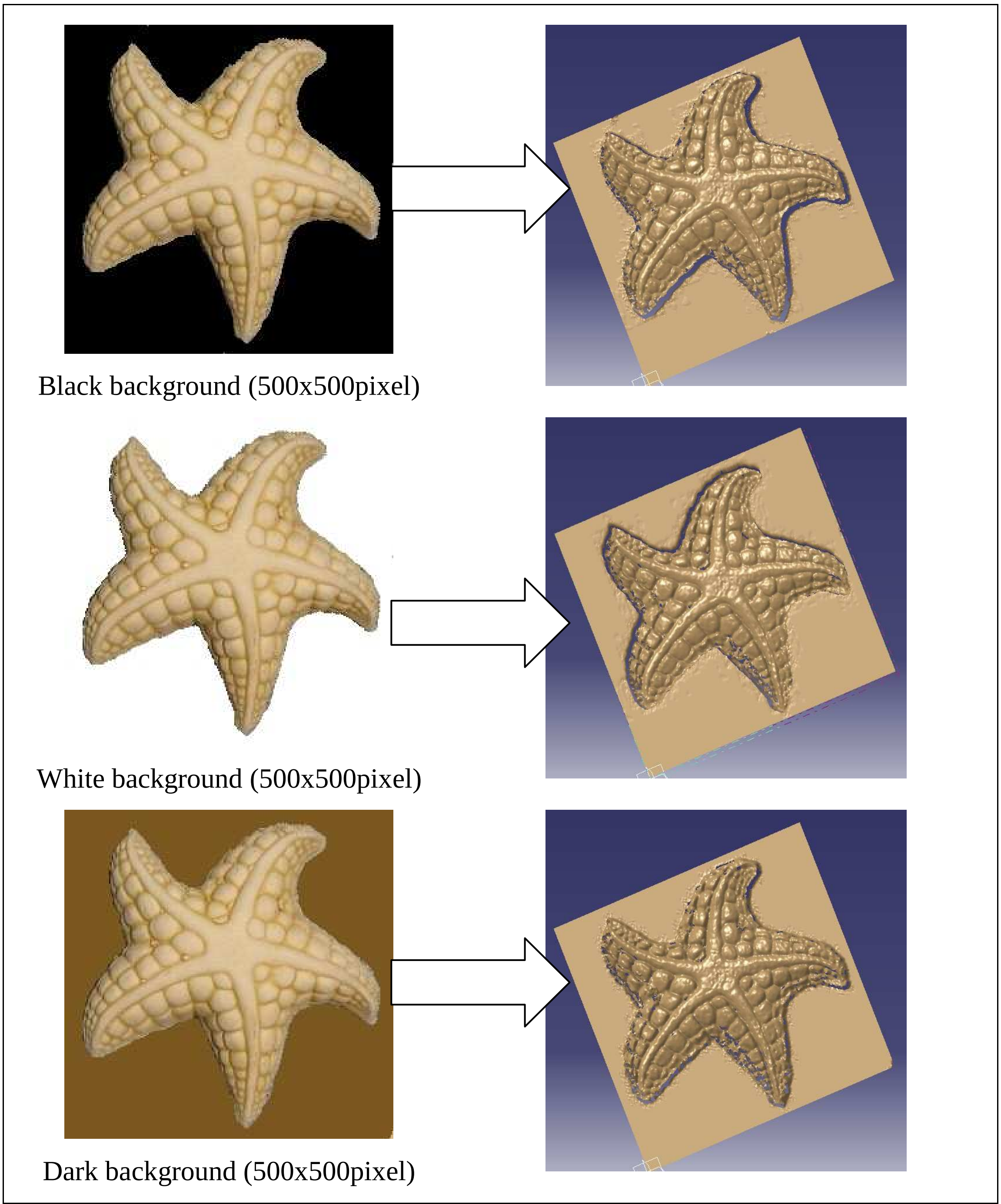

Figure 5.23b Result of background color effect, Black background, White background, Dark background

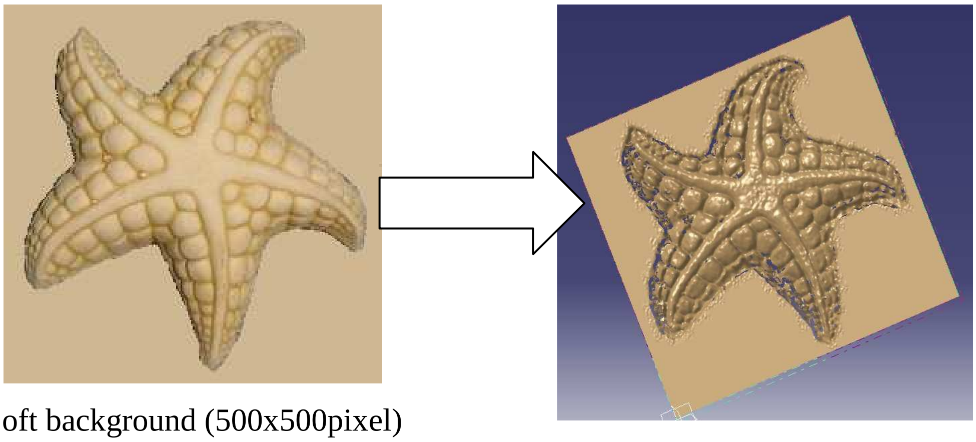

Soft background (500x500pixel)

Figure 5.23c Result of background color effect, Soft background

5.14 Testing effect of image resolution

A result of testing effect of image resolution can be seen on figure 5.24. Without normalization a sharpness of 3D surface was varied by the number of pixel, while according to figure 5.25, with normalization a sharpness of expanding height 3D surface was also varied by the number of pixel, 0.1-fold of pixel width. However, the higher number of pixel is, the more increase of holes takes place on expanding height 3D surface. Details of testing are provided as follows:

Wat Arun

Latitude 13°44'37.14"N Longitude 100°29'20.59"E

Camera direction South Time 2/4/2553 12:16:00

View angle 90°

Star fish

Latitude 13°45'27.95"N Longitude 100°27'50.86"E

Camera direction 330° Time 11/2/2553 12:16:00

View angle 0°

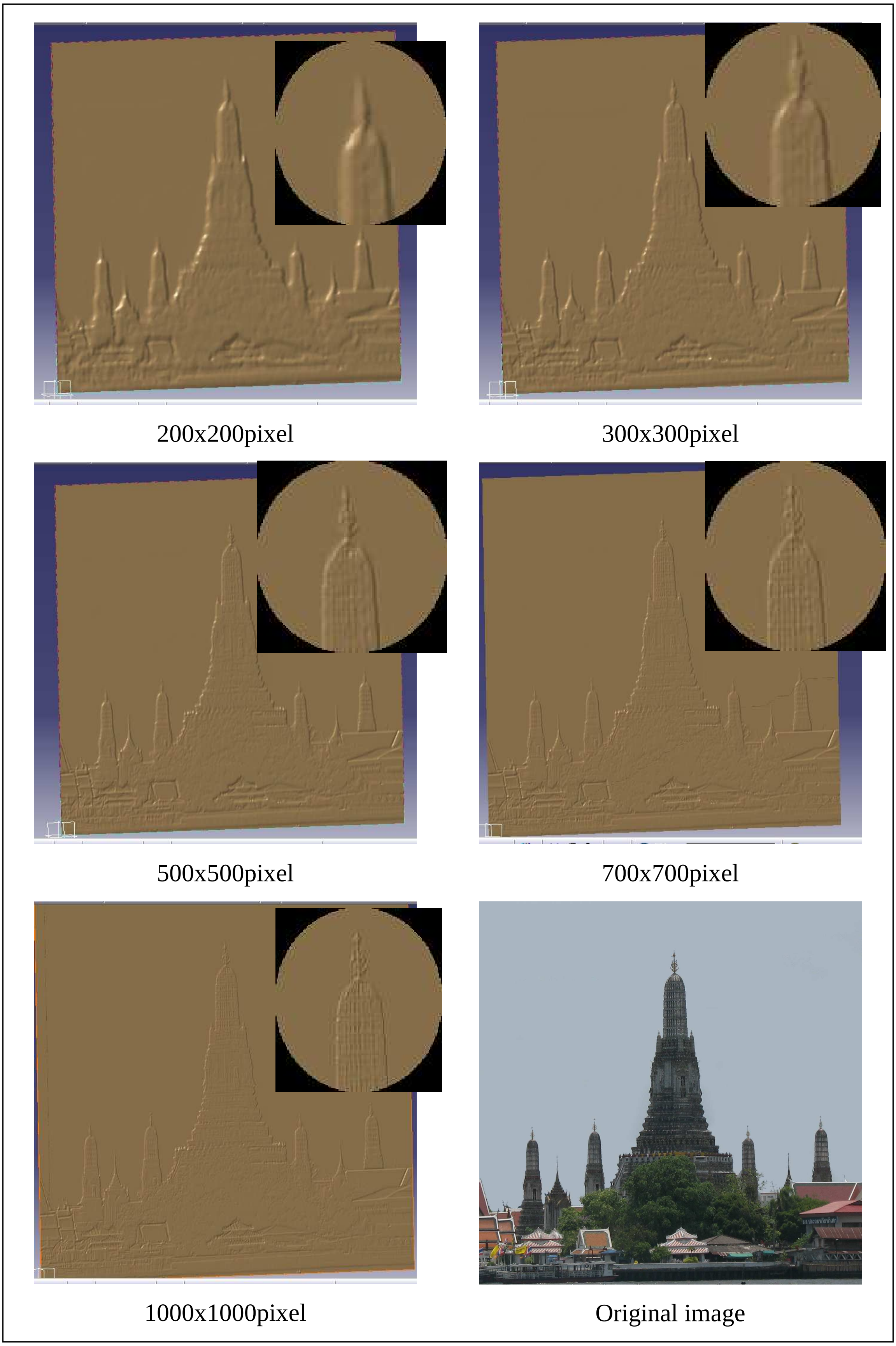

Figure 5.24 Effect of image resolution: Wat Arun.

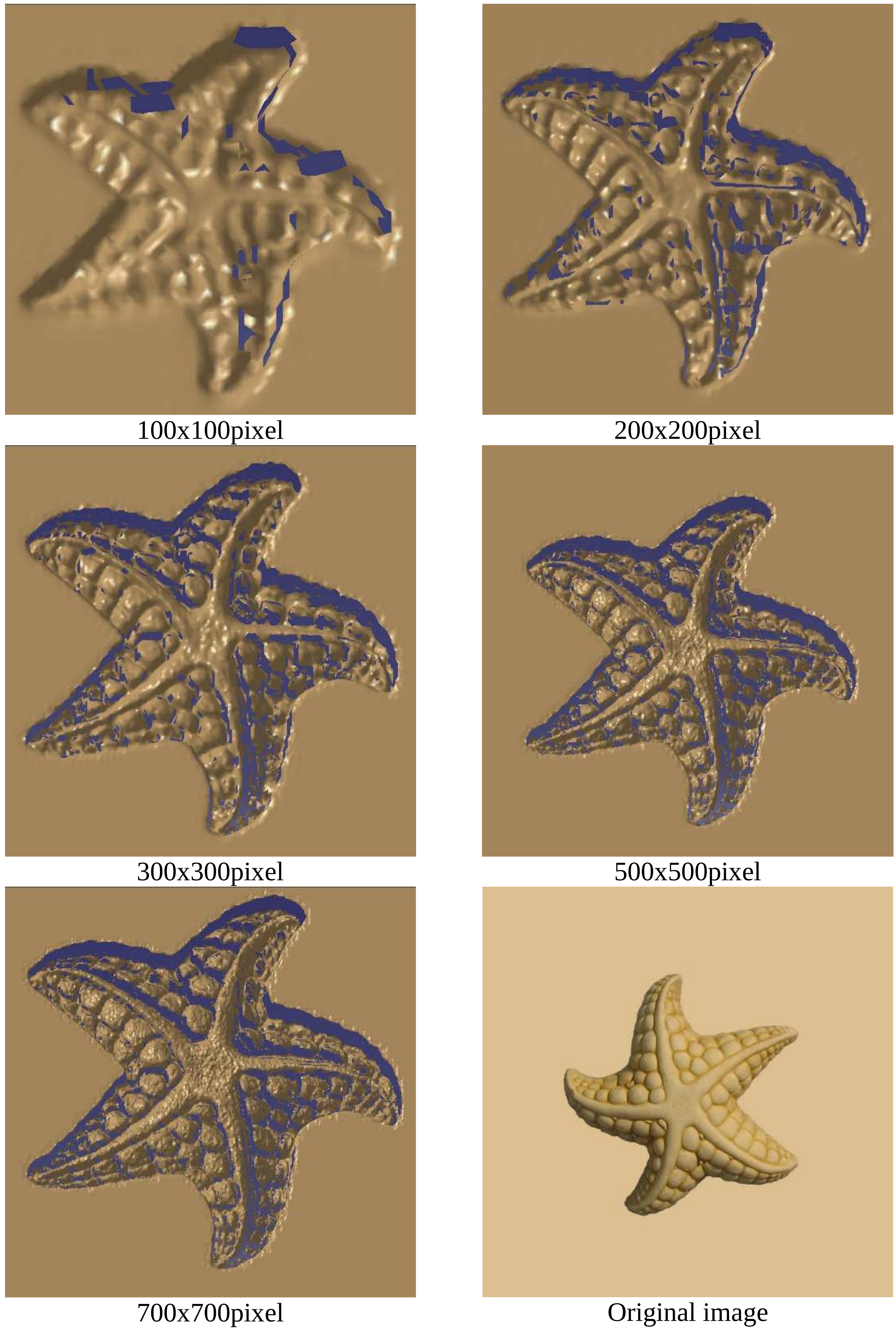

Figure 5.25 Effect of image resolution: star fish.

5.15 Result of reconstruction to 3D bas-relief surface

To generate 3D bas-relief surface must be based on Tsi-Shah SFS's calculation without normalization. Different figures of three materials-Can, Bottle and Starfish- together with a selected place, Wat Arun, were taken into a process of the research according to figure 5.1 without rotation and normalization of SFS black box and the process provided a result of solar light direction shown on table 5.13 and a result of 3D surface shown on figure 5.26 and 5.27. Can, Starfish and Wat Arun were completely perfect, whereas, there was a small spot at the button of bottle which can be fixed by CATIA.

Table 5.13 The results of SPA calculation

Object	Times	Latitude Longitude	Zenith angle (degrees)	Azimuth angle (degrees)
Can	4/2/2553 11:23:10	13 ^{o} 45 '27 "N 100^{o} 27' 51"E	58.9990	160.7521
Bottle	4/2/2553 11:13:00	13 ^{o} 45 '27 "N 100^{o} 27' 51"E	59.6681	158.0736
Starfish	11/2/2553 14:40:05	13 ^{o} 45 '27 "N 100^{o} 27' 51"E	62.1599	215.6715
Wat Arun	2/4/2553 12:16:00	13°44'37.14"N 100°29'20.59"E	35.7057	177.6467

5.26a1 Can 5.26a2 Bottle 5.26a3 star fish

5.26b1 Can result 5.26b2 Bottle result 5.26b3 Star fish result

Figure 5.26 Objects for test in this thesis (5.26a), and their 3D bas-relief surface result (5.26b).

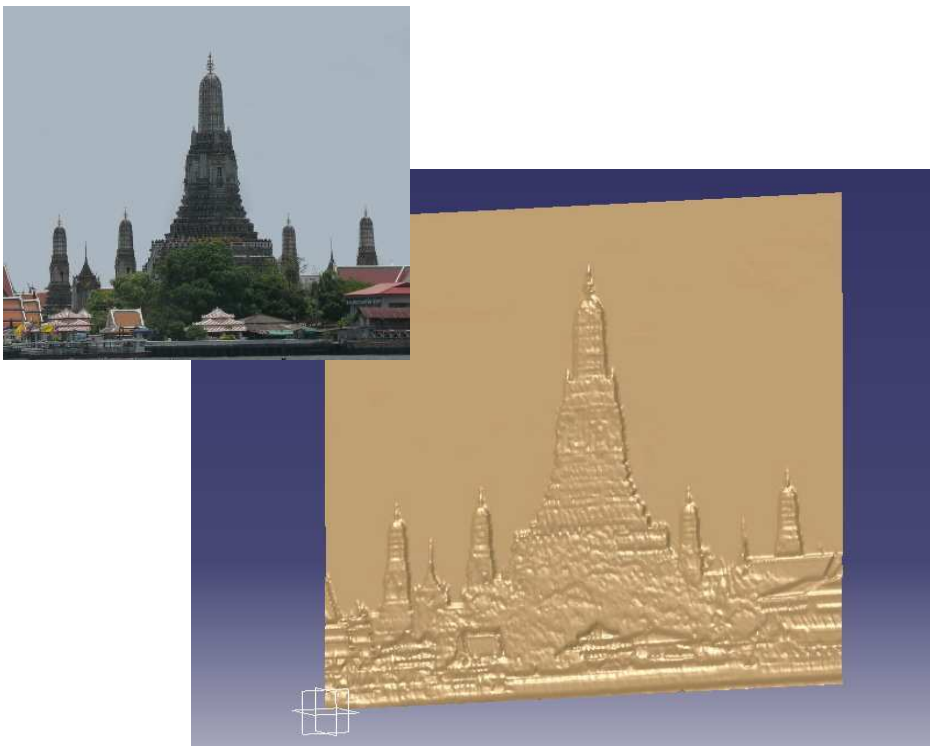

Figure 5.27 Wat Arun and 3D bas-relief surface

5.16 Result of reconstruction to expanding height 3D surface from point cloud with normalization

Due to an error caused by shadow effect, IMG0013, starfish, just a little occurrence of shadow effect was selected. According to figure 5.1, a calculation in this topic was held without rotation, but there was an increase in normalization process on 3D surface expanding height which hardly provided an error as shown on figure 5.28 and detailed as follows:

Object Starfish	Time 21/04/2010 12:45:15
Latitude 130 ^{o} 45 '27 "N	Longitude 100^{o} 27' 51"E
Zenith angle 29.4247 ^{o}	Azimuth angle 194.4769 ^{o}
Slant 29.4245 ^{o}	Tilt 75.5231 ^{o}

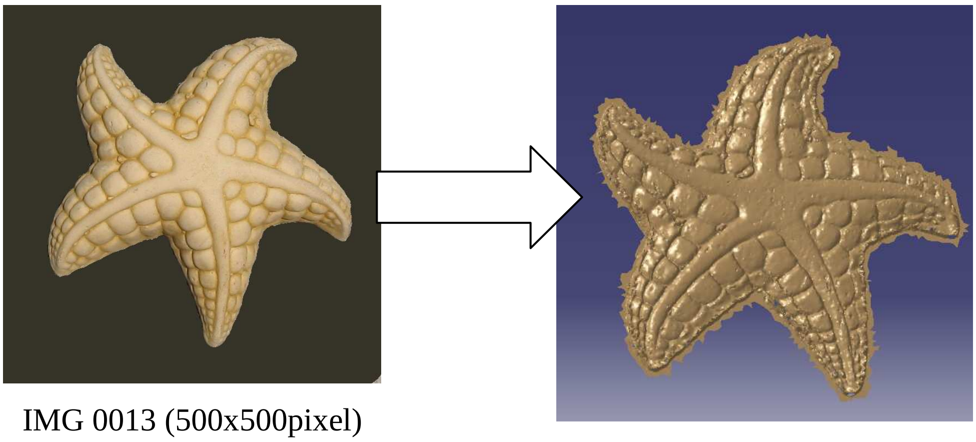

IMG 0013 (500x500pixel)

Figure 5.28 Star fish expanding height 3D surface result

5.17 Result of reconstruction to expanding height 3D surface by combine point clouds

This topic points out a problem solving of a shadow effect by means of combining point clouds sourced by different directions of light. IMG 3038 and 3044, as shown on figure 5.29, were distorted by shadow effect, from curve surface to lean surface. According to figure 5.1, the images will be put into normalization process in order to rotate both of them to be the same position.

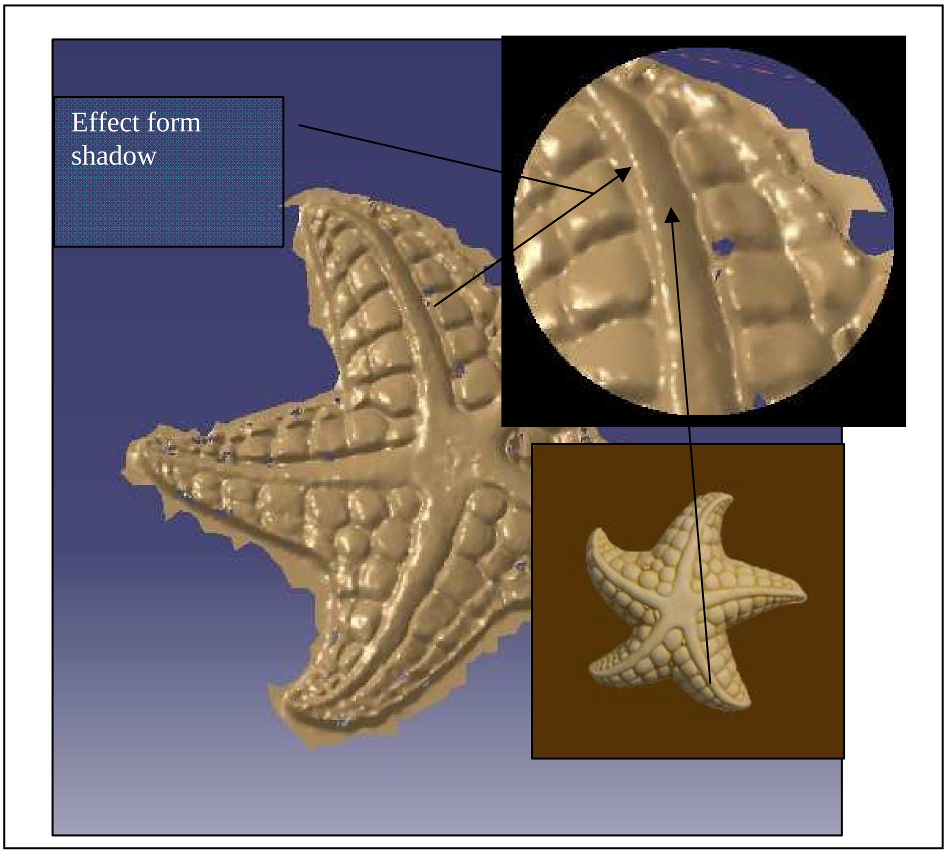

Figure 5.29 Shadow effect

In performing combination point clouds by CATIA, when the point clouds are imported, it is vital for a researcher to align point clouds before picking out each part of them and then merging them altogether. Figure 5.30a – 5.30d show a process of fixing shadow effect by combination each partial well point cloud. Figure 5.30a this step used Adaptive function in point filter for filtering point - specially points on planar elements-. Figure 5.30b, this step will choose partials well point clouds by click Activate 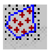 and then merging point clouds by click Merge Clouds 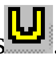. Figure 5.30c, this step is fixing hole using triangle meshes stick together by click Interactive Triangle Creation  and then in Figure 5.30d shown a result of fixing a hold. And when fix all holes, figure 5.31 presents a result of reconstructed expanding height 3D surface fixed by CATTA. By used the same process, in figure 5.32 show a result of wrench surface.

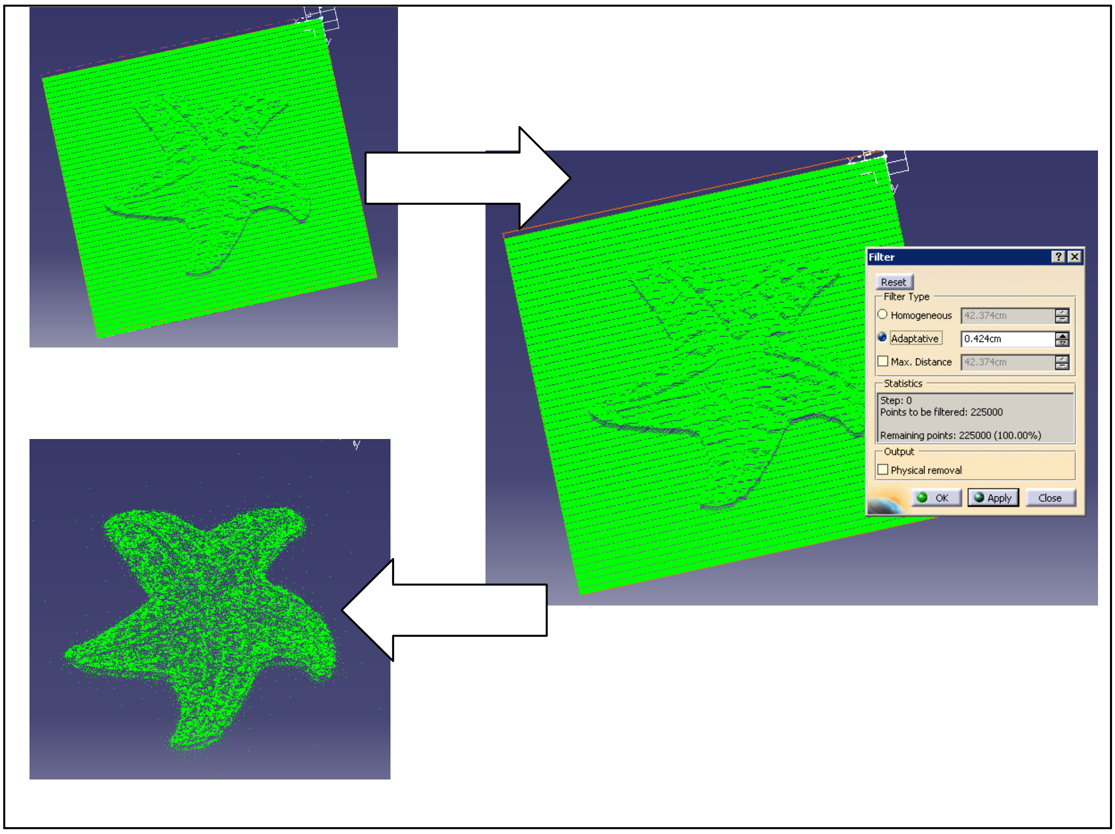

Figure 5.30a CATIA point filter used Adaptive function.

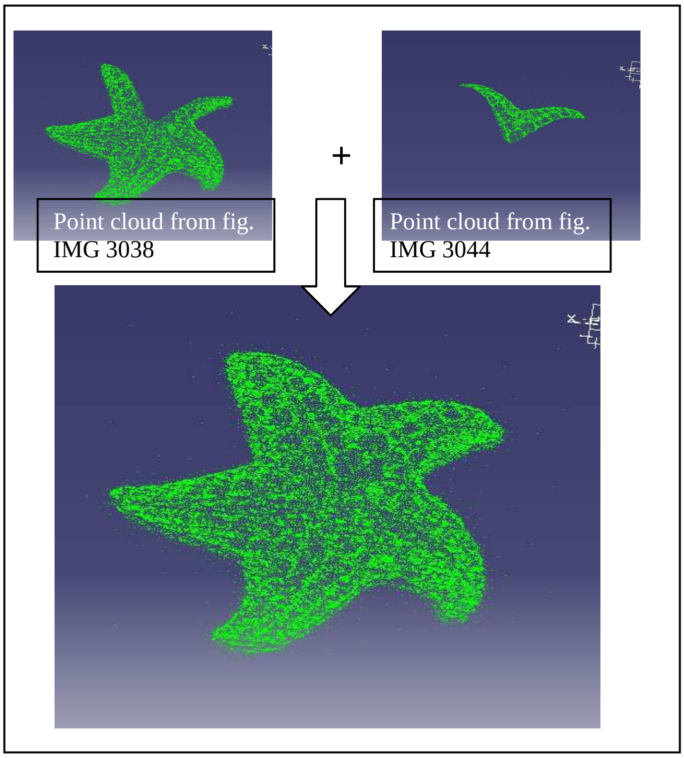

Figure 5.30b merging point clouds by CATIA

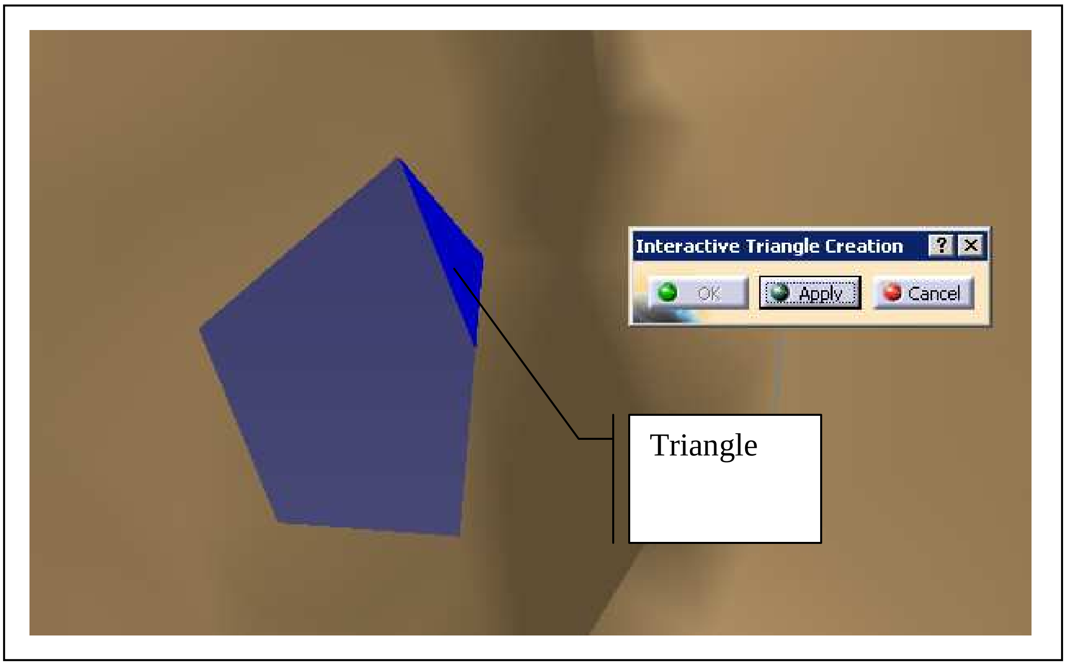

Figure 5.30c Using Interactive Triangle Creation function

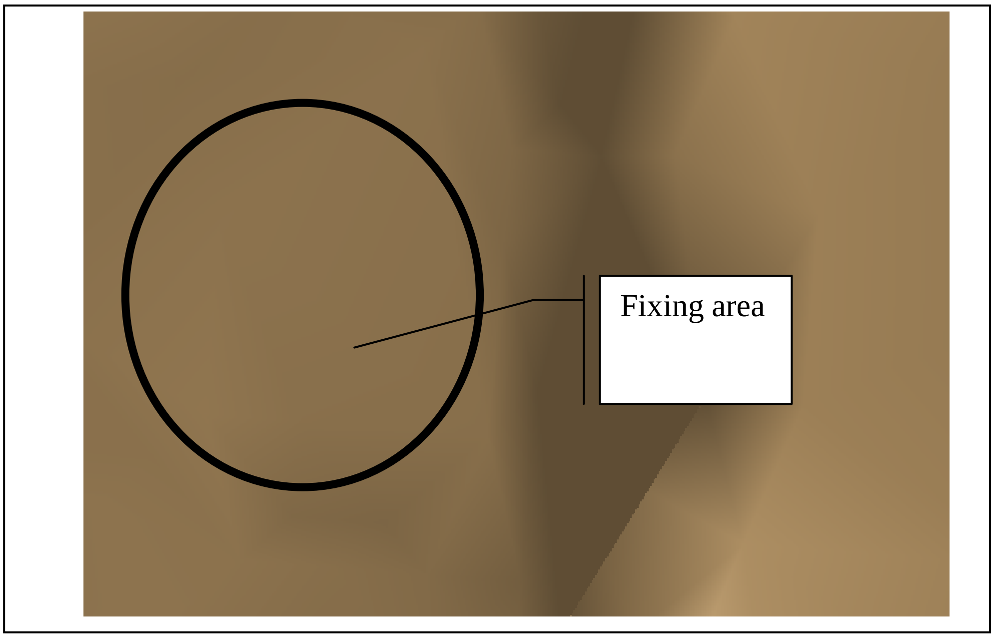

Figure 5.30d Result of using Interactive Triangle Creation function

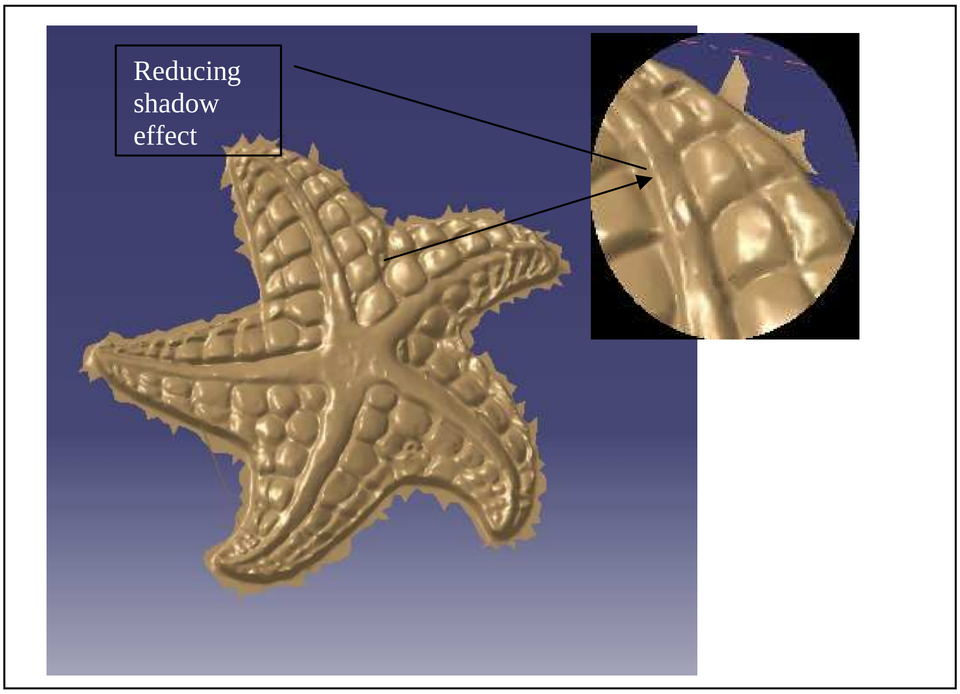

Figure 5.31 Reconstruction expanding height 3D surface after merge point clouds

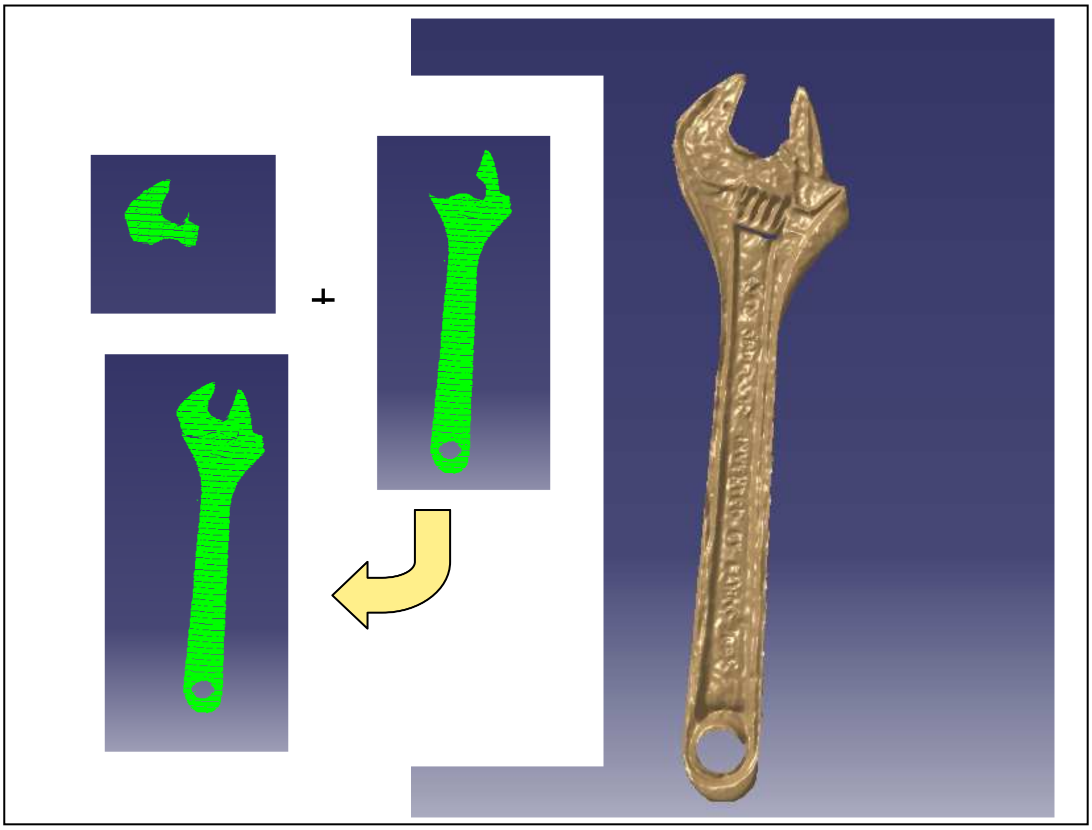

Figure 5.32 Reconstruction expanding height 3D surface (wrench)

5.18 Solving divergence failures problem.

To solve divergence failures problem, a utilization of this research has been conducted by means of rotating image in order to alter its tilt angle. From figure 5.33, a selected IMG3047 with 140.8746-degree tilt angle was rotated along clockwise direction with 90-degree angle, leading to a changing 50.8746-degree tilt angle. Once a whole process was done, a quality of a reconstructed material surface has been obviously improved.

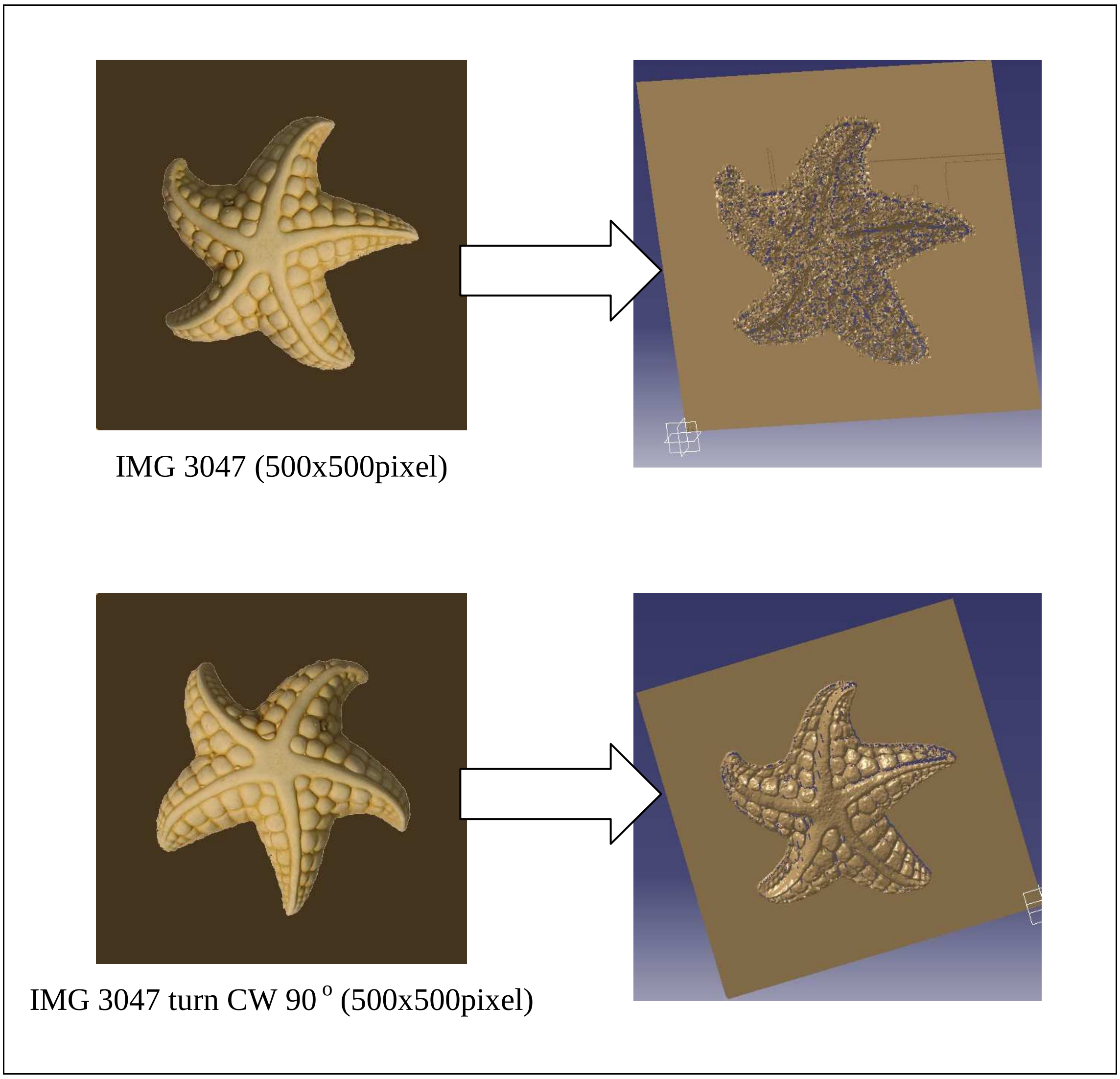

Figure 5.33 Result of solving divergence failures problem

5.19 Test for less condition control

For test capability of developing software for general used so this test use images with less condition control by take photo without adjust place and object,- use only digital camera and compass- . Result of this test show as below.

Table 5.14 Data of Test for less condition control

Item	Figure name	Times	Latitude Longitude	Zenith / Azimuth (degrees)	Direction / View (degrees)	Light direction (degrees)
1	IMG 0062	29/4/2010 13:30:00	13 ° 46 '37 "N 100° 19' 15"E	30.7322 / 216.9791	260 / 90	Sl 76.6, Tl 62.1
2	IMG 0076	6/5/2010	13 ° 45 '27 "N 100° 27' 51"E	49.9311 / 257.6365	135 / 90	Sl 126.1, Tl 22.4
3	IMG 0066	5/5/2010 12:27:00	13 ° 47 '43 "N 100° 19' 26"E	24.4929 / 187.3447	30 / 90	Sl 70.8, Tl 105.4
4	IMG 0067	5/5/2010 13:18:00	13 ° 47 '42 "N 100° 19' 26"E	27.9388 / 213.69936	90 / 90	Sl 105.1, Tl 113.8
5	IMG 0068	5/5/2010 16:14:00	13 ° 47 '42 "N 100° 19' 30"E	56.6323 / 262.94398	260 / 90	Sl 37.0, Tl 66.0
6	IMG 0069	5/5/2010 16:14:10	13 ° 47 '42 "N 100° 19' 30"E	56.6323 / 262.94398	260 / 90	Sl 37.0, Tl 66.0
7	IMG 0070	5/5/2010 16:15:00	13 ° 47 '42 "N 100° 19' 30"E	56.8203 / 263.1221	240 / 90	Sl 66.8, Tl 36.6
8	IMG 0079	10/5/2010 14:35:00	13 ° 47 '42 "N 100° 19' 30"E	37.9766 / 243.3230	215/90	Sl 84.9, Tl 52.3

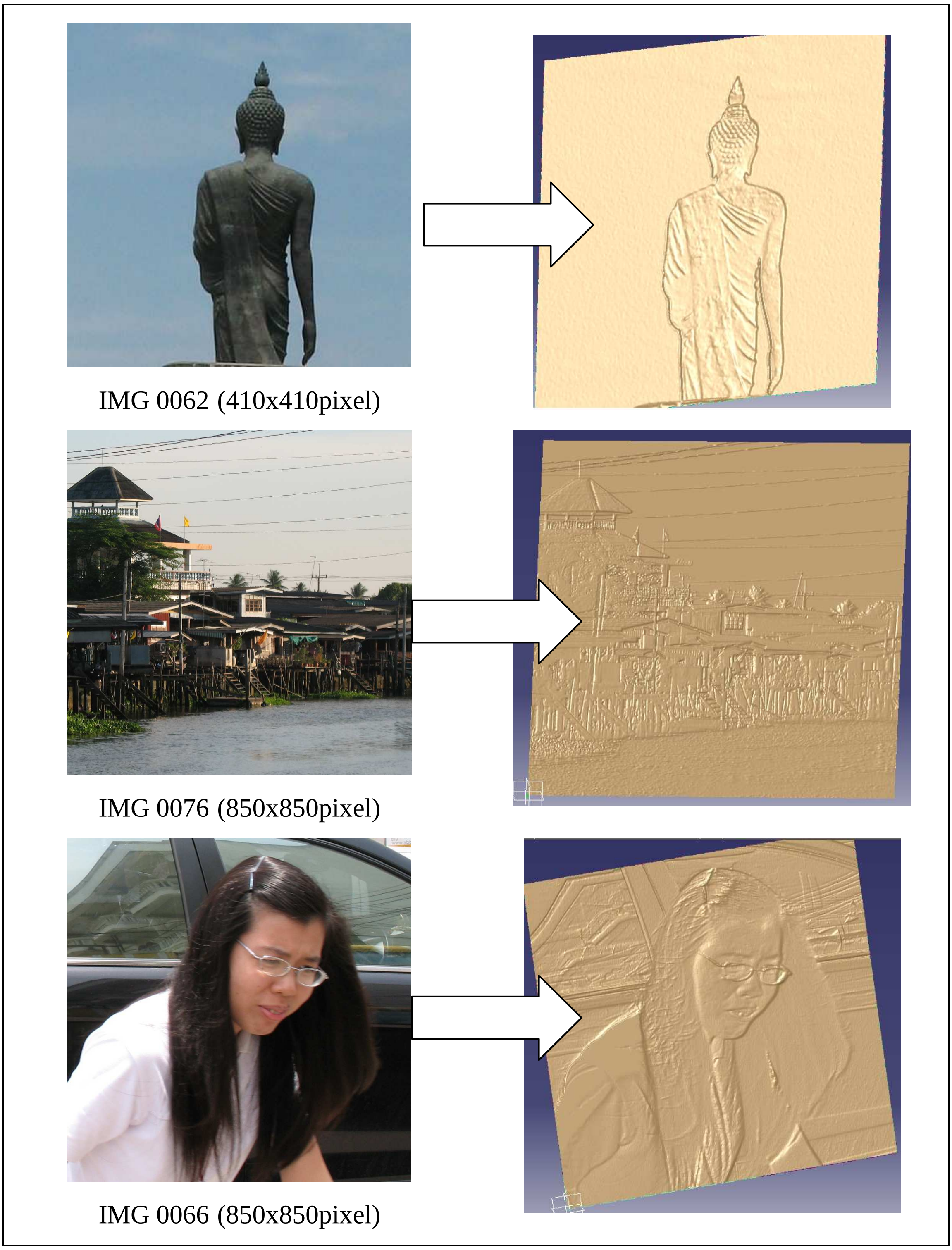

Figure 5.34a Result of less condition control Test, Figure name IMG 0062, IMG 0076, IMG 0066


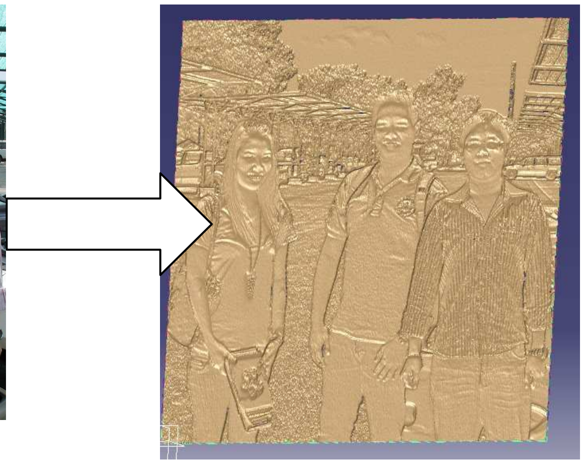

IMG 0067 (900x900pixel)


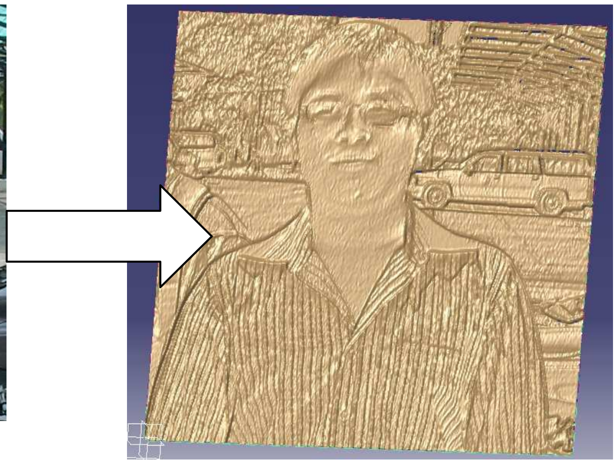

IMG 0067_1 (510x510pixel)


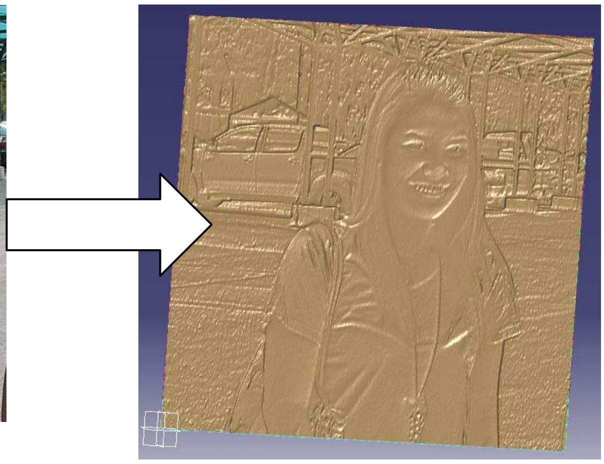

IMG 0067_2 (600x600pixel)

Figure 5.34b Result of less condition control Test, Figure name IMG 0067

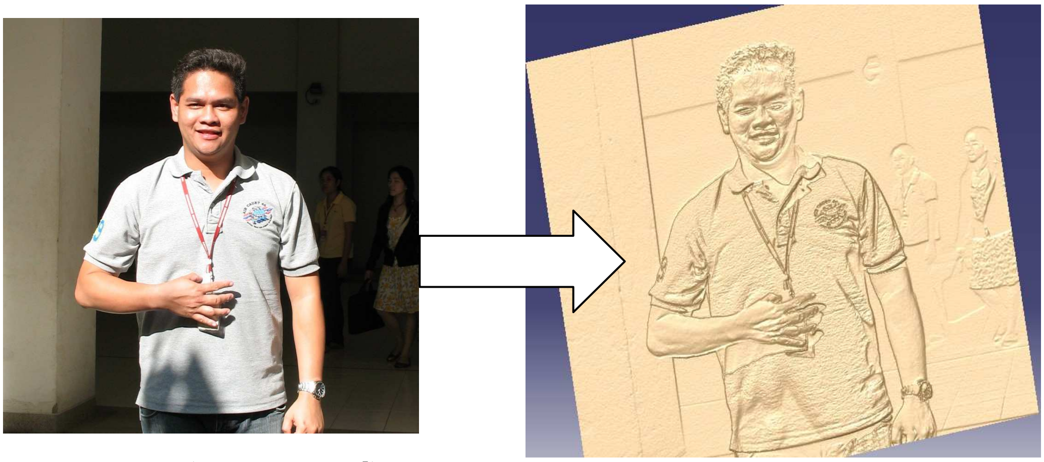

IMG 0068 (900x900pixel)

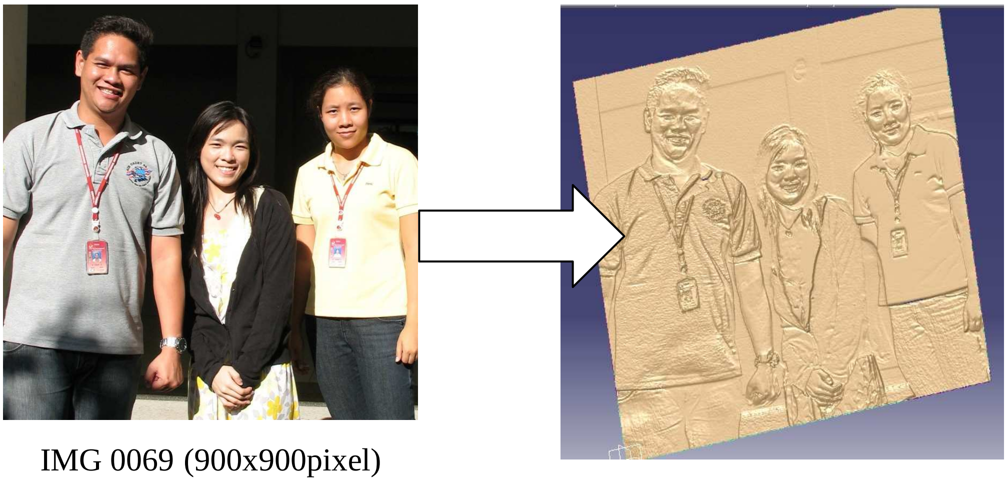

IMG 0069 (900x900pixel)

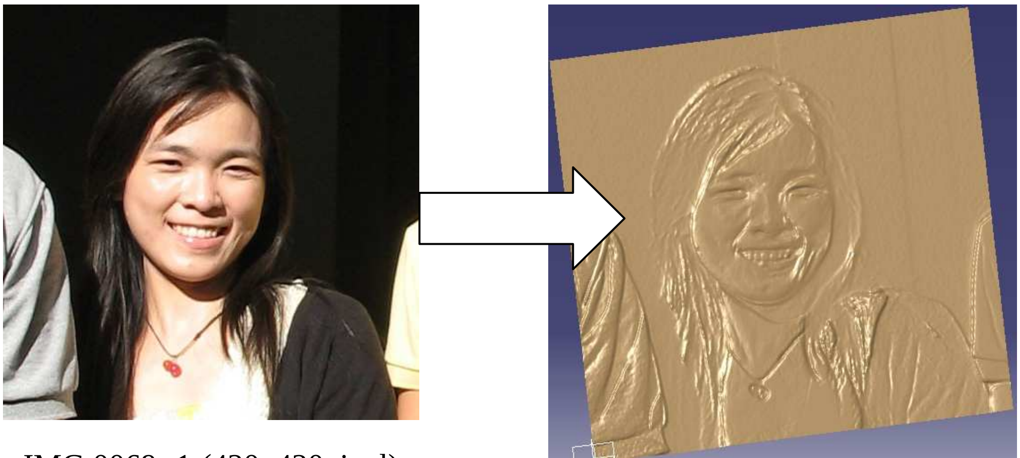

IMG 0069_1 (420x420pixel)

Figure 5.34c Result of less condition control Test, Figure name IMG 0068, IMG 0069

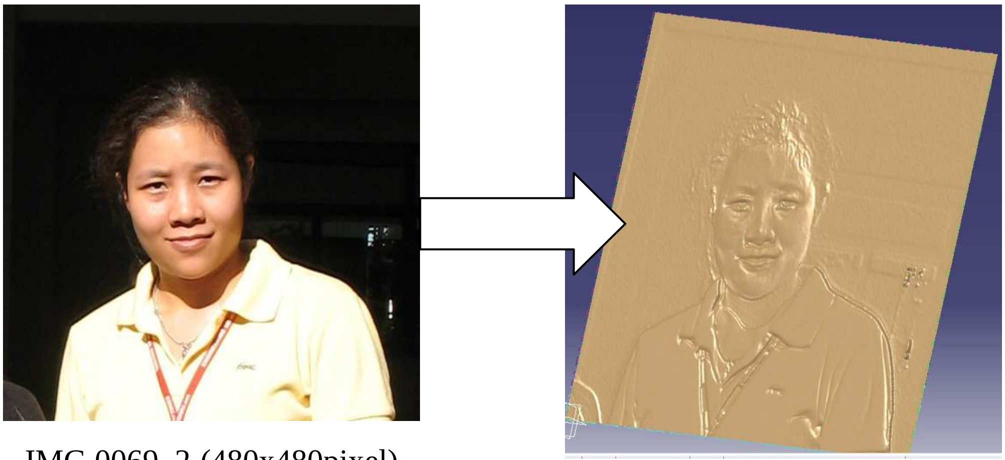

IMG 0069_2 (480x480pixel)

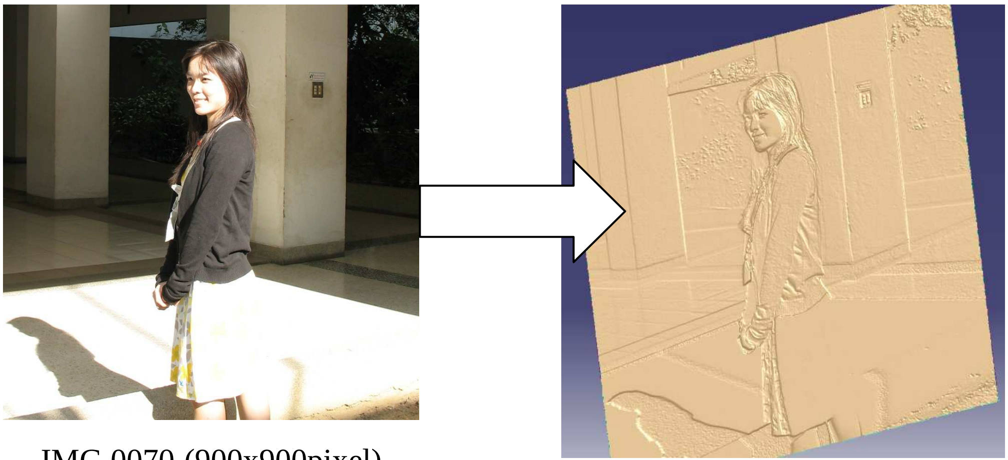

IMG 0070 (900x900pixel)

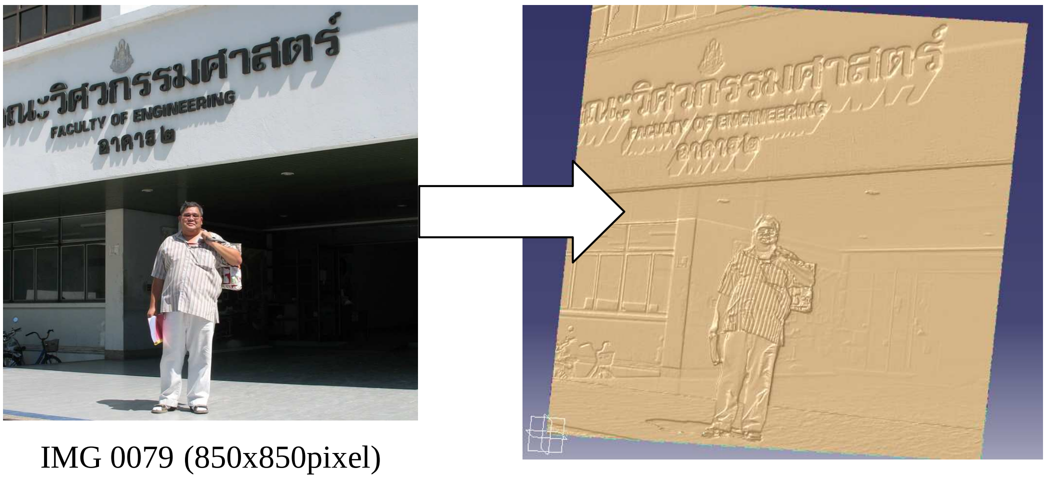

IMG 0079 (850x850pixel)

Figure 5.34d Result of less condition control Test, Figure name IMG 0069, IMG 0070, IMG 0079

CHAPTER VI
DISCUSSION AND RECOMMENDATIONS

1.2. Discussion

6.1.1 Discussion of result and testing

To examine whether created software potentially meets the aims of the research, researcher has determined a few conditions to standardize an effectiveness of a use of created software as follows:

6.1.1.1 In topic 5.10, show that finding a position of the sun can be replaced values by defaults available in developed software if those of changing temperature, air pressure and elevation are unidentified and hardly affect on the calculation.

Another variable such as times, time zone, latitude, longitude and delta T that they don't trouble to find after take a photograph, - for delta T, see manual for SFS with Solar program in Appendix B-, so they don't need as defaults.

6.1.1.2 In topic 5.11, to examine an impact of light intensity on expanding height 3D surface found that a quality of camera is an important factor contributing to a quality of expanding height 3D surface. Camera exposed to the light provides a less impact on expanding height 3D surface than camera unexposed to the light so main discussion of result in this topic is using more clearly image surface result will more high quality.

6.1.1.3 In topic 5.12, an examination of an impact of light direction on 3D surface resulted in two issues as follows:

- Shadow effect caused photo to be distorted; as a result, the time of taking photo must be taken into account. In topic 5.17 select time to photograph with less shadow then surface result less error from shadow too.

- Light direction was sourced by two position,- 135-degree tilt angle and 315-degree tilt angle (recommend +- 10 degree)-. This may lead to divergence failures,-divergence failures happening in Newton-Raphson method by many factors, Pramote (2006)-. However, an occurrence of divergence failures can be fixed by rotating photo to 90-degree angle before feeding them into software program.

6.1.1.4 In topic 5.12, an examination of an impact of background on 3D surface resulted in two issues as follows:

- In case of unpainted background, its impact on 3D surface depends on its pattern; nevertheless, to avoid any failures, background could be modified before feeding photos into software program.

- In case of painted background, material seemed to curve out from its background with darkened color; conversely, it seemed to sink into its background with brightened color

6.1.1.5 In topic 5.13, an examination of image resolution resulted in two issues as follows:

- If photo is not taken into normalization process, there will be an increase in bas-relief surface in line with an increase in pixel.

- If photo is taken into normalization process, there will be an increase in bas-relief surface in line with not only an increase in pixels, but also increases in holes on expanding height 3D surface.

Conclusion in this topic is more resolutely image then surface result will more resolutely but it may have more holes or more size of hole on surface.

6.1.2 The quality of performing SFS with solar light source

6.1.2.1 Compare quality of performing SFS, -in bas-relief manufacturing-, with bas-relief manufacturing of the Royal Thai Mint.

In doing product design job which focuses on bas-relief sculpture, it is necessary to rely on skilled labors such as mintage production or amulet production Computer Aided Design, CAD and Computer Aided Manufacturing, CAM are nowadays used for these industries. However, carving skill is still required for generating prototype, a fundamental process. Such prototype then will be put into Coordinate Measuring Machine or any other valued machines before taken into CAD and CAM processes. As the discussed procedure requires a lot of time and costs, an application of this research with solar calculation by Tsi-Shah SFS can be replaced. Tsi-Shah SFS effectively enables 3D surface to be bas-relief even in a huge material such as buildings or landscape.

For easier to show a utilization of Tsi-Shah SFS in bas-relief work, a coin production by the Royal Thai Mint,http://www.royalthaimint.net/, -show as figure 6.1-, will used for comparison with process with used SFS , -show as figure 6.2-. The comparison can be seen that reduce process and can be concluded utilization of Tsi-Shah SFS as follow

- It does not need much labor skill in carving, independent from their performance or emotion so it able to control leads time in design step.
- It does not need all kind for prototype in design step so it can decrease in material for design step.
- It can reduce number of process.
- It leads to cost reduction as relies on only a small number of equipments-computers digital cameras and compass rather than CMM or another copy surface machine that cloud be use in coin production.
- Administrator can consider and permit the design from virtual design, -surface design-.

.

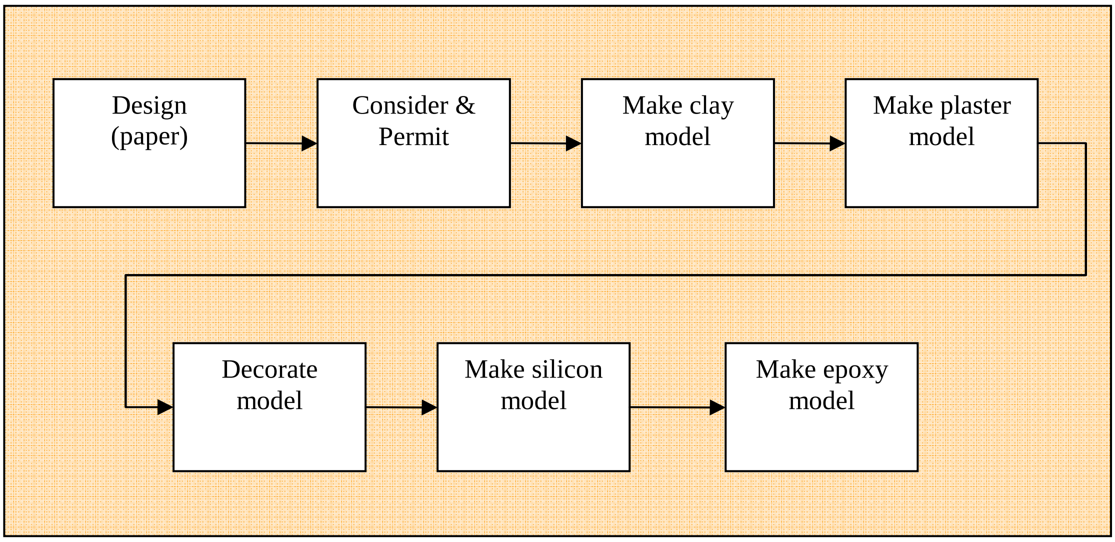

Figure 6.1 Step design of coin production by the Royal Thai Mint

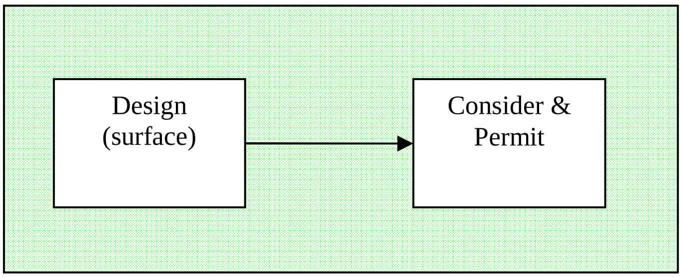

Figure 6.2 Design step when use SFS.

6.1.2.2 Compare quality of performing SFS with solar light source and rotation technique, with SFS unused solar light source and rotation technique

Created software can generate 3D surface at higher level by normalization process, and expanding height 3D surface can be completely utilized when already fixed by CATTA. In this research, the method of combining point clouds has been developed. Its principle is on the basis of generating point clouds from the same photo but different directions of light by rotating around Z axis. After examined with star fish, the result presented that it can improve photo distortion caused by an effect of shadow. So it can conclude quality merit of performing SFS with solar light source and rotation technique that better than with SFS unused solar light source and rotation technique as follow

- Able to reduce effect from showdown by rotation technique And combining point clouds.

- Due to solar light calculation, it give correct light direction so it reduce error from incorrect light direction, besides this it can be performed not only in workshop but also in outdoor with a huge material.

To apply 3D surface with product design job needs to imitate material surface which is rather incompatible with CAD. Capability of generating surface from point cloud by any other software must be taken to operate this job, and when an imitation is produced, consequently an obtained 3D surface will be used for CAD or other applications. However, since there are still a number of errors, -Shen&Yang (2005)-, SFS is not suitable for applying with Revert engineering; conversely, it can be applicable for product design by means of utilizing a group of data with CAD software.

6.2 Discussion for dominant factors and eliminating effects of factors from a surface result

6.2.1 Dominant factors

Dominant factors for bas-relief 3D work and expanding height 3D surface by hinge as follow.

6.2.1.1 *Clearing of the image*: In topic 5.11 that finding all of bas-relief 3D work and expanding height 3D surface, more clearing of the image surface will more contrast or more surface resolution.

6.2.1.2 *Shadow effect*: Shadow should not too much effect to defect meshes and surface resolution in bas-relief 3D work but it has some effect to shape,

As show as topic 5.12, Shadow on objects effects to defect meshes in expanding height 3D surface work that has more than bas-relief 3D work, therefore, these effect to shape of surface.

6.2.1.3 *Divergence effect*: Divergence is the most inferior effect as show as topic 5.12 in IMG 3047 and IMG 3041; - shape and surface resolution will be failure. Furthermore, surface will has a lot of defect meshes-.

6.2.1.4 *Image resolution*: Surface resolution varies to image resolution, but in expanding height 3D surface work, image resolution is an effect to increase shadow effect that make more surface errors.

Note: Time, calculated by using laptop BenQ Intel core 2 duo CPU T8100 2.10 GHz 3 GB of Ram, is one minute for image size ,900x900 pixels limited by CATIA.

.

6.2.2 Eliminating effect of factors from surface result

6.2.2.1 *Eliminating non clearing of the image*: For clearing image, digital camera which has brightness compensation function should be used. A sample is shown as figure 5.28.

6.2.2.2 *Eliminating Shadow effect*: The best solution for reducing shadow effect should avoid light direction that cause shadows or at the least shadow. Therefore, this thesis presents a solution method as topic 5.17 for expanding height 3D surface work by using combination point clouds that can reduce a shadow effect.

6.2.2.3 *Eliminating divergence effect*: For avoided divergence failures, user should beware light direction in 135-degree tilt angle and 315-degree tilt angle or if it can’t be avoided, therefore, the light direction should be solved by using an image rotation technique for a divergence failures problem as show as topic 5.18.

6.2.2.4 *Eliminating Image resolution effect in expanding height 3D surface work*: It is solved problem by a same way in subtopic 6.2.2.2, but a process time will be more waste time for repairing surface by CATIA.

6.2.3 Discussion for effect to process time

Process time is CPU times used for calculating each command in developed program in this thesis and, generating and fixing 3D surface by using the CATIA program. Process time of bas-relief 3D surface follows as in subtopic 6.2.3.1 and expanding height 3D surface follows as in subtopic 6.2.3.2 - 6.2.3.3

6.2.3.1 Surface reconstruction from bas-relief 3D point cloud usually has less defect meshes problem. Therefore, CPU times for fixing surface by CATIA are also less evaluated. Process time about 15 minutes, may be raised to one hour that depends on surface of objects, exception for bas-relief 3D point clouds with divergence effect that it will become to a lot of defect meshes when generate surface.

6.2.3.2 Shadow effect has influence to size of hole and defect meshes. So, if more shadow is also more process time for fixing hole, that will take time 1-2 hours,-shadow effect depends on light direction and a number of resolution for image resolution-.

6.2.3.3 If using combination for point clouds, that can reduce shadow effect but user will spend more time for using CATIA to merge point clouds and fixing surface, -operation as topic 5.17-, that use time between 2.5 – 4 hours depends on surface of objects and effect of shadow.

6.2.4 Factors for reconstruction 3D surface

From information in topic 6.2.1 to 6.2.3, factors could be summarized for bas-relief 3D surface as in table 6.1 and expanding height 3D surface as in table 6.2.

Table 6.1 Factors for reconstruction bas-relief 3D surface

Item	Image clearing	Image resolution	Less shadow	Non divergence	Result	
1	✓	✓	✓	✓	Process time	**15 min.**
					Shape	**Excellent**
					Surface resolution	**Excellent**
					Defect meshes	**Less or non**
2	✓	✓		✓	Process time	**15 min.**
					Shape	**Good**
					Surface resolution	**Excellent**
					Defect meshes	**Less or non**
3	✓	✓	✓		Process time	**-**
					Shape	**failure**
					Surface resolution	**failure**
					Defect meshes	**much**
4		✓	✓	✓	Process time	**15 min.**
					Shape	**Pretty**
					Surface resolution	**Pretty**
					Defect meshes	**Less**
5		✓	✓		Process time	**-**
					Shape	**failure**
					Surface resolution	**failure**
					Defect meshes	**much**
6		✓		✓	Process time	**15 min.**
					Shape	**Pretty**
					Surface resolution	**Poor**
					Defect meshes	**Less**

Table 6.1 Factors for reconstruction bas-relief 3D surface

Item	Image clearing	Image resolution	Less shadow	Non divergence	Result
7		✓			Process time **-** Shape **failure** Surface resolution **failure** Defect meshes **much**
9	✓		✓	✓	Process time **15 min.** Shape **Pretty** Surface resolution **Pretty** Defect meshes **Less**
10			✓	✓	Process time **15 min.** Shape **Pretty -Poor** Surface resolution **Poor** Defect meshes **Less**
11				✓	Process time **15 min.** Shape **Poor** Surface resolution **Poor** Defect meshes **Less**
12			✓		Process time **-** Shape **failure** Surface resolution **failure** Defect meshes **much**
13					Process time **-** Shape **failure** Surface resolution **failure** Defect meshes **much**

Note: *Process time is times since input data in software until finish bas-relief 3D surface.

*Shape is corrective of shape.

*Surface resolution is completely texture of surface.

* Excellent (shape correct and high resolution surface) is the best surface result in each object, which an example is shown IMG 0062 in figure 5.34a.

* Poor (shape error and non resolution surface) is the worth surface result in each object.

Table 6.2 Factors for reconstruction expanding height 3D surface

Item	Image resolution	Image clearing	Less shadow	Non diver-gence	combine point clouds	Solve diver-gence	Result
1	✓	✓	✓	✓	✓		Process time **2-3.5 hours** Shape **Excellent** Surface resolution **Good** Defect meshes **Base on CATIA user**
2	✓	✓	✓	✓			Process time **1-2 hours** Shape **Good- Excellent** Surface resolution **Excellent** Defect meshes **Base on CATIA user**
3	✓	✓	✓		✓	✓	Process time **2-3.5 hours** Shape **Good** Surface resolution **Excellent** Defect meshes **Base on CATIA user**
4	✓	✓	✓			✓	Process time **1-2 hours** Shape **Good** Surface resolution **Excellent** Defect meshes **Base on CATIA user**

Table 6.2 Factors for reconstruction expanding height 3D surface

Item	Image resolution	Image clearing	Less shadow	Non diver-gence	combine point clouds	Solve diver-gence	Result
5	✓	✓	✓		✓		Process time **-** Shape **failure** Surface resolution **failure** Defect meshes **Base on CATIA user**
6	✓	✓		✓			Process time **2.5-3.5 hours** Shape **Pretty** Surface resolution **Good** Defect meshes **Base on CATIA user**
7	✓	✓		✓	✓		Process time **3-4 hours** Shape **Good** Surface resolution **Good** Defect meshes **Base on CATIA user**
8	✓	✓				✓	Process time **1-2 hours** Shape **Good** Surface resolution **Good** Defect meshes **Base on CATIA user**
9	✓	✓					Process time **-** Shape **failure** Surface resolution **failure** Defect meshes **Base on CATIA user**

Table 6.2 Factors for reconstruction expanding height 3D surface

Item	Image resolution	Image clearing	Less shadow	Non diver-gence	combine point clouds	Solve diver-gence	Result
10		✓	✓	✓	✓		Process time **0.5-1 hours** Shape **Good** Surface resolution **Pretty** Defect meshes **Base on CATIA user**
11		✓	✓	✓			Process time **0.5-1 hours** Shape **Good** Surface resolution **Pretty** Defect meshes **Base on CATIA user**
12		✓	✓			✓	Process time **0.5-1 hours** Shape **Good** Surface resolution **Pretty** Defect meshes **Base on CATIA user**
14		✓		✓	✓	✓	Process time **2-3 hours** Shape **Good** Surface resolution **Pretty** Defect meshes **Base on CATIA user**
15		✓		✓		✓	Process time **0.5-1 hours** Shape **Poor** Surface resolution **Pretty** Defect meshes **Base on CATIA user**

Table 6.2 Factors for reconstruction expanding height 3D surface

Item	Image resolution	Image clearing	Less shadow	Non diver-gence	combine point clouds	Solve diver-gence	Result
16		✓		✓			Process time **0.5-1 hours** Shape **Poor** Surface resolution **Pretty** Defect meshes **Base on CATIA user**
17		✓				✓	Process time **0.5-1 hours** Shape **Poor** Surface resolution **Good** Defect meshes **Base on CATIA user**
18		✓					Process time **0.5-1 hours** Shape **failure** Surface resolution **failure** Defect meshes **Base on CATIA user**
19	✓		✓	✓			Process time **1-2 hours** Shape **Good** Surface resolution **Poor** Defect meshes **Base on CATIA user**
20	✓		✓				Process time **-** Shape **failure** Surface resolution **failure** Defect meshes **Base on CATIA user**

Table 6.2 Factors for reconstruction expanding height 3D surface

Item	Image resolution	Image clearing	Less shadow	Non diver-gence	combine point clouds	Solve diver-gence	Result
20	✓		✓				Process time **-** Shape **failure** Surface resolution **failure** Defect meshes **Base on CATIA user**
21			✓	✓			Process time **1-2 hours** Shape **Pretty** Surface resolution **Poor** Defect meshes **Base on CATIA user**
22	✓		✓			✓	Process time **1-2 hours** Shape **Good** Surface resolution **Poor** Defect meshes **Base on CATIA user**
23							Process time **-** Shape **failure** Surface resolution **failure** Defect meshes **Base on CATIA user**

Note: *Process time is times since input data in software until finish 3D surface expanding height,-base on Star fish- .

*Shape is corrective of shape.

*Surface resolution is completely texture of surface.

* Excellent (shape correct and high resolution surface) is the best surface result in each object, which an example is shown in figure 5.28.

* Poor (shape error and non resolution surface) is the worth surface result in each object, which an example is shown as IMG008A in figure 5.20c.

6.3 Recommendations

This topic will recommend to work that can develop from thesis as follow

6.3.1 This thesis points out an application of solar light direction to SFS method suggested by Tsi-Shah; however, solar light direction not only is compatible with Tsi-Shah SFS but also exposes to all SFS methods but may provide various outcomes on material surface.

6.3.2 Due to inability to reconstruct surface surrounding a material, it is necessary to take photo of remaining surface apart from a material, and image perspective must be taken into account by additionally studying a process of merging these surface altogether.

6.3.3 Rotated around Z axis, a material seemingly affects on solar light direction with top view angle during a process of taking photo. After imaging software is used to convert photo to the same direction, a material seemingly directs to the same direction with different solar light direction during a process of taking photo. As a result, an application of solar light to photometric stereo principle can also be performed.

REFERENCES

Ahmed, A. & Farang, A. (2006) A new Formulation for Shape form Shading for Non Lambertian Surfaces. *In Proc. 2006 IEEE Computer Society Conference on Computer Vision and Pettern Recognition*, *2*, 17-22. IEEE Computer Society Press, New York.

Bichsel, M. & Pentland, A.P. (1992) A Simple Algorithm for Shape from Shading. *IEEE Proc. Computer Vision and Pattern Recognition*, 459-465.

Bingham, A.W. & Rees, W.G. (1999) Construction of a High-Resolution DEM of an Arctic Ice Cap Using Shape-from-Shading. *Int. J. Remote Sensing, 2*(15), 3231-3241

Blanco-Muriel, M., Alarcon-Padilla, D.C., Lopea-Monratalla, T.& Lara-Coria,M. (2001) Computing the Solar Vector. *Solar Energy*, *70*(5), 431-441.

Buncha Pasilatesang (2009) *Application Development by using Visual Basic 2008.* SE-ED Ucation Public, Bangkok.

CATIA documentation for CATIA Version 5 Release 18 .

Chang, J.Y., Lee, K.M. & Lee,S.U. (2008) Shape form Shading using Graph cuts. *Pattern Recognition, 41*, 3749-3757.

Cheung, W.P., Lee, C.K. & Li, K.C. (1997) Direct Shape form Shading with Improved Rate of Convergence. *Pattern Recognition*, 30(3), 353-365.

Courteille, F.,Crouzil, A., Denis Durou, J. & Gurdjos, P. (2007) Shape form Shading for the Digitization of Curved Documents. *Machine Vision and Applications, 18,* 301-316.

Daniel, P., Durou, J.-D.(2000). From Deterministic to Stochastic Methods for Shape from Shading. *Proceeding of the fourth Asian Conference on Computer Vision*, Taipei, Taiwan,187-19.

Durou, J.-D., Falcone, M. & Sagona, M. (2008). Numerical Methods for Shape-form-Shading:A new Survey with Benchmarks.*Computer Vision and Image Understanding*, *109*, 22-43.

Falcone, M., Sagona, M.(1997). An algorithm for the Global Solution of the Shape-form-Shading Model. *Proceeding of the Nith International Conference on Image Anaylysis and Processing, 1*, Lecture notes in Computer Science, Florence, Italy, 596-603.

Grena, R. (2008) An Algorithm for the Computation of the Solar Position. *Solar Energy, 82*, 462-470.

Gibson, J. J. (1950a). The Perception of the Visual World. Boston, MA Haughton Mifflin. *Int. J. Computer Vision, 14*(3), 227-251.

Gibson, J. J. (1950b). The Perception of Visual Surfaces. *American Journal of Psychology, 63*, 367–384.

Horn, B.K.P., Sjoberg, R. W. (1978) Calculating the Reflectance Map. *Artificial Intelligence Laboratory*, MIT.

Horn, B.K.P. (1970) Shape form Shading: A Method for Obtaining the Shape of a Smooth Opaque Object From One View: *Artificial Intelligence Laboratory*, MIT

Horn, B.K.P. & Brooks, M.J. (eds.) (1989).*Shape form shading*, MIT press, Cambridge, MA.

Horn, B.K.P. (1981) Hill Shading and the Reflectance Map, *Proceeding of the IEEE, 69*(1).

Hsieh, J.W., Yuan Mark Liao, H., Tat Ko, M.& Fan, K.C. (1995) Wavelet-based Shape form Shading. *Graphical Models and Image processing, 57*(4), 343-362.

Hu, M.K. (1962) Visual Pattern Recognition by Moment Invariants, IRE. *Trans. Inf. Theory ,8* (1) ,179–187.

Lambert, J.H. (1760) Photometria Sive de Mensura de Gratibus Luminis. *Colorum et embrae Augsberg*, Germany, Eberhard klelt.

Leclerc, Y.G.& Bobick, A.F. (1991) The Direct Computation of Height form Shading. *Proceeding of the IEEE Conference on Computer Vision and Pattern Recognition*, Maui, Hi, USA.

Lee, C.H. & Rosenfeld, A. (1985) Improved Methods of Estimating Shape from Shading Using the Light Source Coordinate System. *Artificial Intelligence, 26*, 125-143.

Lee, K.M. & Kou, C.C.J. (1993) Shape form Shading with a Linear Triangular Element Surface Model. *IEEE Trans. Pattern Analysis and Machine Intelligence, 15*(8), 815-822.

Michalsky, J.(1988) The Astronomical Almanac's Algorithm for Approximate Solar Position (1950-2050).*Solar Energy, 40*(3),b227-235.

Nicodemus, F.E., Richmond, J.C., & Hsia, J.J. (1977) *Geometrical Considerations and Nomenclature for Reflectance.U.S.A.*: Nation Bureau of Standard,U.S. Department of Commerce.

Oren, M. & Nayer, S. (1995) Generalization of the Lambertian model and implications for machine vision. *Int. J. Computer Vision*, *14*(3), 227 – 251.

Pramote Dechaumpai (2006) *Numerical Methods in Engineering*. 5th ed. Chulalongkorn University Press, Thailand, 46-54.

Pentland, A.P. (1984) Local Shading Analysis. *IEE Transactions on Pattern Analysis and Machine Intelligence*, *6*(2), 170-187.

Pentland, A.P. (1988) Shape Imformation from Shading: A Theory about Human Perception. *In'l conf. Computer Vision*, 404-413.

Pentland, A.P. (1990) Linear Shape form Shading. *International Journal of Computer Vision, 4*, 153-162.

Phong, B.T. (1975) Illumination for Computer Generated Picters. *Communications of the ACM*, *18*(6), 311 – 317.

Richard, H.E. (2000) *Computer Algebra Recipes for Mathematical Physics,* 87-124. New York: Birkhauser Boston.

Reda, I.& Andreas, A.(2004) Solar Position Algorithm for Radiation Applications. *Solar Energy , 76*, 577-589.

Reda, I.& Andreas, A.(2005) *Solar Position Algorithm for Radiation Applications* (revised). Technical Report by National Renewable Energy Laboratory**,** USA.

Robles-Kelly, A., & Hancock, E.R.(2007) Shape-From-Shading Using the Heat Equation. *IEEE Transactions on Image Processing*, *16*(1), 7-21.

Roderrick,M.L. (1992) *Methods for Calculating Solar Position and Day Length Including Computer Programs and Subroutines*. Resource Management Technical Report No.137. South Perth: Department of Agriculture Western Australian.

Roj Hongprasit (1974) *Naval Astronomy*. Naval Education Department of Loyal Thai Navy press.

Royal Thai Mint, Coin Production Process. [cited 2010 May 31] : Available from: http://www.royalthaimint.net/ .

Shen, X. & Yang, L. (2005) Shape form Shading Models .In Suri,S.J., Wilson, D.L., & Laxminarayan, S., *Hand Book of Biomedical Image Analysis Engineering International ,1* (A), 257-304. Topics in Biomedical Engineering, International Book Series. New York: Kluwer Academic.

Sitichoke Yodrayub. (2007*) Digital mage processing programming by Visual Basic*. Technology Promotion Association (Thailand-Japan) Press., Thailand.

Tsai, P.S. & Shah, M. (1994) Shape form Shading Using Linear Approximation. *Image and Vision Computing*, *12*(8), 487-498.

Vogel, O., Breuß, M. & Weickert, J. (2008) Perspective Shape form Shading with Non Lambertian reflectance. In Rigpll, G. (ed) DAGM 2008. *LNCS*, *5096*, 517-526. Springer, Heideberg.

Vogel, O., Valgaerts, L., Breuß, M. & Weickert, J. (2009) Making Shape form Shading Work for Real-World Images. In Denzler, J., Notni,.G. & Süße, H. (Eds.) *Pattern Recognition Lecture Notes in Computer Science,* 191-200. NewYork: Springer Berlin Heidelberg .

Wacharaporn Suriyapiwat (2002) Basic Computer and New age of programming technique. Thaijareankanpimp press. Bangkok.

Woodham,R.J.(1980) Photometric Method for Determining Surface Orientation from Multiple Images. *Optical Engineering*, *19*(1), 139-144.

Zheng, Q. & Chellappa (1991) Estimation of Illuminat Direction Albado and Shape from Shading. *IEEE Trans Pattern Analysis and Mechine Inteligence, 13*(7), 680-702.

Zhang, R., Tsai, P.S., Cryer, J.E. & Shah, M. (1999). Shape form Shading: a Survey . *IEEE Transaction on Pattern Analysis and Machine Intelligence*, *21*(8), 690-706.

APPENDICES

APPENDIX A

DATA TABLE FOR SOLAR POSITION CALCULATION

Table A1.1 Earth Periodic Terms L0

Row Number	A	B	C
0	175347046	0	0
1	3341656	4.6692568	6283.07585
2	34894	4.6261	12566.1517
3	3497	2.7441	5753.3849
4	3418	2.8289	3.5231
5	3136	3.6277	77713.7715
6	2676	4.4181	7860.4194
7	2343	6.1352	3930.2097
8	1324	0.7425	11506.7698
9	1273	2.0371	529.691
10	1199	1.1096	1577.3435
11	990	5.233	5884.927
12	902	2.045	26.298
13	857	3.508	398.149
14	780	1.179	5223.694
15	753	2.533	5507.553
16	505	4.583	18849.228
17	492	4.205	775.523
18	357	2.92	0.067
19	317	5.849	11790.629
20	284	1.899	796.298
21	271	0.315	10977.079
22	243	0.345	5486.778
23	206	4.806	2544.314
24	205	1.869	5573.143
25	202	2.4458	6069.777
26	156	0.833	213.299
27	132	3.411	2942.463
28	126	1.083	20.775
29	115	0.645	0.98
30	103	0.636	4694.003
31	102	0.976	15720.839
32	102	4.267	7.114
33	99	6.21	2146.17
34	98	0.68	155.42
35	86	5.98	161000.69
36	85	1.3	6275.96
37	85	3.67	71430.7
38	80	1.81	17260.15
39	79	3.04	12036.46
40	71	1.76	5088.63

Table A1.1 Earth Periodic Terms L0 (Cont.)

Row Number	A	B	C
41	74	3.5	3154.69
42	74	4.68	801.82
43	70	0.83	9437.76
44	62	3.98	8827.39
45	61	1.82	7084.9
46	57	2.78	6286.6
47	56	4.39	14143.5
48	56	3.47	6279.55
49	52	0.19	12139.55
50	52	1.33	1748.02
51	51	0.28	5856.48
52	49	0.49	1194.45
53	41	5.37	8429.24
54	41	2.4	19651.05
55	39	6.17	10447.39
56	37	6.04	10213.29
57	37	2.57	1059.38
58	36	1.71	2352.87
59	36	1.78	6812.77
60	33	0.59	17789.85
61	30	0.44	83996.85
62	30	2.74	1349.87
63	25	3.16	4690.48

Table A1.2 Earth Periodic Terms L1

Row Number	A	B	C
0	628331966747	0	0
1	206059	2.678235	6283.07585
2	4303	2.6351	12566.1517
3	425	1.59	3.523
4	119	5.796	26.298
5	109	2.966	1577.344
6	93	2.59	18849.23
7	72	1.14	529.69
8	68	1.87	398.15
9	67	4.41	5507.55
10	59	2.89	5223.69
11	56	2.17	155.42
12	45	0.4	796.3
13	36	0.47	775.52

Table A1.2 Earth Periodic Terms L1 (Cont.)

Row Number	A	B	C
14	29	2.65	7.11
15	21	5.34	0.98
16	19	1.85	5486.78
17	19	4.97	213.3
18	17	2.99	6275.96
19	16	0.03	2544.31
20	16	1.43	2146.17
21	15	1.21	10977.08
22	12	2.83	1748.02
23	12	3.26	5088.63
24	12	5.27	1194.45
25	12	2.08	4694
26	11	0.77	553.57
27	10	1.3	3286.6
28	10	4.24	1349.87
29	9	2.7	242.73
30	9	5.64	951.72
31	8	5.3	2352.87
32	6	2.65	9437.76
33	6	4.67	4690.48

Table A1.3 Earth Periodic Terms L2

Row Number	A	B	C
0	52919	0	0
1	8720	1.0721	6283.0758
2	309	0.867	12566.152
3	27	0.05	3.52
4	16	5.19	26.3
5	16	3.68	155.42
6	10	0.76	18849.23
7	9	2.06	77713.77
8	7	0.83	775.52
9	5	4.66	1577.34
10	4	1.03	7.11
11	4	3.44	5573.14
12	3	5.14	796.3
13	3	6.05	5507.55
14	3	1.19	242.73
15	3	6.12	529.69
16	3	0.31	398.15

Table A1.3 Earth Periodic Terms L2 (Cont.)

Row Number	A	B	C
17	3	2.28	553.57
18	2	4.38	5223.69
19	2	3.75	0.98

Table A1.4 Earth Periodic Terms L3

Row Number	A	B	C
0	289	5.844	6283.076
1	35	0	0
2	17	5.49	12566.15
3	3	5.2	155.42
4	1	4.72	3.52
5	1	5.3	18849.23
6	1	5.97	242.73

Table A1.5 Earth Periodic Terms L4

Row Number	A	B	C
0	114	3.142	0
1	8	4.13	6283.08
2	1	3.84	12566.15

Table A1.6 Earth Periodic Terms L5

Row Number	A	B	C
0	1	3.14	0

Table A2.1 Earth Periodic Terms B0

Row Number	A	B	C
0	280	3.199	84334.662
1	102	5.422	5507.553
2	80	3.88	5223.69
3	44	3.7	2352.87
4	32	4	1577.34

Table A2.2 Earth Periodic Terms B1

Row Number	A	B	C
0	9	3.9	5507.55
1	6	1.73	5223.69

Table A3.1 Earth Periodic Terms R0

Row Number	A	B	C
0	100013989	0	0
1	1670700	3.0984635	6283.07585
2	13956	3.05525	12566.1517
3	3084	5.1985	77713.7715
4	1628	1.1739	5753.3849
5	1576	2.8469	7860.4194
6	925	5.453	11506.77
7	542	4.564	3930.21
8	472	3.661	5884.927
9	346	0.964	5507.553
10	329	5.9	5223.694
11	307	0.299	5573.143
12	243	4.273	11790.629
13	212	5.847	1577.344
14	186	5.022	10977.079
15	175	3.012	18849.228
16	110	5.055	5486.778
17	98	0.89	6069.78
18	86	5.69	15720.84
19	86	1.27	161000.69
20	85	0.27	17260.15
21	63	0.92	529.69
22	57	2.01	83996.85
23	56	5.24	71430.7
24	49	3.25	2544.31
25	47	2.58	775.52
26	45	5.54	9437.76
27	43	6.01	6275.96
28	39	5.36	4694
29	38	2.39	8827.39
30	37	0.83	19651.05
31	37	4.9	12139.55
32	36	1.67	12036.46
33	35	1.84	2942.46
34	33	0.24	7084.9
35	32	0.18	5088.63
36	32	1.78	398.15
37	28	1.21	6286.6
38	28	1.9	6279.55
39	26	4.59	10447.39

Table A3.2 Earth Periodic Terms R1

Row Number	A	B	C
0	103019	1.10749	6283.07585
1	1721	1.0644	12566.1517
2	702	3.142	0
3	32	1.02	18849.23
4	31	2.84	5507.55
5	25	1.32	5223.69
6	18	1.42	1577.34
7	10	5.91	10977.08
8	9	1.42	6275.96
9	9	0.27	5486.78

Table A3.3 Earth Periodic Terms R2

Row Number	A	B	C
0	4359	5.7846	6283.0758
1	124	5.579	12566.152
2	12	3.14	0
3	9	3.63	77713.77
4	6	1.87	5573.14
5	3	5.47	18849

Table A3.4. Earth Periodic Terms R3

Row Number	A	B	C
0	145	4.273	6283.076
1	7	3.92	12566.15

Table A3.5 Earth Periodic Terms R4

Row Number	A	B	C
0	4	2.56	6283.08

Table A 4.1 Periodic Terms for the Nutation in Longitude and Obliquity Coefficients for $\Delta\psi$ & $\Delta\varepsilon$

Coefficients for $\Delta\psi$		Coefficients for $\Delta\varepsilon$	
a	b	c	d
-171996	-174.2	92025	8.9
-13187	-1.6	5736	-3.1
-2274	-0.2	977	-0.5
2062	0.2	-895	0.5
1426	-3.4	54	0
712	0.1	-7	0
-517	1.2	224	-0.6
-386	-0.4	200	0
-301	0	129	-0.1
217	-0.5	-95	0.3
-158	0	0	0
129	0.1	-70	0
123	0	-53	0
63	0	0	0
63	0.1	-33	0
-59	0	26	0
-58	-0.1	32	0
-51	0	27	0
48	0	0	0
46	0	-24	0
-38	0	16	0
-31	0	13	0
29	0	0	0
29	0	-12	0
26	0	0	0
-22	0	0	0
21	0	-10	0
17	-0.1	0	0
16	0	-8	0
-16	0.1	7	0
-15	0	9	0
-13	0	7	0
-12	0	6	0
11	0	0	0
-10	0	5	0
-8	0	3	0
7	0	-3	0
-7	0	0	0
-7	0	3	0

Table A 4.1 Periodic Terms for the Nutation in Longitude and Obliquity Coefficients for $\Delta\psi$ & $\Delta\varepsilon$ (Cont.)

Coefficients for $\Delta\psi$		Coefficients for $\Delta\varepsilon$	
-7	0	3	0
6	0	0	0
6	0	-3	0
6	0	-3	0
-6	0	3	0
-6	0	3	0
5	0	0	0
-5	0	3	0
-5	0	3	0
-5	0	3	0
4	0	0	0
4	0	0	0
4	0	0	0
-4	0	0	0
-4	0	0	0
-4	0	0	0
3	0	0	0
-3	0	0	0
-3	0	0	0
-3	0	0	0
-3	0	0	0
-3	0	0	0
-3	0	0	0
-3	0	0	0

Table A 4.2 Periodic Terms for the Nutation in Longitude and Obliquity
Coefficients for Sin terms

Y0	Y1	Y2	Y3	Y4
0	0	0	0	1
-2	0	0	2	2
0	0	0	2	2
0	0	0	0	2
0	1	0	0	0
0	0	1	0	0
-2	1	0	2	2
0	0	0	2	1
0	0	1	2	2
-2	-1	0	2	2
-2	0	1	0	0
-2	0	0	2	1
0	0	-1	2	2
2	0	0	0	0
0	0	1	0	1
2	0	-1	2	2
0	0	-1	0	1
0	0	1	2	1
-2	0	2	0	0
0	0	-2	2	1
2	0	0	2	2
0	0	2	2	2
0	0	2	0	0
-2	0	1	2	2
0	0	0	2	0
-2	0	0	2	0
0	0	-1	2	1
0	2	0	0	0
2	0	-1	0	1
-2	2	0	2	2
0	1	0	0	1
-2	0	1	0	1
0	-1	0	0	1
0	0	2	-2	0
2	0	-1	2	1
2	0	1	2	2
0	1	0	2	2
-2	1	1	0	0
0	-1	0	2	2
2	0	0	2	1

Table A 4.2 Periodic Terms for the Nutation in Longitude and Obliquity Coefficients for Sin terms (Cont.)

2	0	1	0	0
-2	0	2	2	2
-2	0	1	2	1
2	0	-2	0	1
2	0	0	0	1
0	-1	1	0	0
-2	-1	0	2	1
-2	0	0	0	1
0	0	2	2	1
-2	0	2	0	1
-2	1	0	2	1
0	0	1	-2	0
-1	0	1	0	0
-2	1	0	0	0
1	0	0	0	0
0	0	1	2	0
0	0	-2	2	2
-1	-1	1	0	0
0	1	1	0	0
0	-1	1	2	2
2	-1	-1	2	2
0	0	3	2	2
2	-1	0	2	2

APPENDIX B
MANUAL FOR DEVELOPED SOFTWARE TOOL

B1. Introduction

This program is developed from principle of Linear Shape Form Shading in method of Tsi-Shah and the solar position in method of Reda-Andreas, calculate by input image data and solar data.

The preliminary agreement in use.

Text Box when background color is red, can not enter data. That happens when users enter data in another text box that is same kind data.

Text Box that background is yellow. User can both enter data or not that has default data.

Almost Text Box must only enter numerical data in Text Box. Text box which must input alphabet data are Cal Sun Light Direction/Latitude/N or S and Cal Sun Light Direction /Longitude/E or W.

B2. Usability

When users open this program will see a Form Main window as shown as figure B1 which 3 button for choose as follows.

-Cal SFS: Users click this button when users want to use SFS calculation first. And then users can choose both enter light source by self and enter sola light source that will more explanation in topic A 2.2.4

-Cal Sun Light Direction: Users click this button when users want to use Solar position calculation first and then sent solar position to calculation SFS.

- Close form used for close all active sub-form.

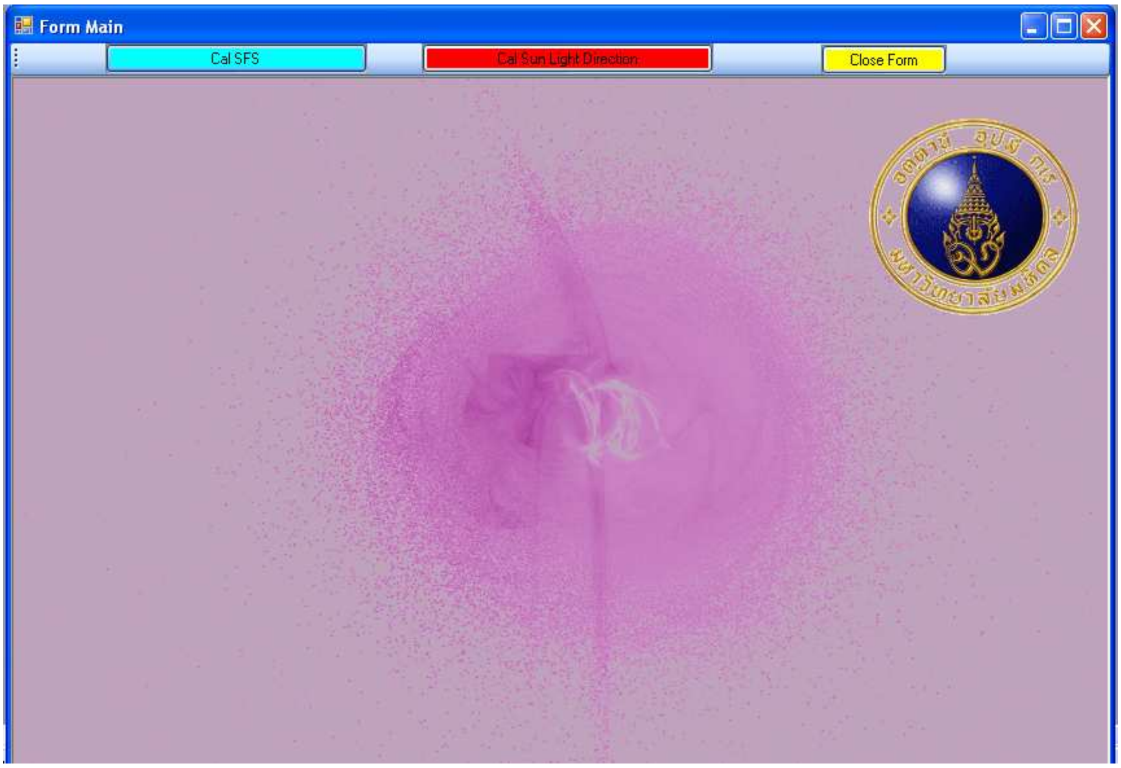

Figure B1 Form Main Window

When Users click Cal SFS button in Form Main window then the Shape Form Shading Tsi window as show as figure B2 will appear. The Shape Form Shading Tsi window can be divided to 7 parts as follows.

- Enter and show the image part (1)
- Enter light source data in the Cartesian coordinate part (2)
- Enter light source data in the Stereographic Coordinate part (3)
- Enter object height part (4)
- Choice of light source direction part (5)
- Operation part (6)

B2.1 Shape Form Shading Tsi-Shah window

B2.1.1 Enter and show the image part is for find image directory by click Brows Pic button (user can't enter directory in textbox). Images much in group of BMP, and much have width equal to length and size of image too big CPU times will too long.

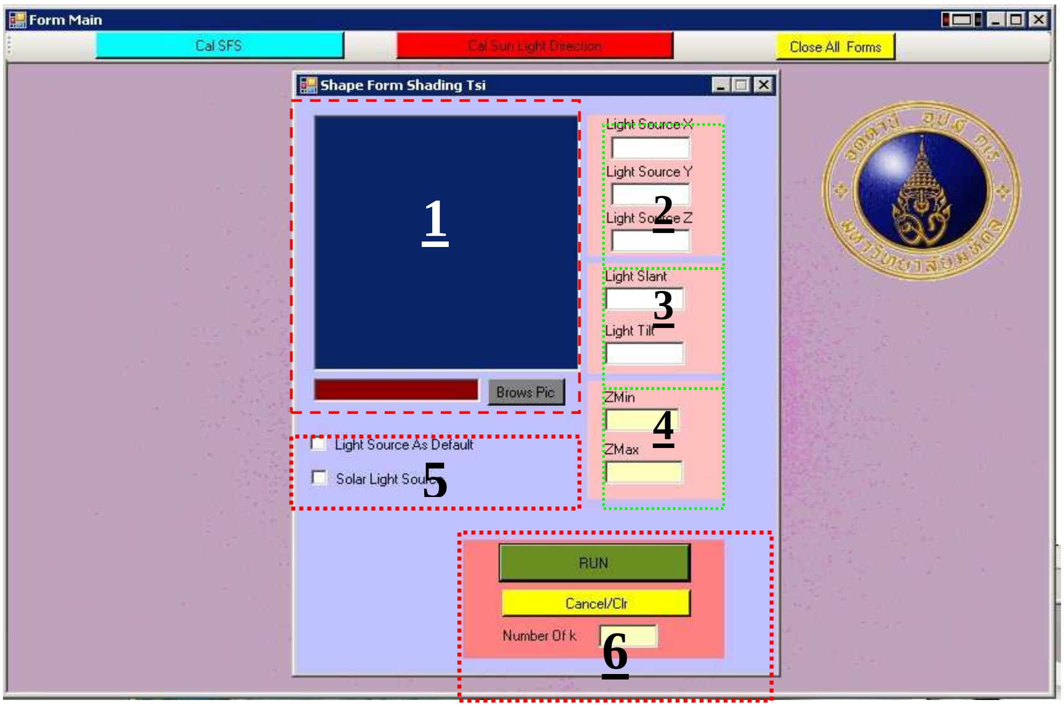

Figure B2 the Shape Form Shading Tsi window.

B2.1.2 If users know light source coordinate can use only one of The Enter light source data in the Cartesian coordinate part and the Enter light source data in the Stereographic Coordinate

B2.1.3 Enter object height part is not required to enter any information. If users want to calculate normalization, enter the object lowest in Z min textbox and the object highest in Z max textbox in unit pixel. En example for find height in pixel unit such as object that has width 2 meters and its width in figure is 200 pixel, then user use to multiply object height ,- 1 meters-, by 100. Now we have the object height in pixel equal to 100.

B2.1.4 The Choice of light source direction part has 2 check boxes. If both of 2 check boxes are was check another entering data of light source will inactive. The Light Source as Default check box that for test run FSF or run SFS by you have unknown with light source direction. And the Solar light source check box when was checked the Cal Sun Light Direction will appear and then see next in topic B2.2

B2.1.5 Operation part combine of Run, Cancel/Clr and Number of k , they are used as follows.

Run button was click for run SFS when user enter data complete. Before SFS calculation end a saving window as figure B3 will appear user much choose directory for save file and then when finish calculation as figure B4 users use to click OK for end operation. Cancel/ Clr button used for delete data in all textbox and back to origin state of the Shape from Shading window.

Number of k is has default equal to 6,- recommend number- . If users want to enter by self, remind that number is smaller CPU times are more less and more error result and bigger CPU times are more times and more close to exact result.

Save used for save result in .text file type.

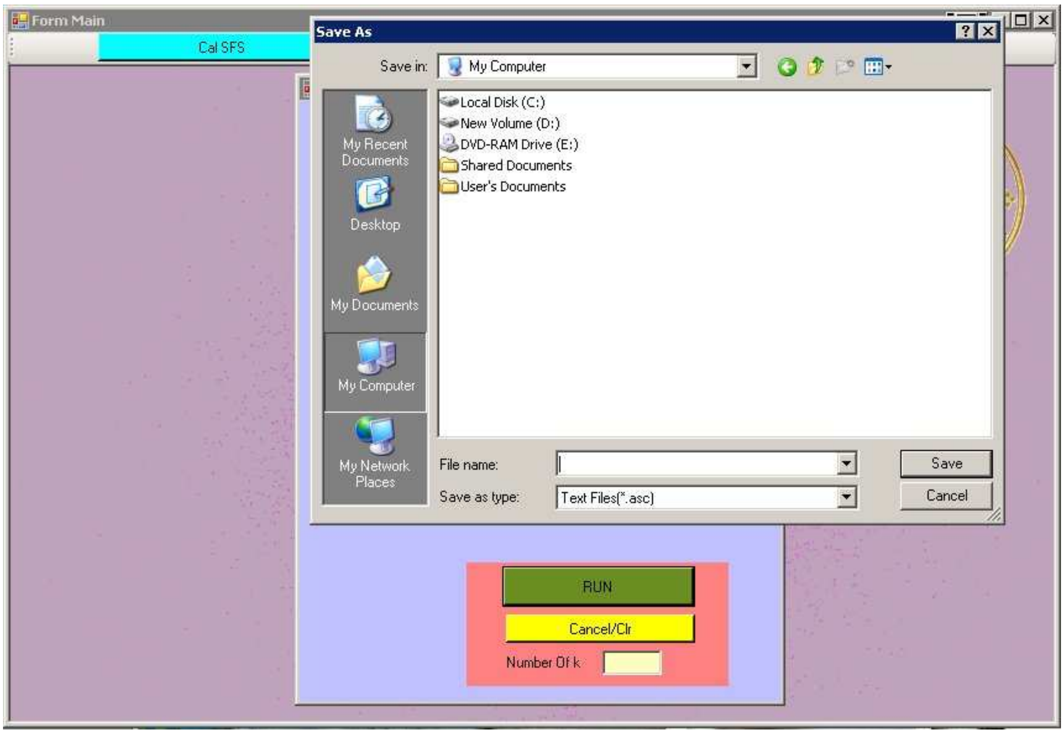

Figure B3 Saving window for saving Shape From Shading result.

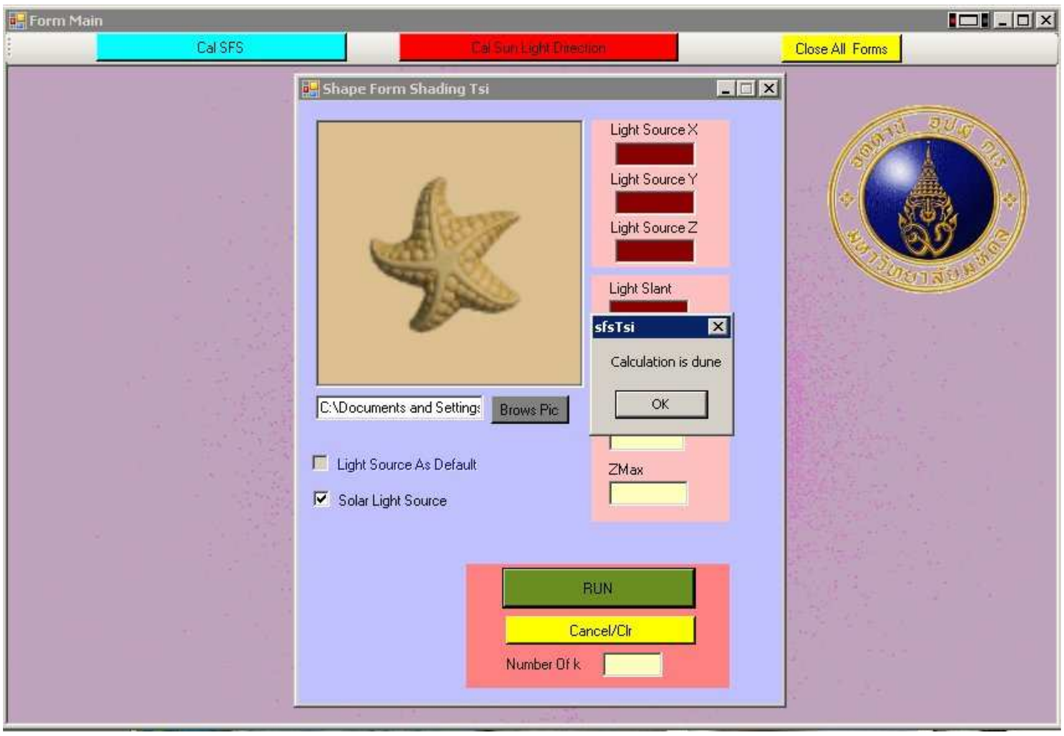

Figure B4 The Shape from Shading when end calculation.

B2.2 Cal Sun Light Direction

When user both click the Cal Sun Light Direction button from Form Main and choose Solar Light Source from the Shape Form Shading Tsi window then the Solar Light Source window will generate as shown as figure B5. The Solar Light Source window can be divided to 6 parts as follows.

- Time data part (1)
- Location part (2)
- Atmosphere part (3)
- Delta T part (4)
- Height of objects part (5)
- Operation part (6)

Data that much enter is part 1, 2, 4 and 5. The Atmosphere part (part 3) has default as mean of pressure and mean of temperature of Thailand in 2008.

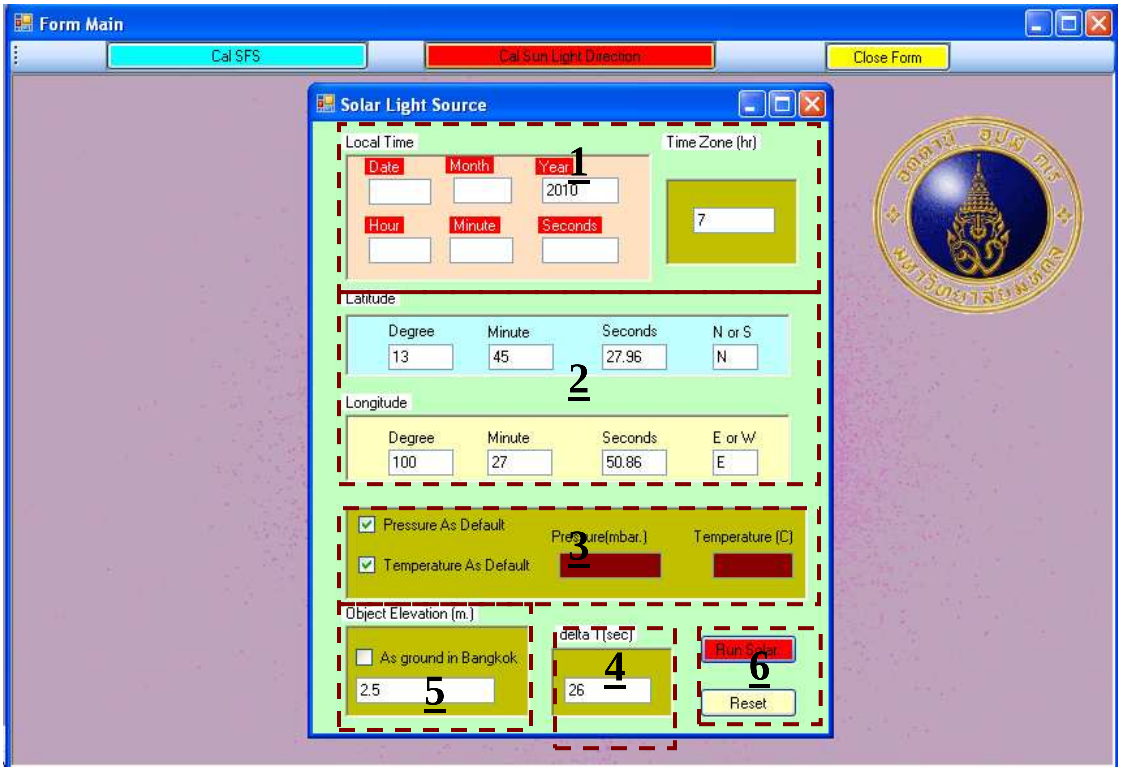

Figure B5 The Cal Sun Light Direction window.

B2.2.1 Time data part is for enter local time data. If user need to calculation by precisely times, can Compared Thailand standard time from website the National Institute of Metrology (Thailand), -www.nimt.or.th-, or from website of the Loyal Thai Navy Hydrographic Department, -http://www.navy.mi.th/hydro/time/-, Time Zone textbox for enter time zone that far from Greenwich, Thailand has time zone equal to +7.

B2.2.2 Latitude and Longitude can enter as both 2 form as follows.

- Enter Latitude, Longitude as integer not more than 180 degrees, 90 degrees, and enter Minute textboxes and Second textboxes as integer not more than 60 degrees.

- Enter Latitude, Longitude as real number with decimal such as 39.349, in this form no need enter in Minute and Second textbox.

If in the Northern Hemisphere Latitude enter N or n, if not enter S or s.

If in the west of Greenwich Longitude enter W or w, if not enter E or e.

B2.2.3 Pressure has default as 840 mbar and temperature has default as 30^{o}c.

B2.2.4 Delta T can be found in yearly journal of the Astronomical Almanac, or_easier way use weekly report of the US Naval Observatory from website http://www.usno.navy.mil/ or the easiest way, but the most error by use the delta T prediction graph for year 2000 to 2050 as shown as figure B6

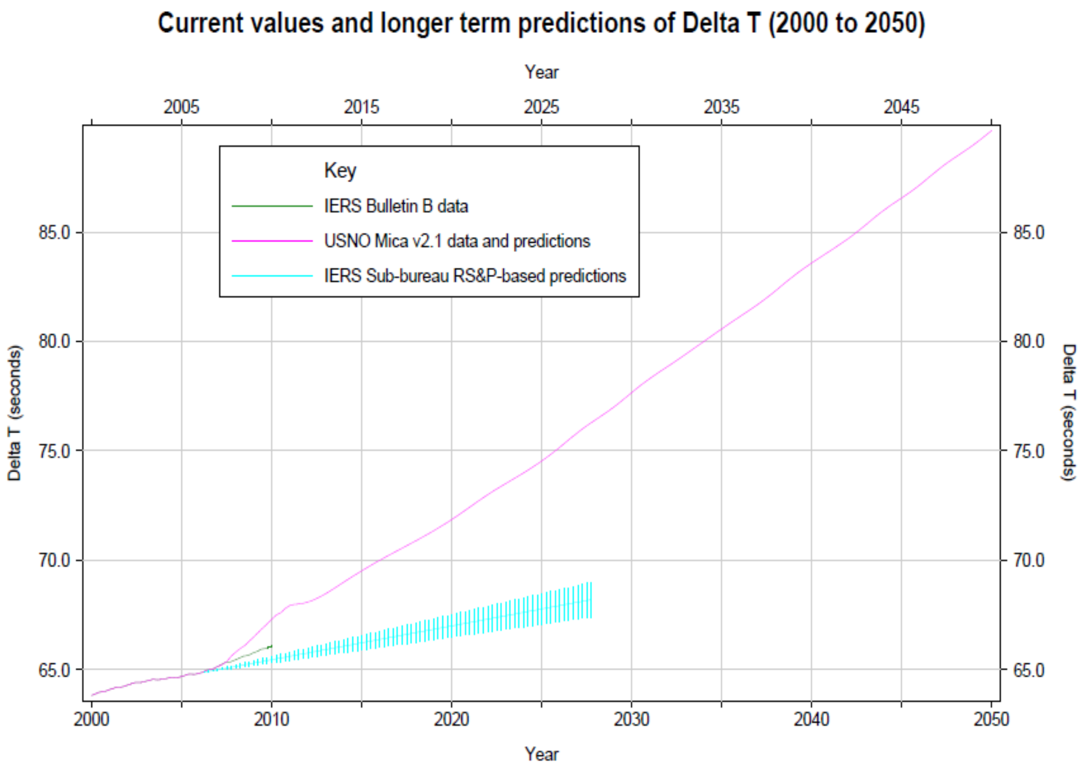

Figure B6 The prediction of delta T, data from http://www.usno.navy.mil/

B2.2.5 The Height of objects part is height above sea level of objects. In Thailand, user can download height above sea level data by website of The National Statistical Office Thailand, service.nso.go.th/nso/g_data23/stat_23/toc_23/23.1-1.xls.

B2.2.6 Reset button will be pressed for back to origin state of the Cal Sun Light Direction window.

B2.2.7 A Run Solar button is used for run calculation of solar position when finish calculation a Massage Box as shown as figure B7 will appear. Then if users press Cancel button Zenith angle and Azimuth angle will shown as figure B8 and SFS will not be calculate. If users press OK button, the TurnSunLight window will active.

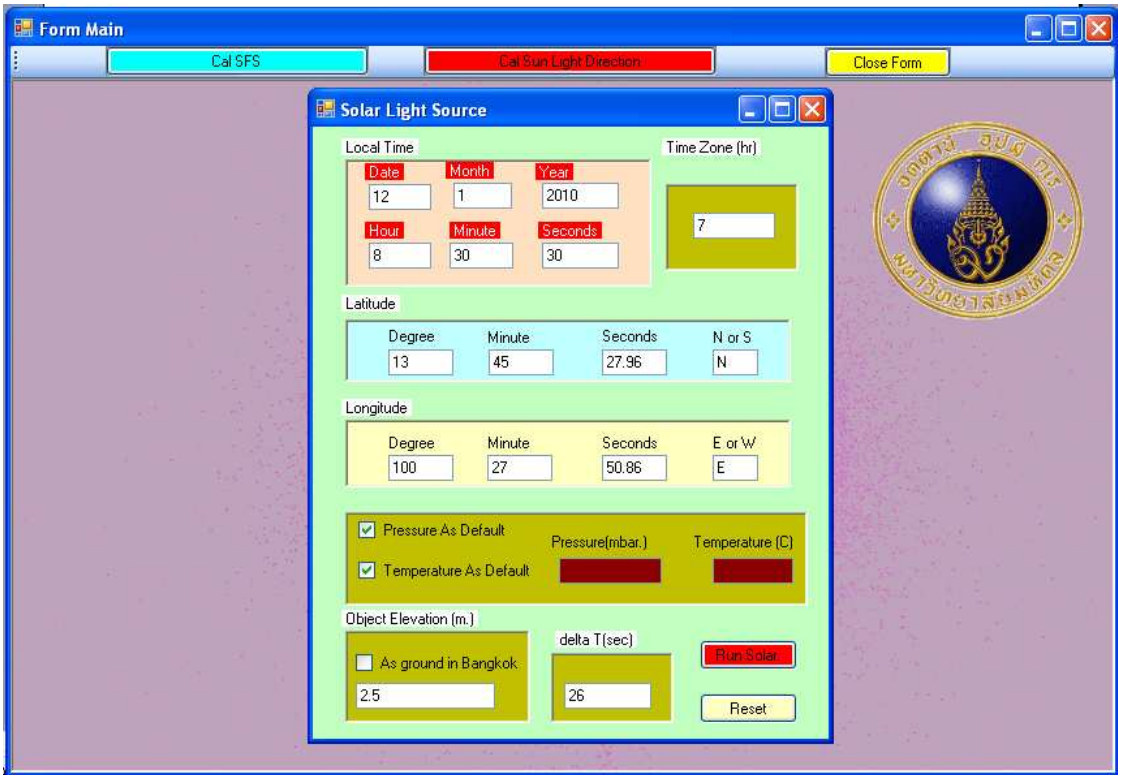

Figure B7 The Cal Sun Light Direction with enter data.

B2.3 The TurnSunLight is used for transformation solar light direct to SFS coordinate, have 3 part as shown as figure B9 as follows.

- Rotation of Z axis (1)
- Rotation of X axis (2)
- Operation part (3)

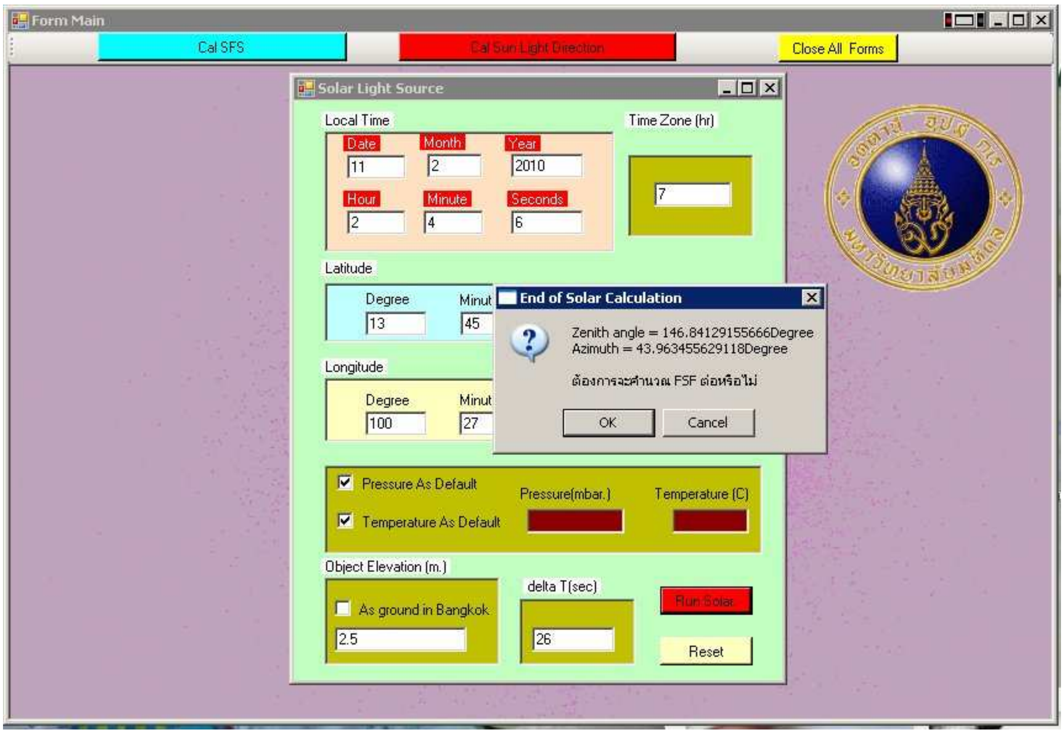

Figure B8 Result of the Cal Sun Light Direction

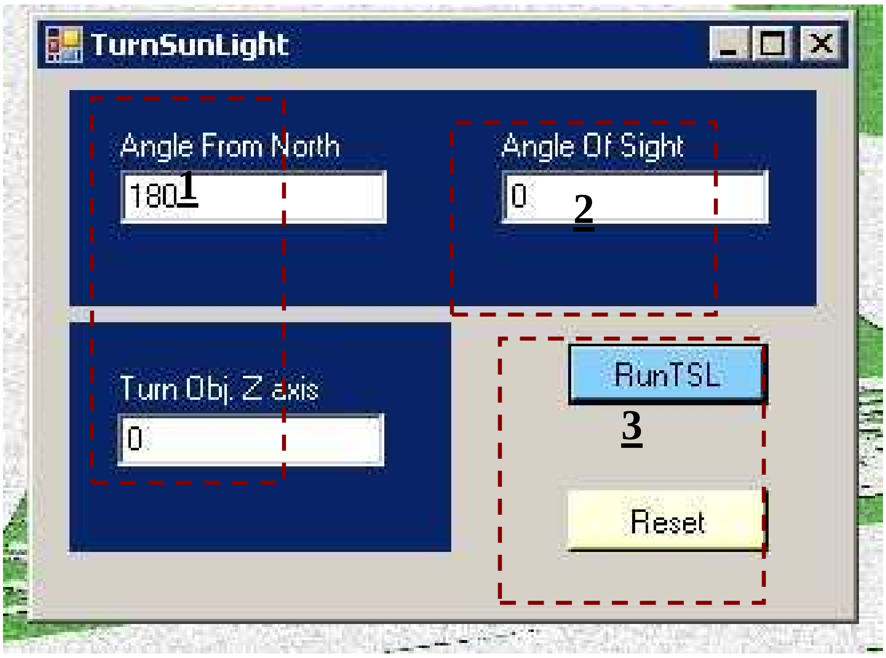

Figure B9 The TurnSunLight window

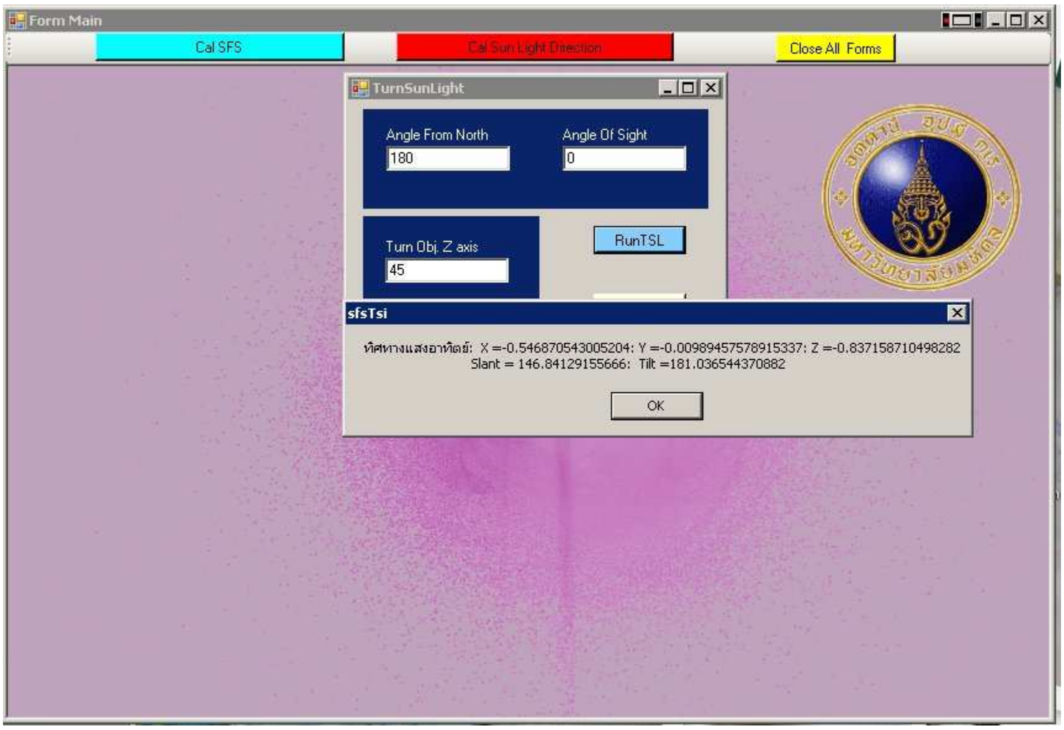

Figure B10 The TurnSunLight result

Usability of the TurnSunLight window as follow.

B2.3.1 If number in the Angle From North textbox equal 0 mean you take photo direct to the North. Otherwise if put other number much count angle counter clock wise

B2.3.2 If number in Turn Obj. Z axis textbox equal 0 mean object does not turn. Otherwise if put other number much count angle counter clock wise

B2.3.3 If number in the Angle of Sight textbox equal 0 that mean you take photo in top-view. Otherwise if put other number much count angle counter clock wise

B2.3.4 Run button will be pressed for run TurnSunLight and then the Shape Form Shading Tsi window will open automatically. The Shape Form Shading Tsi window was explained in topic B2.1.

B2.3.5 Reset button will be pressed for back to origin state of the TurnSunLight window.

When TurnSunLight end calculation it will show result as figure B10

BIOGRAPHY

NAME	LCDR. Wittaya Aueprasert
DATE OF BIRTH	17 June 1973
PLACE OF BIRTH	Ratchaburi, Thailand
INSTITUTIONS ATTENDED	Royal Thai Naval Academy, 1993-1998 Bachelor of Engineering (Marine Engineering) Mahidol University, 2007-2010 Master of Engineering (Industrial Engineering)
RESEARCH GRANTS	-
HOME ADDRESS	19/6 VILLAGE 4 SOI TAR-IT TAR-IT SUB-DISTRICT PAK-KRET DISTRICT NONTHABURI PROVINCE 11120 Tel. 0-2962-4117 E-mail : jokelaa@gmail.com
EMPLOYMENT ADDRESS	ROYAL THAI NAVY Tel. 0-2475-5184 Web-site: http://www.navy.mi.th
PUBLICATION / PRESENTATION	Eastern Asia University conference, second